Characterizing Microbial Communities Using Droplet Microfluidic Technology

by

Sida Wang

A dissertation submitted in partial fulfillment
of the requirements for the degree of
Doctor of Philosophy
(Chemical Engineering)
in The University of Michigan
2017

Doctoral Committee:

Professor Mark A. Burns, Co-Chair
Associate Professor Xiaoxia Lin, Co-Chair
Professor Betsy Foxman
Associate Professor Sunitha Nagrath
Professor David H. Sherman

Sida Wang

sidawang@umich.edu

ORCID iD: 0000-0001-8101-8883

To Mom, Dad, and Amy

ACKNOWLEDGEMENTS

Looking back at these last six years, I can't believe I signed up for this crazy ride. There have been so many ups and downs, but I've loved every minute of it and doing this has been one of the greatest experiences I will ever have. I couldn't be prouder of what I've accomplished, but I could never have done this alone. Without the support of my colleagues, friends and family, I never would have crossed this finish line. Now that I'm here, I'm excited about starting the next step of my life, but also sad to say goodbye to so many people who've been with me these last six years.

First, I'd like to thank my advisors Mark and Nina for all their support throughout my PhD here at Michigan. Mark and Nina are the most intelligent, well-respected, and caring people I've ever had the pleasure of knowing. They taught me how to be a better scientist, presenter, and colleague. Throughout my PhD, I've had doubts about my progress and accomplishments. However, Mark and Nina have taught me to have confidence in myself and even in those moments where I doubted myself, they always supported in me. Most importantly, their sense of humor has made these last six years a joy to work with them. Some people are lucky to get one advisor who has these qualities, but I was blessed to have two. I will always consider them my academic mom and dad. I know the lessons they have taught me I will carry for the rest of my career.

To my other committee members Professors Sunitha Nagrath, Betsy Foxman, and David Sherman, thank you for your useful advice throughout my dissertation. Professor Nagrath taught me in one of my first courses in graduate school and her course helped reignite my passion for microfluidics and biology. Her advice on microfluidics has been very helpful. Professor Foxman has provided so much insight in the microbiological aspect of my research during my prelim and data meeting. In addition, her advice in deciding my career path has been insightful. Professor Sherman and Dr. Michael Schoefield have been a wonderful collaborator in our tunicate work together. Their knowledge on solving this difficult topic and help providing tunicate samples were invaluable.

To my lab mates in the Burns and Lin Group, thank you for all your help throughout my PhD career. To the past Burns lab members Dr. Ji-hyang Park, Dr. Eric Livak-Hale, Dr. Jaesung Lee, Dr. Lavinia Li, Dr. Wen-chi Lin, Dr. Liang Zhang, and Ioana Nadra, thank you for all of your advice and guidance in all of my work. Ji-hyang was instrumental in starting the droplet co-cultivation project and without her training and advice, I would not even have a project. And to Eric, Jaesung, Wen-chi, and Liang who I've spent most of my PhD career with, I'd especially like to thank you for your friendship. To Lavinia, my classmate and office buddy, we have been through it all together and I can't imagine having somebody better to lean on for support. And a special thanks to Ki-Joo Sung for being the best undergraduate a graduate student could ask for. I'd like to thank the current Burns lab members Brian Johnson, Dr. Sarah Mena, Zach Pritchard, Martin de Beer, and Alyse Krausz for their support on my projects and the wonderful time we spent in lab and group meetings. Brian Johnson is the best resource any graduate student could ask for. He has provided everyone in our lab with so much technical support on experiment design and lab equipment he should have 6 PhDs by now. To the past Lin lab members Dr.

Jeremy Minty, Dr. Yu Chen, Dr. Fengming Lin, Dr. Alissa Kerner, Dr. Changkyu Byun, Dr. Mike Nelson, Dr. Chun Wan, Mathieu Rossion, Scott Mansfield thank you for all your support dealing with everything microbiology related. A big thank you to Mathieu and Scott for their helps with various projects I've worked on. To the current Lin lab members Scott Scholz, Tatyana Saleski, Corine Jackman, Adam Krieger, David Carruthers, and James Tan thank you for the times in lab working and sharing laughs together. Corine, your help and insight working with me on the microbiome projects have been wonderful. And James, thank you for taking the time to help me with the sequencing work in such a short timeline. I will greatly miss each of you and good luck on your future endeavors wherever it may take you. I hope our paths will cross again someday.

To Kelly Raickovich and Susan Hamlin, thank you for being wonderful administrators and making sure the graduate students were fed. To my undergraduate mentor, Dr. Arul Jayaraman, working in your lab during my undergraduate at Texas A&M University ignited my passion for microfluidics and microbiology. Thank you to all of the collaborators I've worked with: Professor Vincent Young, Professor Alex Rickard, Judy Opp, Derek Samarian, the staff at the LNF, sequencing cores at the University of Michigan and Sam Hunter at the University of Idaho. To the GradTONES members, singing with you guys has been a wonderful experience, but becoming friends with everyone has been even better. And a special thank you to Dr. Andrew Brouwer and Dr. Michael Brown for their friendship over the years. And to Lavinia and Zach, I'm glad to have found people to geek out over board games with.

I'd like to thank my family I'd like to say a special thank you. My parents are immigrants from China and without them, I would never have the opportunities afforded to me today. They worked so hard to ensure we'd have a better life in the US and sacrificed everything

to get here. From them I learned about the importance of hard work and perseverance to achieve my goals. To Amy, I'm so glad to call you my sister and I can't wait to see all you will accomplish in life. Finally, I'd like to thank Jad Khattab for his love, patience and support these last two years. Thank you for all you put up with and I can't wait to see what the future holds for us.

TABLE OF CONTENTS

LIST OF FIGURES

LIST OF TABLES

ABSTRACT

Bacteria are ubiquitous organisms that play a role in nearly every facet of life from health to the environment. A majority of bacteria live in synergistic communities but many of these bacteria have yet to be cultured and studied in the laboratory. The key to producing new drugs and treating incurable polymicrobial diseases may lie in these uncultured organisms. The objective of this dissertation is to develop a microdroplet platform for co-cultivation and characterization of mixed populations that will enable study of novel bacteria and interactions in microbial community.

Previously, our lab successfully developed a proof of concept droplet generation device for co-culturing *E. coli*. In this dissertation, we continue this work by developing microfluidic technologies to analyze droplets after cultivation. We first developed a device that can separate droplet content. Using streptavidin-functionalized beads, we bound targeted biotinylated microparticles in droplets. Then, using a pneumatically operated separation device, the series of posts in the device trap the beads while the remaining droplet content is removed. The bound targets can be re-encapsulated in a new droplet generated on-chip. We were able to achieve up to 98% purity and 100% yield using this device.

Next, we developed a device for separation and dispensing of single droplets. This device is a pneumatically operated two-layer device with a partially closed valve. We tested this device using *E. coli* cultures in droplets and subsequently amplified the DNA in each isolated droplet. We verified the fidelity of amplification by RT-PCR and whole genome sequencing and showed that the whole genome from each droplet dispensed was successfully amplified. Finally, we demonstrated multi-species amplification in droplets using *E. coli* and *P. putida* and verified with RT-PCR both genomes could be amplified regardless of composition.

Using this technology, we developed a platform for co-cultivation of human gut bacteria in droplets and used sequencing to elucidate interactions between cultured species. Droplets containing different initial cell numbers and media were incubated under anaerobic conditions. The droplets were then isolated individually for DNA amplification. After amplification, we sequenced the DNA and analyzed one meta-genome to determine functional relationships between two species in a droplet. We found complementary amino acid metabolism pathways for valine, leucine, isoleucine and lysine between the two species as well as differing glycan metabolic pathways in the two species.

This platform was re-adapted for cultivation of endosymbiotic bacteria in tunicate. We developed a methodology for extracting endosymbionts from tunicate cells and verified by T-RFLP analysis. Subsequently, the extracted bacteria were cultured in droplets using media from the host extract.

This dissertation demonstrates a microfluidic platform for stochastically decomposing complex microbial communities into manageable subsets for studying

bacterial interactions using co-cultivation and DNA sequence analysis. This is a powerful tool for high-throughput cultivation and analysis with small sample sizes. Using this platform, we can isolate, culture, and characterize specific interactions between bacteria within a microbial community providing insight that culture-independent metagenomic analysis cannot.

Chapter 1

Research Objective and Background

1.1 Microbial Communities

Bacteria are the most prevalent organisms on Earth. Some species have been well characterized and engineered for various applications such as production of biofuels and value commodities. A majority of these bacteria exist in microbial communities, defined as a multi-species assemblage where bacteria as well as fungi and archaea live in a contiguous environment and interact with one another [10]. In the human body, microbial communities exist in various body sites including the mouth, gut, skin, and urogenital regions [11]. In each of these various sites, species can vary greatly with each site having it's own unique community as seen in Figure 1.1 and collectively, these communities define the human microbiome through their complex interactions with the human body. In fact, the bacteria from the human microbiome outnumber human cells 1-to-1 [12] demonstrating just how prevalent bacteria are within the human body and how important they are to its function. Microbiomes are also unique to each person with a number of factors affecting the composition including lifestyle (e.g. diet and exercise),

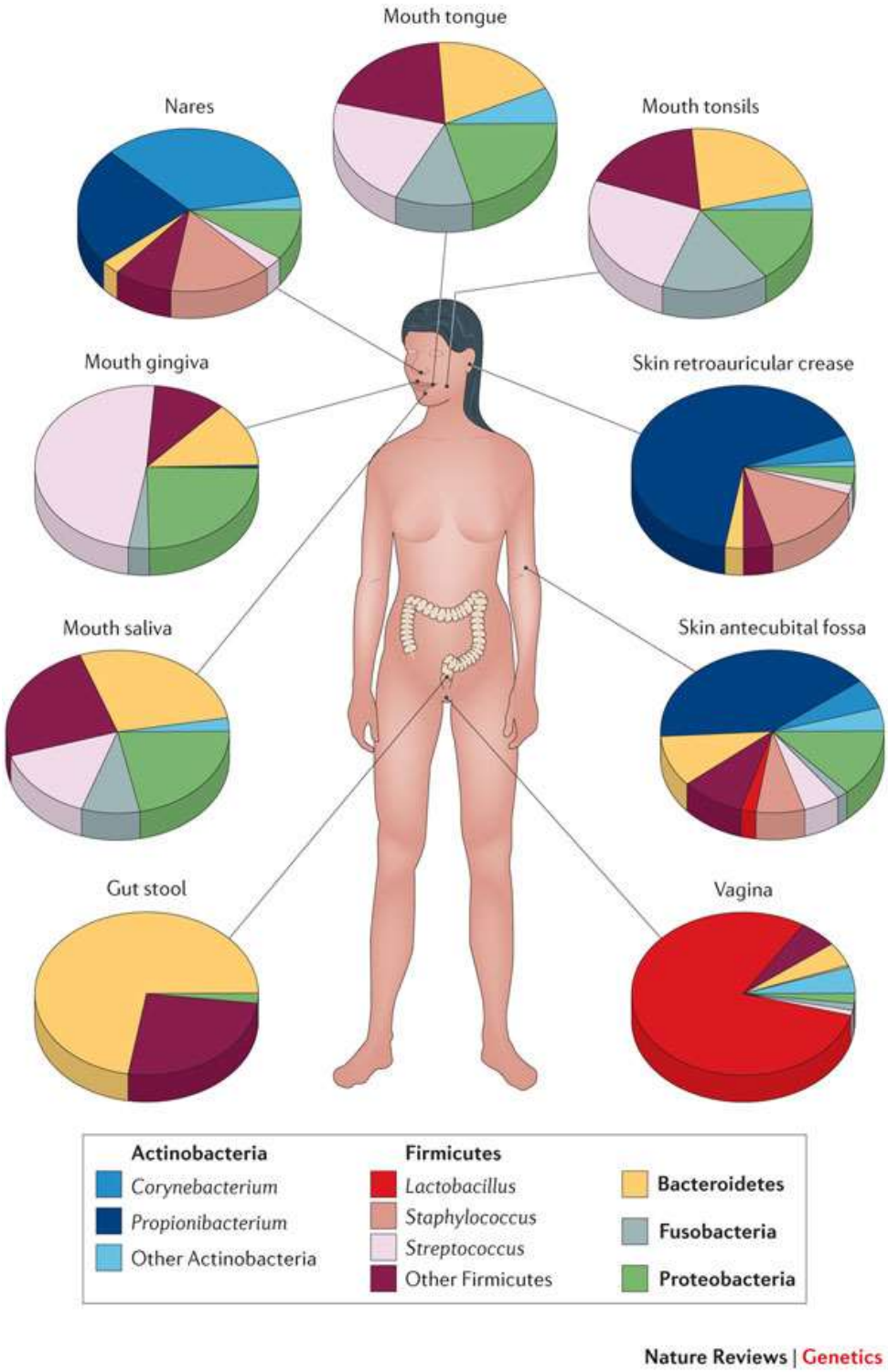

Figure 1.1: The locations of microbial communities typically found on the human body and the s compositions within each community. The microbial communities vary in function and diversity depending on the various body sites. Adapted from [3].

environmental exposures (e.g. place of residence or work), genetic factors, immune system, and disease (Figure 1.2). However, it has been estimated up to 99% of all the

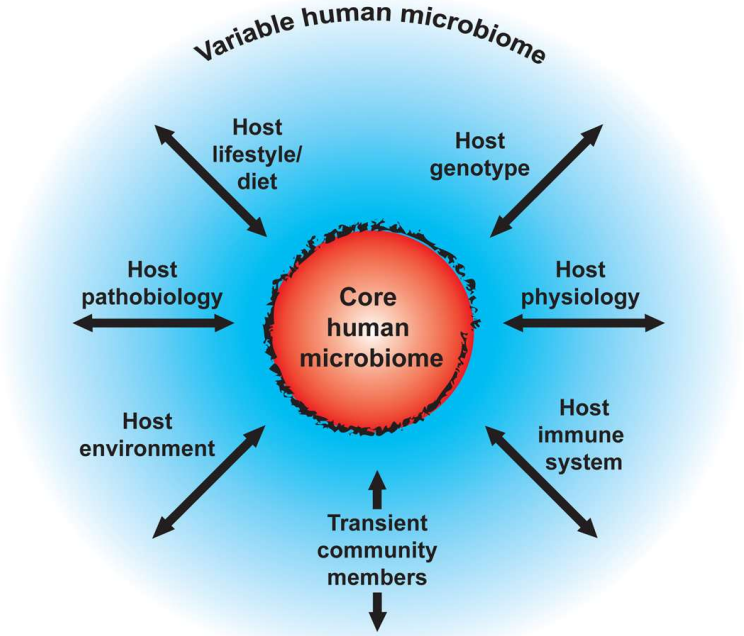

Figure 1.2: Examples of the various factors that affect a microbiome's composition. In some cases, the microbiome can affect these factors such as immunity and environment. Figure adapted from [4]

bacteria in the world have yet to be studied, let alone cultured in the laboratory [13-15]. These uncultured bacteria could be used to treat diseases, produce highly desirable chemicals, and clean up contamination in the environment. This is because these microbial communities are complex and not well understood due to the innumerable interspecies interactions [16]. These interactions can range from mutualistic to parasitic and everything in between [17]. Very few of bacteria that exist have been isolated and characterized and even fewer interactions between bacteria have been analyzed.

Studying and understanding these bacteria is paramount for future advancements in human health. As the number of antibiotic resistant bacteria continues to rise [18], new strategies must be developed to prevent this increasingly alarming phenomenon. Microbial community interactions in humans could be utilized to naturally fight these infections rather than using antibiotics that select for and proliferate these resistant

bacteria. Beyond this issue, microbial communities that are part of the human microbiome can potentially treat other diseases such as obesity and diabetes as previous studies have indicated a link between microbiome composition and these diseases. Understanding these microbial communities will allow us to understand the microbiome better, but we must be able culture and analyze the bacteria within the community. To do this, co-cultivation methods must be used to study these bacterial interactions within a community.

The barriers to culturing many unculturable bacteria include unknown nutrient requirements, culture bias [19], oxygen concentrations, and bacterial interactions. Obtaining site-specific media and controlling oxygen exposure to the bacteria can address the first few challenges. However, bacterial interactions pose a bigger challenge especially when dealing with more complex communities. Bacterial interactions are extremely important in understanding microbial communities, as these interactions are the basis for why these communities thrive where single species of bacteria might fail. As previous studies have indicated [20], biotic and abiotic stresses on bacteria such as invaders and lack of resources are better handled with more diversity within a community. Many species in the community might create niche roles for themselves, thus relying on other species for other vital functions. While these properties enable species to thrive in nature, isolation of individual species for further study in the laboratory is difficult as many species are unable to be cultured without it's necessary partners.

There is a need for laboratory techniques focused on co-cultivation but performed in a high-throughput manner. Challenges include the need to select specific species to

pair and the sheer number of possible pairings. Conventional laboratory culturing equipment such as flasks and 96-well plates are not sufficient when working with communities of hundreds of different species. Instead, modern microbiological techniques to study microbial communities focus primarily on DNA analysis detailed in the next section.

1.2 Microbial Community Analysis Techniques

Microbial community analysis has made significant progress over the last few decades with the advent of next generation sequencing technology [21,22]. Many traditional techniques are still useful for partial community analysis such as Polymerase Chain Reaction (PCR) (conventional or quantitative), Terminal Restriction Fragment Length Polymorphism (T-RFLP), and Fluorescence *in-situ* Hybridization (FISH). Whole community analysis methods such as whole genome sequencing, metagenomics [23], and metaproteomics [24] are more useful for whole community analysis and in-depth studies. See Figure 1.3 for a full list of analysis techniques.

PCR is a popular technique for partial community analysis because it is easy to use and results can be achieved quickly. Many techniques in PCR of microbial communities use the 16S rRNA gene, the workhorse of microbial community analysis [25], as it is a gene found in all bacteria consisting of many regions. Each region is either a conserved region (universal across all bacteria) or a variable region (different for each species) and these regions alternate to make up the 16S gene. In bacteria, there are 9 variable regions separated by conserved regions. Using this knowledge, microbiologists have devised various methods to identify community composition and individual species. One technique is identifying unique species by using the known variable region

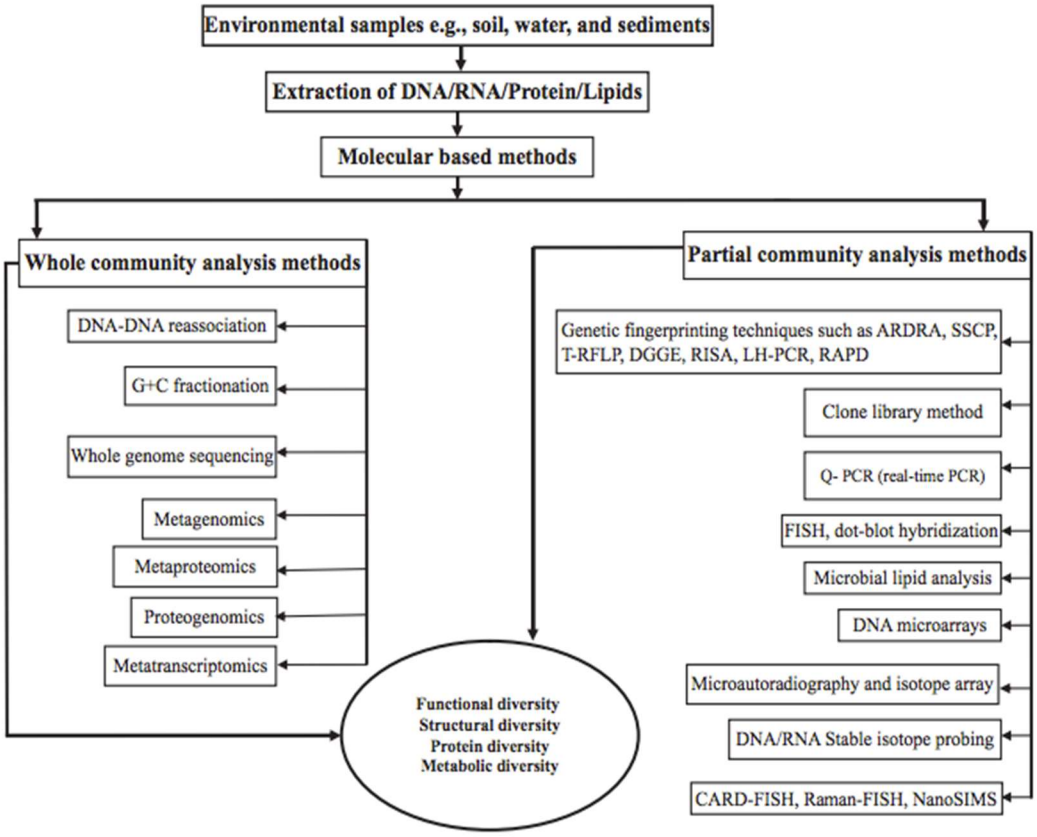

Figure 1.3: Chart demonstrating the two types of molecular analysis methods for microbial communities. Partial community methods are typically cheaper and faster to perform, but provide limited information about the community. Used for fingerprinting the community. Whole community methods take longer and cost more to perform, but provide more in-depth information. Adapted from[5]

sequences of the target. [26,27] During PCR, only the target's 16S sequence will be amplified. Sanger sequencing of the amplified DNA allows for target verification by comparing the amplified sequence to the target's sequence. Target specific PCR is only useful for partial analysis of specific species and only applicable for known 16S rDNA sequences. It cannot be used on a community to identify all species in the community. To characterize the number of species and abundance in a community, T-RFLP [28] is often used. In T-RFLP, the 16S rDNA of all species in a community is PCR amplified and fragmented by enzyme digestion. The fragment located at the beginning of the 16S is fluorescently tagged during amplification. Gel electrophoresis separates the fragments

and as each species will have a different length fragment, each fragment length represents a species in the sample. In addition, fluorescence intensity also quantifies abundance of each species. See Figure 1.4. T-RFLP does not identify species unless fragment length

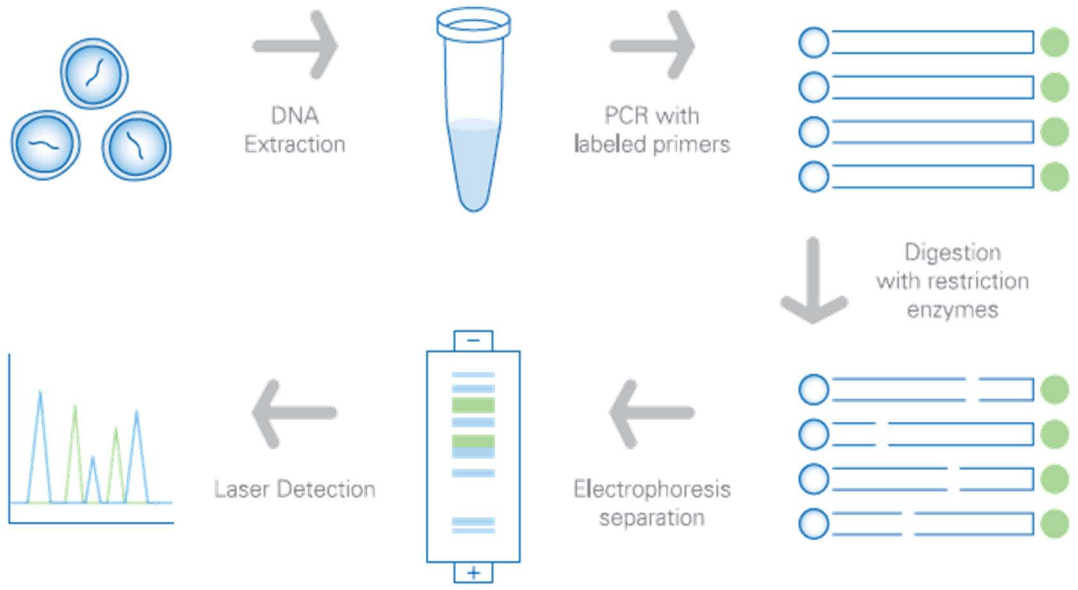

Figure 1.4: Flow diagram of the process of T-RFLP. The DNA is extracted from the all bacteria and PCR is performed to amplify the 16S gene. Primers targeting the conserved regions amplify the 16S of all bacteria and a fluorophore is attached to the forward primer. Enzyme digestion breaks down the 16S in pieces where each resulting fragment containing the adapter is detected after an electrophoresis separation. The resulting fragment length and fluorescent intensity approximates number of species and relative quantity. Adapted from [2]

for each species is known.

It is possible to study some communities when the number of species is low using PCR or T-RFLP, but many communities found in the human gut or mouth can contain up to a thousand species [29]. Whole genome sequencing allows for a better understanding of the functionality of the species within their genetic make-up. It will reveal relationships between different species in a community and allow us to understand what role each species plays. Sequencing technology from Roche©, Ion Torrent©, Pacific Biosciences©, and Illumina© have drastically altered the way microbial communities can

be analyzed. Sequencing can provide species number, abundance, and whole genomes. And as sequencing technology improves, it has become possible to study more diverse communities more accurately. A comparison of the current sequencing technologies is show in Figure 1.5. Sequencing technology still has many challenges such as incorrect reads, gaps, and sufficient read lengths [30] that can hinder accuracy of genome construction at low coverage. Cost and time are other barriers, as larger read numbers requires thousands of dollars and can require weeks to months including library preparation and data analysis. Finally, sequencing still fails to address features of the community such as cell morphology, spatial and temporal data, and interactions within a community. When looking at complex communities, it is difficult to identify interactions when looking at the enormous data sets generated through sequencing. One opportunity that addresses this issue is microfluidic technology, which can aid in isolating interactions within the community.

	Roche 454	IonTorrent PGM	Illumina	PacBio RSII[a]
Maximum read length (bp)	1200	400	300[b]	50,000
Output per run (Gb)	1	2	1000[c]	1
Amplification for library construction	Yes	Yes	Yes	No
Cost/Gb (USA Dollar)	$9538.46	$460.00	$29.30	$600
Error kind	Indel	Indel	Substitution	Indel
Error rate (%)	1	~1	~0.1	~13
Run time	20 h	7.3 h	6 days	2 h

Adapted from Glenn, T. 2014 NGS Field Guide—Table 2a—Run time, Reads, Yield|The Molecular Ecologist. Available online at: http://www.molecularecologist.com/next-gen-fieldguide-2014/ (Accessed Aug 17, 2015).
[a] P6-C4 chemistry.
[b] MiSeq read length.
[c] Illumina HiSeq 2500 Dual flowcell yield.

Figure 1.5: Comparison of different sequencing technologies currently on the market. Adapted from [6]

1.3 Droplet Microfluidics

Droplet microfluidics is the manipulation of discrete volumes of fluids in immiscible phases under laminar flow regimes. [31] Recently, droplet microfluidics has become powerful tool for studying biological systems because it provides two important functionalities: stochastic confinement and high-throughput analysis. Droplets in this dissertation are defined as discrete volumes generated by two immiscible phases. The continuous (outer) phase is oil and the discontinuous (inner) phase is aqueous. The mechanism by which these droplets form is the competing stresses created by the interfacial tension and viscosity difference. [32] The interfacial tension reduces the interfacial area while the viscous stress drags this interface downstream. The Capillary number, a dimensionless parameter, defines these two properties (interfacial and viscous stress) as show here:

$$Ca = \frac{\eta U_0}{\gamma} \tag{1}$$

where Ca is the capillary number, η is the dynamic viscosity, U_0 is the characteristic velocity, and γ is the interfacial tension. The Capillary number is the governing force on how droplets are generated. At low Capillary number ($Ca < 10^{-2}$), the interfacial forces are dominant and ratio of flowrates between the two phases governs the droplet formation. At high Capillary numbers ($Ca > 10^{-2}$), the viscous forces are dominant and the channel dimensions, channel geometries, and fluid flow properties control droplet formation. [33] There are three primary channel designs for droplet generation: co-flow, T-junction, and cross-flow.

When usedd in microfluidics, droplets are generated in a high-throughput manner to produce large quantities in short time frames (up to 1000 droplets/second). The ability

to generate large numbers of samples makes this a powerful tool for many biological applications such as PCR and cell cultures [34]. Current technology for PCR and culturing are limited by the equipment capacity (up to a few hundred simultaneous operations) and cannot achieve the throughput droplet microfluidics can. Furthermore, surfactant additions allow for multiple droplets to remain in contact with one another for extended periods of time allowing for bulk droplet storage for cell culturing [35,36]. Manipulation to perform analysis in droplets such as merging/reagent addition [37,38], splitting [39], and sorting [40] have been developed (Figure 1.6), collectively providing a powerful asset in studying systems like microbial communities.

1.4 Droplet Microfluidics for Microbiological Applications

Droplet microfluidics solves two of the biggest challenges facing microbiological studies: the ability to isolate single cells from a bulk sample into individual compartments and high-throughput culturing and analysis. This enables us to study bacterial interactions by partitioning complex communities into smaller subsets, addressing the challenge meta-genomic approaches faces with respect to communities being too complex to decipher interactions. Technologies beyond generation of these droplets allow for rapid downstream analysis. A comparison of some different approaches for culturing bacteria including droplet microfluidics is show in Figure 1.7.

The usage of droplet as micro-reactors for microbiology began in 1954 when Joshua Lederberg used mineral oil on glass slides to separate and compartmentalize bacteria in a sample. [41] Since then, droplet microfluidic applications for microbiology has rapidly expanded into applications for screening enzymatic activity [42,43], anti-bacterial susceptibility [44,45], and directed evolution [46,47].

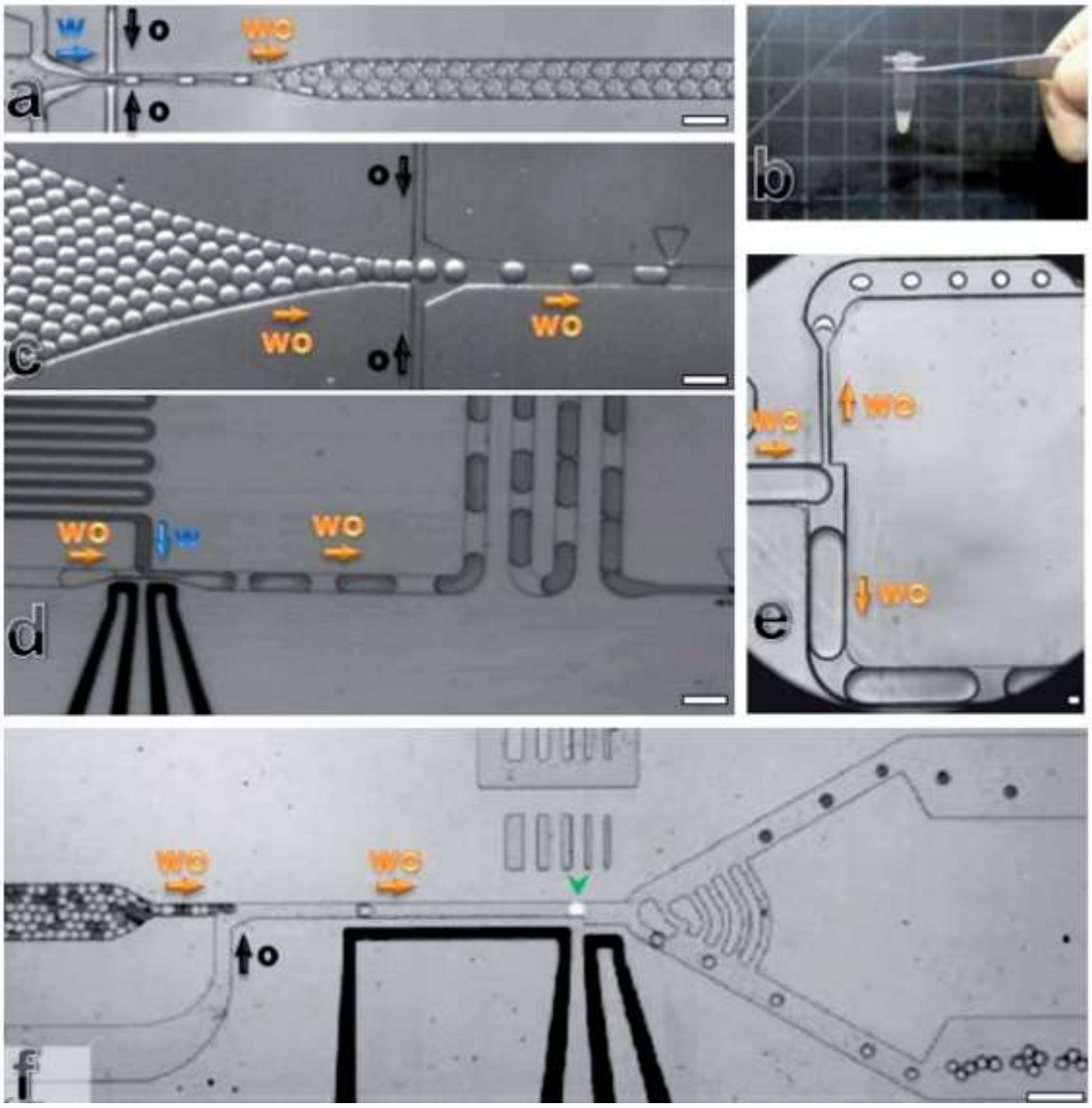

Figure 1.6: (a) Droplet generation on a flow focusing device (b) Bulk volume of droplets in a PCR tube (c) Device for reinjecting formed droplets into another microfluidic device (d) Reagent injection device for droplets (e) Droplet splitting device (f) Droplet sorting device based on fluorescence signal. Adapted from [4]

Additionally, droplet microfluidics for studying bacterial physiology and interactions has been demonstrated. Gordrian *et al.* were the first to demonstrate this technique using droplet plugs to isolate and culture single cells from an environmental soil sample. [48] Work by Park *et al.* used symbiotic *E. coli* strains to show bacterial interactions are observable in droplets (Figure 1.8a). [49] Additionally, Weitz *et al.* demonstrated the use of droplets for bacterial communication by diffusing signaling molecules from one droplet to another (Figure 1.8b). [50] Finally, Ma *et al.* utilize

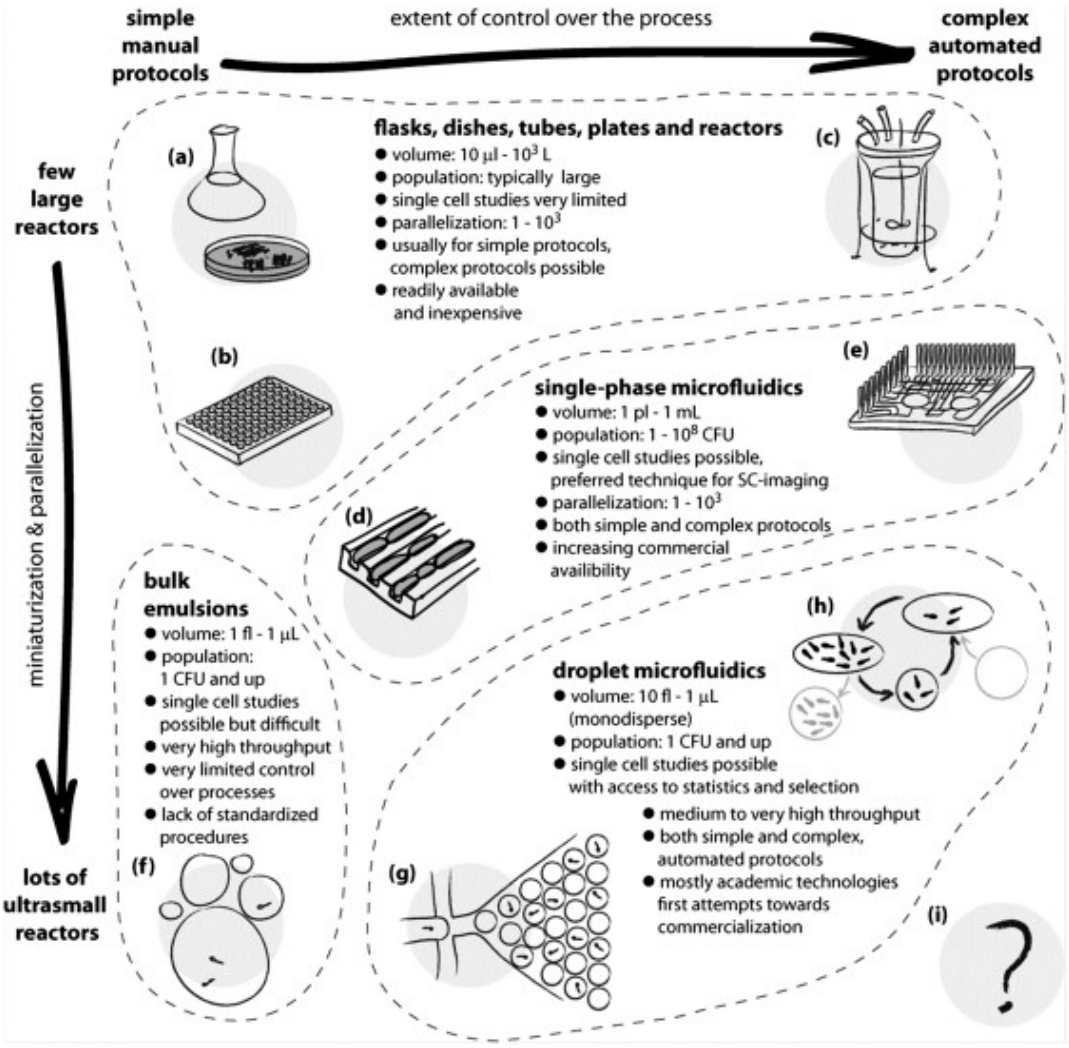

Figure 1.7: Different techniques for culturing bacteria. Droplet microfluidics offers both finee-tuned control and rapid parallelization. Future techniques could expand further with the addition of media exchange and higher throughput. Adapted from [6]

droplets to perform single cell culturing from the human gut and successfully isolated a previously unculturable bacterial species. [51] Droplet microfluidics offers an innovative way to approach studying microbial community. However, microfluidic technologies that allow us to manipulate these droplets after cultivation for analysis such as dispensing and content separation need to be developed. In this dissertation, we seek to address some of these needs.

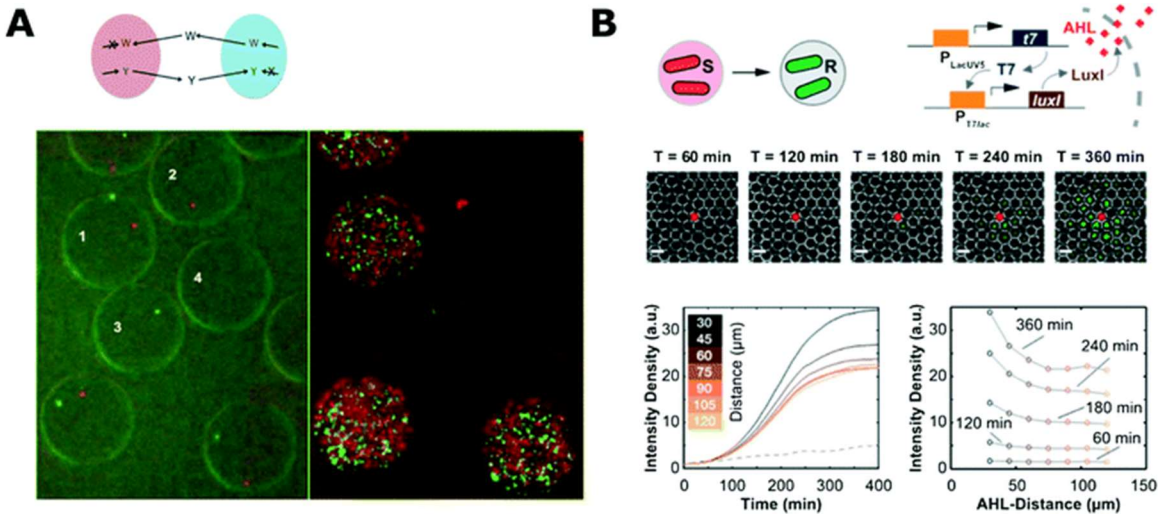

Figure 1.8: (a) Figure adapted from Park *et al.* demonstrating co-cultivation of symbiotic *E. coli* strains. [5] The two *E. coli* strains are auxotrophic with knockouts for Tryptophan (red fluorescence) and Tyrosine (green fluorescence) capable of cross-feeding the component the other is lacking. Droplets containing both species grew after incubation but droplets containing only one species do not grow. (b) Demonstration of bacterial communication using droplets (Weitz *et al.*). [13] Bacteria only fluoresce when AHL diffuses from a sender droplet to the recipient droplet containing the bacteria. Bacteria closer to the vicinity of the sender droplet receive higher concentrations, thus fluoresce more intensely than droplets further away.

1.5 Dissertation Overview

To advance the field of droplet microfluidics for cultivation and analysis of natural microbial communities, we first designed a microfluidic device for separation of droplet content by using surface functionalized beads in chapter 2. The device is pneumatically operated and has a series of posts capable of trapping beads of a desired size. These beads can capture a target by the streptavidin-biotin bond within a droplet. During device operation, the bead(s) bound to the target are trapped at the posts while the remaining droplet content is removed. Then, a new droplet can be generated in the device to recapture the bead(s) containing the target to complete the separation process. We demonstrated the efficacy of this device by separating biotinylated microparticles from non-biotinylated microparticles. Potential applications for this device include separation of desired targets within a droplet and removal of undesirable content.

In chapter 3, we continued device development by designing and fabricating a pneumatically operated droplet spacing device. The device is two layers with a partially closed valve that spaces and dispenses a bulk volume of droplets. We combined the device with Multiple Displacement Amplification (MDA) on *E. coli* bacteria after cultivation and dispensing to demonstrate whole genome amplification of low cell material from droplets. We further analyzed the resulting amplicon to determine fidelity and bias of amplification. This process was reapplied to multiple bacterial species for feasibility on microbial communities. This device was combined with co-cultivation and sequencing to develop a platform for studying microbial communities.

To demonstrate the droplet cultivation and analysis platform we have developed, we co-cultured bacteria from the gut obtained from human fecal samples in droplets in chapter 4. Using different media and cell concentration conditions, we successfully cultivated various species within each droplet. We isolated several droplets via spacing and dispensing and amplified the DNA via MDA. After some preliminary DNA analysis using T-RFLP and cluster analysis to screen for ideal samples, we performed whole genome sequencing. After sequencing analysis, we found some gene complementarity in amino acid metabolic pathways between two potential species in a droplet.

Finally, in chapter 5 we worked with the droplet microfluidic system to attempt culturing endosymbiotic bacteria found in tunicate, a marine animal in the Caribbean. First, techniques for extracting the bacteria from within the eukaryotic cells were developed. Using PCR and T-RFLP, we successfully identified the presence of the target within our extracted samples. We cultured the extracted bacteria in droplets and were able to culture a bacterial species. However, upon further analysis, we found the species

cultured was not the target. Ultimately, we developed a method for extracting and culturing endosymbiotic bacteria in droplets.

Chapter 2

Bead Mediated Separation of Droplet Content

2.1 Summary

Separation of components such as particles and cells in droplets is important and highly desired in droplet microfluidic assays. Bead-based microfluidic techniques offer an approach that uses the bead's solid surface to immobilize targets like particles or biological material. We demonstrate a bead-based technique for exchanging droplet content by separating fluorescent micro-particles in a microfluidic device. The device uses posts to filter surface-functionalized beads from a droplet and re-capture the filtered beads in a new droplet. With post spacing of 7 μm, beads above 10 μm had 100% capture efficiency. The efficiency of this system was determined using targeted particles that bind onto the functionalized beads and are, therefore, transferred from one solution to another in the device. The microfluidic device successfully separated the targeted particles from the non-targeted particles with up to 98% purity and 100% yield.

2.2 Introduction

Bead-based microfluidic technology has been used extensively in research in recent years for applications such as protein analysis [52,53], bacterial detection systems

This chapter was partially modified from a previously published work by *Wang et al*. [1]

[54,55], and other biological applications [56,57]. Bead-based microfluidic systems hold many advantages over conventional techniques including low reagent consumption, faster reaction times and high sensitivity [58]. These systems pair well with droplet microfluidics as droplet-based devices offer the same advantages and can be used for the same types of applications [34]. Previous papers have demonstrated the use of droplet microfluidics for PCR [59,60], cell growth, and cell sorting [40,49,61]. In these applications, droplets must remain intact and distinct from one another for long periods of time. To keep droplets separated requires the use of surfactants to decrease surface energy and prevent droplet merging [35]. However, difficulties arise when droplets need to be manipulated for further downstream analysis. In particular, techniques such as merging [37,38] and separation of droplet content become challenging since these actions require the manipulation of the droplet interface. Additional challenges to designing a viable method for these techniques include the need to maintain separate and distinct droplets after performing the manipulation.

Separating components in a droplet or moving a component from one droplet to another is a complex technique that is important in assays. The goal of the technique is to maintain a component or target in the droplet while removing the rest of the unwanted solute and solution, and the technique should ultimately be achieved in a high-throughput manner. State-of-the-art work in the segregation of droplet content focuses primarily on two areas: electrowetting on diodes (EWOD) and magnetic particles to separate droplet content. EWOD manipulates the effective droplet surface tension and wetting properties by an electric field [62,63]. Various techniques such as merging, splitting and separation have been demonstrated in previous works using this concept [64-66]. Techniques using

magnetic beads bind the target and separate them from the rest of droplet by a magnetic field generated on-chip. Works by Brouzes *et al*. and others focus on separating content by pulling magnetic beads in one direction while the rest of the droplet is split [67-70]. Another paper by Kim *et al.* demonstrates the separation by pulling the magnetic beads through a series of aqueous and oil phases separated by posts [71]. All of the above-described systems require fabrication or use of an electric or magnetic system on-chip. Some other works have demonstrated separation or enrichment using acoustic waves [72,73] or flow fields [74,75].

We fabricated a PDMS particle separation device that uses surface functionalized polystyrene beads to capture target particles capable of separating surfactant-stabilized droplets. Beads are trapped in a row of posts, and a new droplet is generated on-chip to re-encapsulate the trapped beads thus retaining the target particles. We determined optimal operating parameters and demonstrated successful capturing of the particles. Then we tested the capability of the bead's binding to the target particles. Finally, using our device and surface functionalized polystyrene beads, we demonstrated the exchange of droplet content during which targeted particles were retained whereas non-targeted particles were removed.

2.3 Materials and Methods

2.3.1 Materials

Beads for testing capture efficiency at the posts were 1.99 μm (Spherotech), 4.16 μm (Spherotech), 6 μm (Interfacial Dynamics Corporation), 7.32 μm (Bang Laboratories, Inc), 8.62 μm (Polysciences, Inc), 10.2 μm (Spherotech), 11.3 μm (Spherotech), and 16.2 μm (Spherotech) in average diameter.

In droplets experiments, the continuous oil phase was fluorocarbon oil (HFE-7500, 3M) containing 2% perfluoropolyether-polyethyleneglycol surfactant (RAN Biotechnologies). It was made with 10% stock solution through sonication and dilution into a 2% solution. The dispersed aqueous phase consists of 1X PBS (Fisher Scientific) with 0.05% Tween-20 (Sigma Aldrich) in the original and recaptured droplets. 14-17.9 μm diameter polystyrene beads functionalized with streptavidin (Spherotech) were used as the capturing beads. Pink fluorescent polystyrene particles with diameter range of 1.7-2.2 μm (Spherotech) were used as the target particle. Green fluorescent latex beads (Polysciences, Inc.) with diameter range of 1.7-2.2 μm were used as the non-target particle. Polydimethylsiloxane (PDMS) (Sylgard 184 Silicone Elastomer, Dow Corning), silicon wafers (Silicon Valley Microelectronics), and SU-8 (Microchem) were used for device fabrication.

2.3.2 Fabrication of PDMS Device

Photomasks were designed on L-Edit and made in the Lurie NanoFabrication Center at the University of Michigan. The SU-8 mold was made by negative etching on a silicon wafer. The silicon wafer was spin coated with SU-8 2035 at a thickness of 50 μm. The wafer was pre-baked at 65°C and then at 95°C. The wafer was then exposed and a post-exposure bake was performed at 95°C. After baking, the wafer was silanized with (tridecafluoro-1,1,2,2,-tetrahydrooctyl)-1-trichlorosilane using a desiccator. PDMS was poured on top of the SU-8 mold, vacuumed to remove air bubbles and heated to solidify the polymer. The devices were cut, punched with holes to create openings for the channels, and bonded on glass slides using plasma-activated bonding using a corona discharge wand.

2.3.3 Particle Binding to Beads

Streptavidin beads were mixed with pink fluorescent biotinylated particles, green fluorescent non-biotinylated particles, and a combination of both at various ratios in 100 µL of 1X PBS with 0.05% Tween-20. Beads and particles were incubated overnight in room temperature or on a Fisher Scientific vortexer mixer set to shake at a setting of 1 (300 rpm) in a micro-centrifuge tube. Beads and particles were centrifuged at 5,000 rpm on a centrifuge for one minute. Resuspension was performed using a vortexer set at max rotational speed (3200 rpm). Beads were separated from non-bound particles by a 5 µm filter. The beads were washed off the filter and resuspended in PBS. All counting of particles bound was done via microscopy by fluorescence to identify targeted and non-targeted particles.

Beads and particles were counted using a hemocytometer to determine their concentrations. They were then diluted to generate one streptavidin-functionalized bead and 25 mixed targeted and non-targeted particles per droplet. Droplets were generated on a flow-focusing PDMS droplet generation device. Droplets were collected using an Eppendorf tube that has tubing and a syringe connected to it. Droplets were incubated overnight at room temperature.

2.3.4 Droplet generation and device operation

The device was operated using pressurized air to flow the droplets and solutions in the channels. Droplets were introduced in the droplet inlet/collection channel by applying pressure to the syringe connection. There were three inlets connected to the pressure source by a syringe tip, tubing and syringe. The pressure was controlled by a voltage box, which regulates the pressure range between 0-5 psig. The voltage was

regulated using a LabVIEW program. Droplets previously generated were introduced by applying a pressure of 0.028 to the droplet inlet channel. A pressure of 0.016 psig was applied to the spacing oil channel and aqueous channel while flowing the droplet toward the post region. Once the bead has been captured, the pressure in the aqueous phase was increased to 0.020 psig to generate a plug. The pressure was decreased to 0.016 psig once the plug has been generated. The pressure was turned off once the plug has re-encapsulated the bead and the plug becomes the desired droplet size. Droplets that contain the retained beads and particles were taken out of the device through the droplet inlet. All counting of particles bound was done via microscopy by fluorescence to identify targeted and non-targeted particles.

2.4 Results and Discussion

2.4.1 Device Operation and Characterization

To perform the complete process of droplet separation, two steps are needed: separation of the target from the droplet and re-encapsulation of the target in a new droplet (Figure 2.1a). For the purposes of this chapter, droplets were generated on a separate device. The generated droplets contained beads and target micro-particles, which bind to the surface of the bead via streptavidin-biotin. Non-targeted micro-particles with no surface functionalization were used for the negative control. The microfluidic device has several features that were used to capture the beads, generate new droplets and recapture the beads. Droplets can be introduced from the inlet channel and become trapped at the posts located downstream of the main channel (Figure 2.1b). New droplets were generated in the channel labeled aqueous phase at the T-junction with the main channel. The beads that were trapped can be recaptured with the newly generated

droplets and removed from the device through the droplet inlet channel. The device operation process is summarized in Figure 2.2a-d. The images demonstrate the ability to transport and store an intact droplet out of the device for downstream analysis.

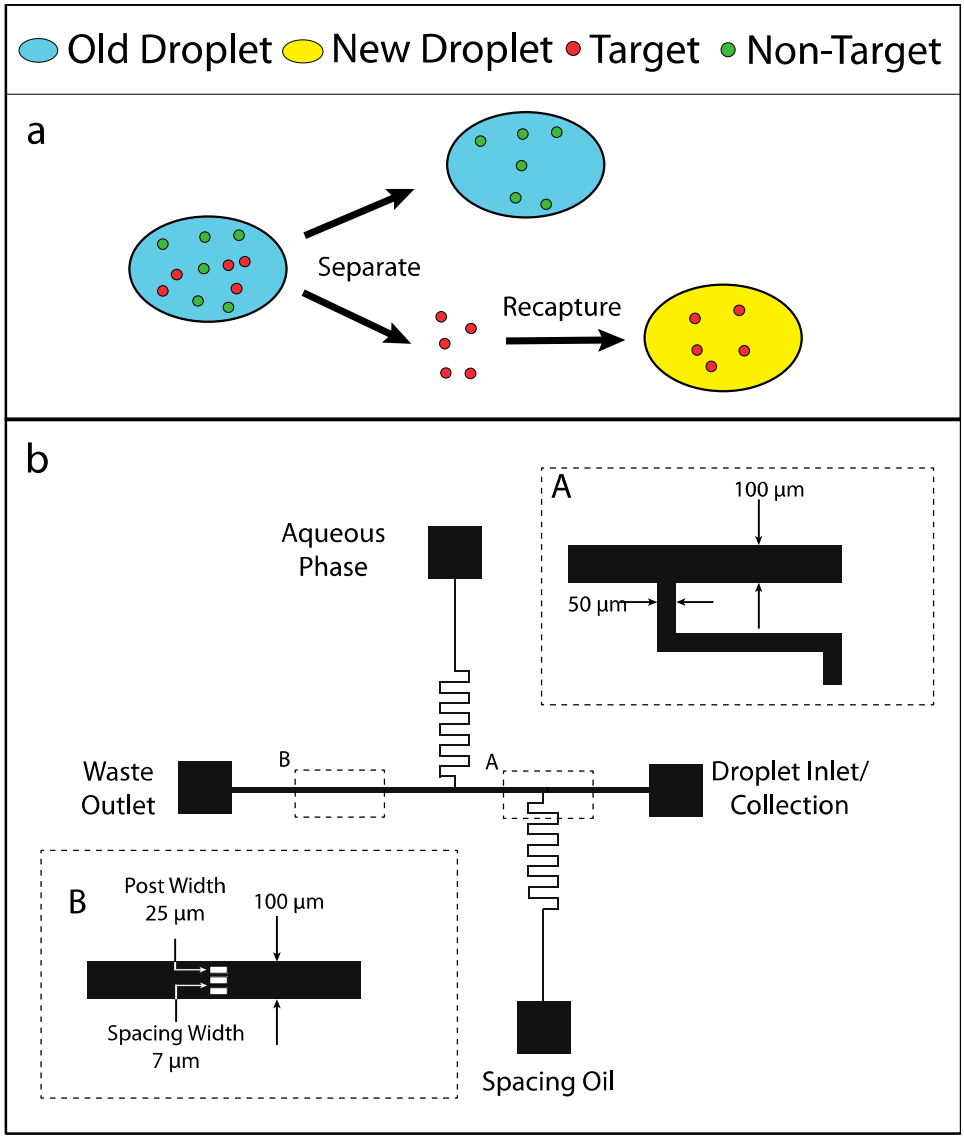

Figure 2.1: (a) Overall operation of separating a target in a droplet and recapturing the target in a new droplet. (b) Schematic of the device used for the droplet separation device. Zoomed in image A shows the dimensions of the main and side channels. Zoomed in image B shows dimensions of the posts for bead capturing.

Initially, the capture region of the device was designed with 6 µm gaps to maintain feasibility of fabrication while remaining viable for usage of different sized beads. However, the actual post spacing was measured to be between 7-8 µm due to

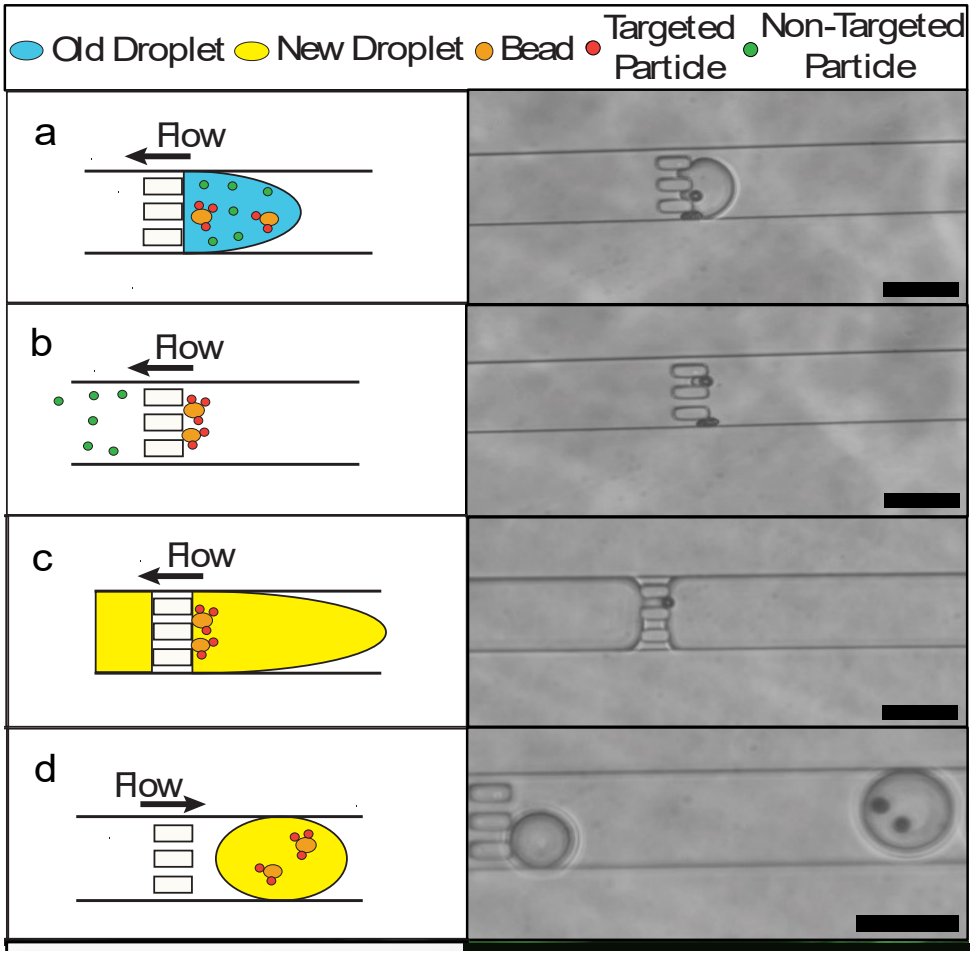

Figure 2.2: (a-b) Schematic and images shows process during bead capture and target separation. (c-d) Schematic and images shows process of bead re-encapsulation. Note for image that shows two beads that the beads were overlapped in the previous image.

deformation of the device during fabrication. The device is designed so that only a single droplet is moved to the posts, preventing multiple droplets from entering this region and/or merging into larger droplets. When a droplet reaches the posts, the resistance in the channel increases due to the surface tension of the droplet and the resulting resistance applied the post. The increase in resistance prevents subsequent droplets in the inlet reservoir from entering the channel. This phenomenon ensures that only a single droplet can be separated at any one time. To ensure that subsequent droplets do not enter the channel once a droplet has completely passed the posts, the pressure applied to the inlet is

adjusted. Note that, because the presence of the posts increases the fluidic resistance, pressure at the aqueous and spacing oil reservoirs also had to be increased slightly. In addition, 90-degree bends in the oil and aqueous channels increased resistance in those channels.

Accurate pressure settings are crucial for successful device operation. Laplace pressure required to push the droplet through the inlet was determined by the Young-Laplace equation:

$$\Delta P = \gamma \left(\frac{1}{R_1} + \frac{1}{R_2}\right) \cos\theta \qquad (2)$$

where ΔP is the Laplace pressure, γ is the surface tension of the oil with surfactant, R_1 and R_2 are the principle radii of curvature and θ is the contact angle. The droplet was assumed to have a spherical shape for the radii of curvature. The surface tension (~5 mN/m) of the oil with surfactant was determined from a paper by Brousseau et al. [76] that studies the effects of the surfactant FC-40's (similar perfluorinated surfactant) with HFE-7500 (same oil). Experimentally, the contact angle was observed to be approximately 60-70° before the droplet enters the post region. The Laplace pressure was calculated at least 0.210 psig. The experimental Laplace pressure needed to push the droplet through the post was 0.044 psig indicating a higher contact angle (approximately 86° in the post region). This difference could be a result of many factors including differences in shape at the post edges and dimensions of the post channels. New droplets were generated by calibration of pressures in the channels to ensure that the bead remains trapped on the posts while a new droplet is being generated. When the plug is being pushed through the posts, the final size can be manipulated by stopping the flow when the plug becomes the droplet of desired size. The total time of operation for the device is 3-4

minutes per droplet. To test the optimal bead range for capturing at the posts, beads ranging from 2 μm to 16 μm were introduced into the device's filtering region and the number of beads captured was counted manually via microscopy. The different sized particles will determine the minimum size at which all beads will be captured to ensure no beads are lost during the capture process. For device post spacing of 6 μm, beads of 6 and 7 μm diameters were captured at 10-20% efficiency (Figure 2.3). During the fabrication process, the posts were distorted due to the elastic nature of PDMS, which can deform the post spacing width that results in gap sizes greater than the designed size. Measurement of gap size by image analysis shows the constriction size can increase up to 8 μm. For bead with diameters greater than 10 microns, 100% of the beads were captured at the posts. For maximum capturing efficiency, beads to be captured should be

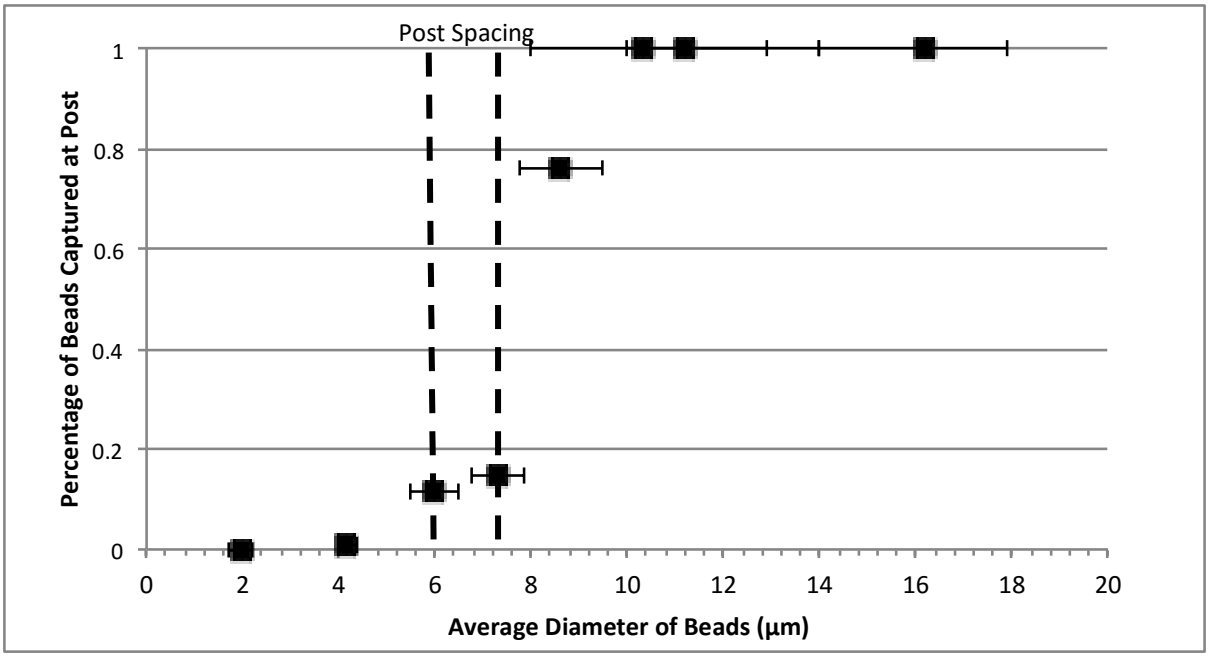

Figure 2.3: Percentage of beads captured between the post spacing with varying bead size. 100% trapping of the beads occurred with 10 μm diameter beads suggesting variance in bead size and deformation of posts affected trapping rate. Each bead size had a total of 150-200 beads to obtain data points of percentage of beads captured. Horizontal error bars denote standard deviation from average bead diameter obtained from manufacturer.

50% greater than the designed gap size.

2.4.2 Targeted Particle Binding to Functionalized Beads

To ensure efficient separation of targets from non-targets in droplets, optimal conditions for binding biotinylated particles to streptavidin-functionalized beads were determined. Polystyrene beads with streptavidin-functionalized surface were mixed with polystyrene particles with biotin-functionalized surface in the aqueous phase to determine the maximum extent to which they bind. For quantification, pink fluorescent biotinylated particles were the target and green fluorescent non-biotinylated particles were the non-target (Figure 2.4a-b).

There were several factors that influenced the binding of the target and non-target particles to the beads (Figure 2.4c). For particles successfully bound, increasing the ratio of biotinylated particles to streptavidin beads proportionally increased the number of particles bound. On average, no shaking during binding improves the number of particles bound most likely due to decreased shear between the particles. In addition, the absence of shaking causes the beads and particles to precipitate to the bottom of the tube and allows for extended contact between them. The low number of particles bound is likely due to the short lengths of the streptavidin and biotin molecules [32,33] and steric hindrance from the size of the particles [34,35]. Since the beads settle in layers, there is uneven exposure of the biotinylated particles to the streptavidin beads. This phenomenon accounts for the high variance of the number of particles bound to individual streptavidin beads.

Optimization of binding by changing incubation parameters led to increased binding capacity and high specific binding (>90%). A series of experiments revealed

conditions that would result in more particles bound while decreasing the variance (Figure 2.4d). In these experiments, both biotinylated and non-biotinylated fluorescent particles were used to determine the specificity. Using a rotator set at 60 rpm to increase contact time of particles to beads while still mixing the beads, the number of biotinylated particles bound increased by 33%, but the variance across beads remained high. Therefore, to increase contact between biotinylated particles and streptavidin beads while still maintaining uniform surface contact, beads were repeatedly centrifuged down into a pellet and re-suspended, binding increased fivefold using this technique and variance halved. The four and eight centrifugation/re-suspension techniques offered higher specificity (95-96%) than rotating at 60 rpm (86%).

2.4.3 Targeted Particle Separation

The distribution of targeted and non-targeted particles in each droplet is shown in Figure 2.5 for four conditions with a constant total number of beads and particles. Beads and particles encapsulated in surfactant-stabilized droplets follow the Poisson distribution. Under each condition, varying ratios of targeted vs. non-targeted particles were observed across different droplets. The average value was close to the expected ratio, indicating that the average number and ratio of particles and beads in each droplet can be manipulated effectively. The device described in Figure 2.2a was tested with targeted and non-targeted particles to determine the separation efficiency. The streptavidin beads could bind most targeted particles, as shown in Figure 2.6a. Experiments conducted to optimize particle-to-bead binding described in Figure 2.4b demonstrated that optimally, an average of 5-targeted particles could be bound onto a single streptavidin bead. This result was consistent with what was observed in droplets

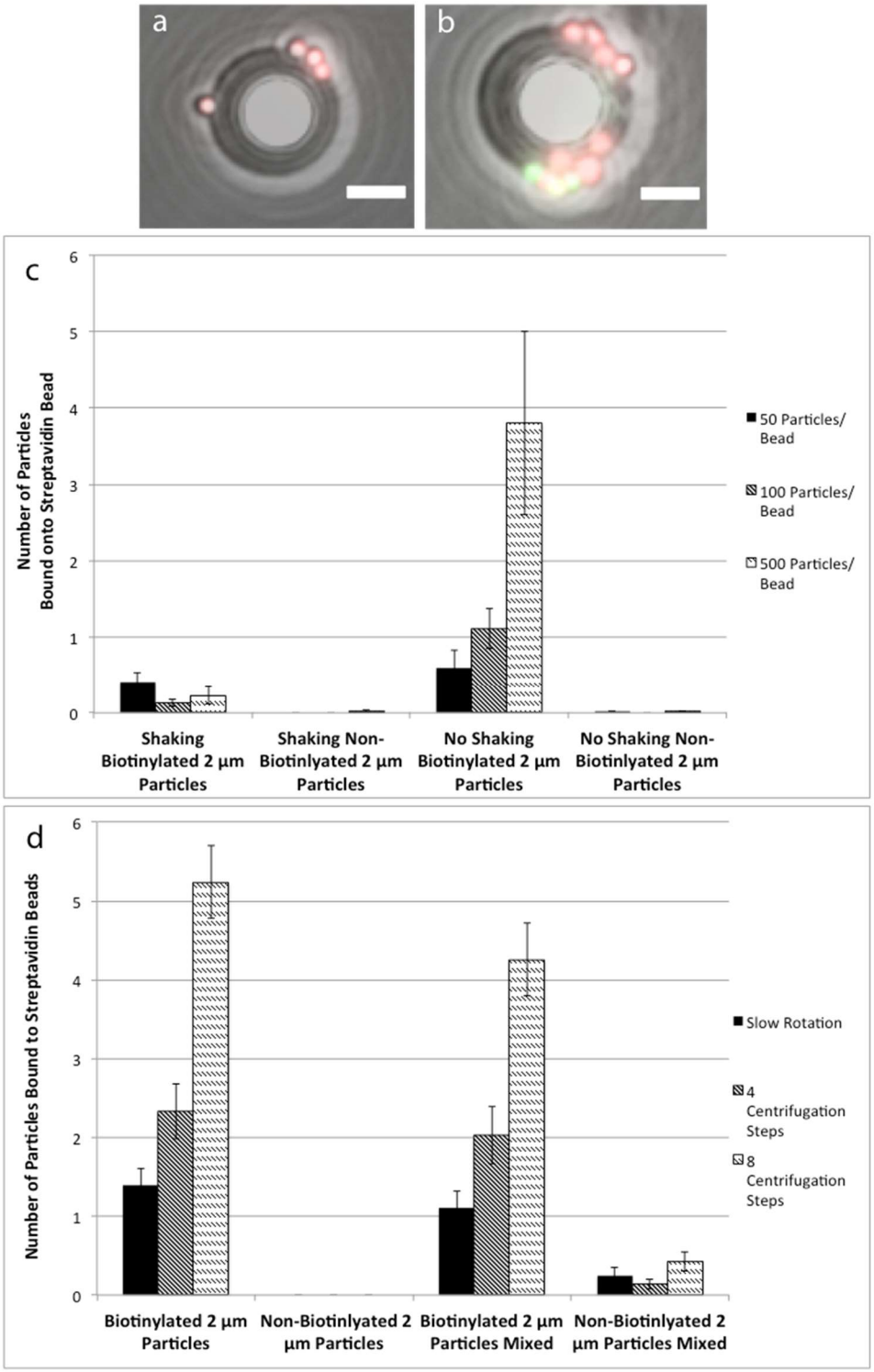

Figure 2.4: (a-b) Images of the targeted and non-targeted particles bound onto beads after filtration. Targeted particles fluoresce red and non-targeted particles fluoresce green. Scale bar is 8 µm. (c) Binding of particles to beads using streptavidin-biotin bond with shaking and no shaking conditions with varying ratios of particles to beads. Compared to a control with non-biotinylated particles. (d) Binding of particles to beads using different techniques to optimize binding. Trials included adding targeted and non-targeted particles together with beads to look at specificity. Trials performed at 100 particles per bead. All error bars denote standard error.

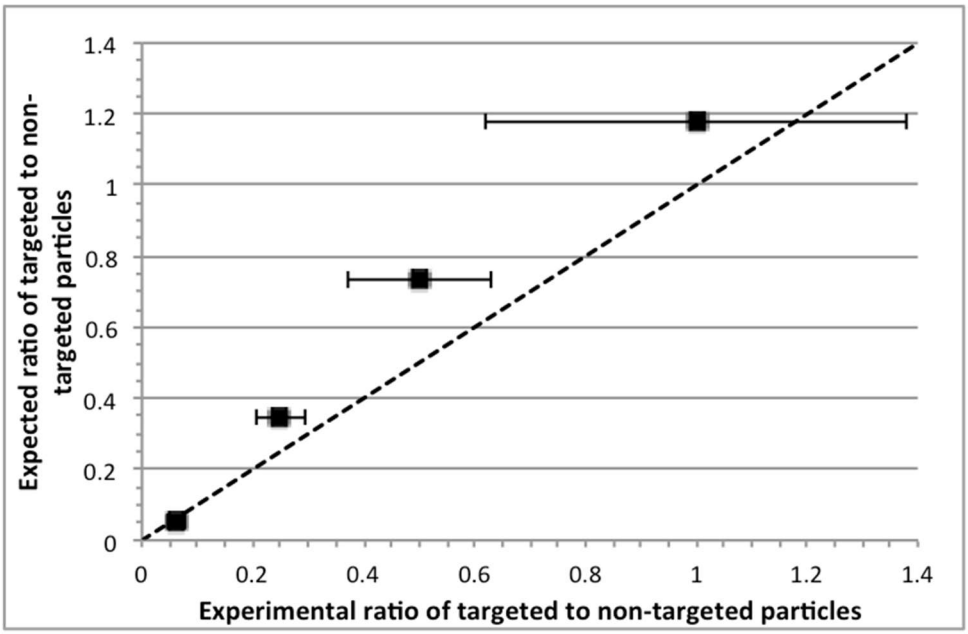

Figure 2.5: Distribution of targeted to non-targeted particles in droplets once generated. Dotted line indicates the calculated average ratio expected. Total number of beads in each droplet was set to 25. 22 droplets were used for each data point. All error bars are standard error.

as increasing the number of initial targeted particles resulted in a rough maximum equivalent to the 5-particle limit. To increase the number of target particles captured, the number of beads per droplet can be increased. We have successfully used up to 10 beads per droplet to capture particles, and have re-encapsulated all the beads. Overall, the system can specifically recover up to 98% of the targeted particles in droplets. Note that, for non-targeted particles, less than 10% of the particles bound to streptavidin beads (Figure 2.6b). Even with non-specific binding, it was shown that the re-encapsulation process could remove many of the non-specifically bound non-targeted particles. In principle, it is possible to remove essentially all the non-specifically bound non-targets by applying the washing procedure multiple times to a droplet.

To define the efficiency of the system, two metrics were used: specific recovery and specific yield.

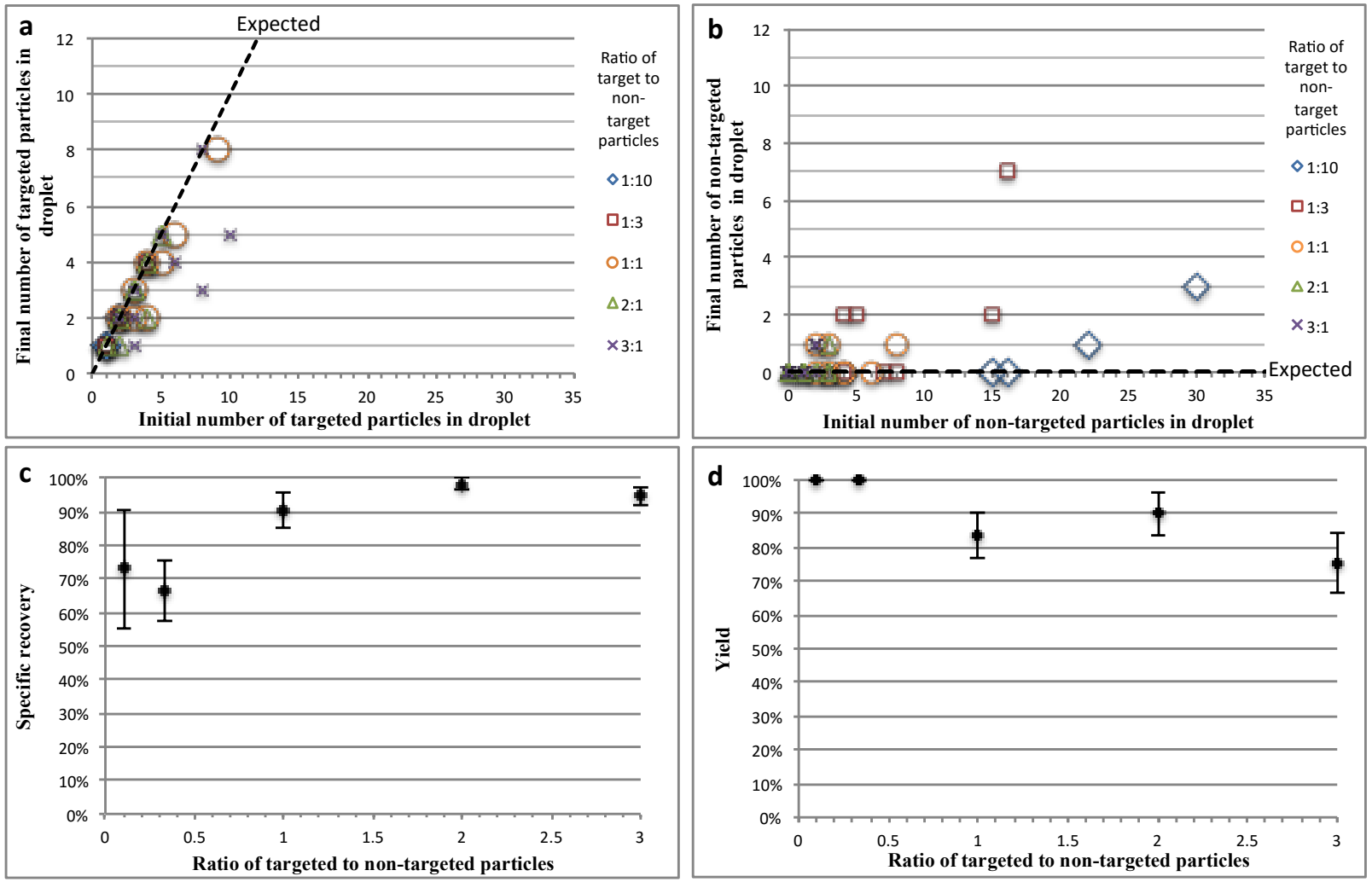

Figure 2.6: (a) Number of the targeted particles bound onto the streptavidin beads. (b) Number of the non-targeted particles bound onto the streptavidin beads. All ratios shown are ratio of targeted to non-targeted particles in individual droplets. (c) Specificity of binding the target particles to the streptavidin beads. Specific recovery determined by final number of targeted particles bound compared to the total number of particles bound. (d) Yield of the number of targeted particles bound to streptavidin beads. Yield determined by the final number of targeted particles bound compared to the initial number of targeted particles in the droplet. A total of ten droplets were separated for replicates. All errors bars denote standard error.

`

$$Specific\ Yield = \frac{Number\ of\ Targeted\ Microparticles\ Bound\ After\ Separation}{Number\ of\ Targeted\ Microparticles\ in\ Droplet\ Before\ Separation} \quad (2)$$

$$Specific\ Recovery = \frac{Number\ of\ Targeted\ Microparticles\ Bound\ After\ Separation}{Number\ of\ Total\ Microparticles\ Bound\ After\ Separation} \quad (3)$$

As shown in Figure 6c, the specific recovery of targeted particles approached 100% for higher ratios of targeted to non-targeted particles. However, the yield decreased at these higher ratios (Figure 6d). This is an expected trend, as higher number targeted particles will result in saturation of the binding sites on the beads, and the total number of beads per particle can be adjusted depending on the application. Also, the lower specificity at lower target to non-target ratios can be improved using multiple separation and recovery steps.

2.5 Conclusion

We have demonstrated a pneumatically operated device capable of separating targets from non-targets in a droplet. We determined optimum parameters for the device and beads and demonstrated successful binding of the target both on-and off-chip. We demonstrated successful operation of the device and characterized the separation efficiency. Using streptavidin surface-functionalized particles, we could capture up to 100% of the biotinylated particles under certain conditions. The operation requires no external magnetic or electrical fields for performing the washing process. This reduces the cost of fabrication and operation of the device by only requiring pneumatic lines. Without the need for magnetic particles, a wide variety of bead materials and surface-chemistry can be used increasing the versatility.

`

Chapter 3

Droplet Microbial Cultivation and Multiple Displacement Amplification

3.1 Summary

Droplet microfluidics is a powerful tool owing to its ability to create many discrete samples while consuming very little material. Once generated, droplets are pooled but due to each droplet's volume, isolating single droplets becomes a challenging task. Even after isolation, the amount of material, such as DNA, that can be extracted from the droplets is often not sufficient for analytical techniques such as sequencing. We demonstrate a pneumatic, partially closed valve device capable of spacing and dispensing single droplets from a large pool. We could achieve up to 83% accuracy in dispensing a single droplet. Once dispensed, we successfully amplified the genomic DNA from *E. coli* cells cultured in a single droplet via Multiple Displacement Amplification (MDA). We verified the fidelity of the amplified genome by RT-PCR and whole genome sequencing. We also amplified DNA from droplets containing two species of bacteria and used RT-PCR to confirm that both genomes were amplified by MDA. Our platform

`

is a simple microfluidic device capable of isolating single droplets for downstream DNA amplification and analysis.

3.2 Introduction

Droplet microfluidic technology has become a powerful tool for many biotechnology applications. The inherent small volumes (femto – picoliter) for each droplet-contained reaction as well as the ability to keep samples intact and distinct make this technology highly desirable for many applications that require small sample volumes and high-throughput operation. [34] However, the small volumes associated with droplet microfluidics can hinder downstream analysis and handling in approaches that require larger volumes (micro – milliliters), such as next generation sequencing and scale-up of cell cultures. In addition, droplet generation results in large pools of droplets that make isolating single droplets extremely difficult to accomplish.

Technologies in droplets microfluidics have been developed to accomplish generation [77], merging [37,38], and sorting [78,79]. In operations like merging and sorting, magnetic fields or piezoelectric systems are used. These techniques have been used for high-throughput operations but they can be challenging to fabricate as well as operate. Alternatively, pneumatic systems are easier to fabricate and operate for single droplet isolation systems requiring less than 1000 operations per minute.

Dispensing of single droplets from a single solution has been well studied, and publications have primarily focused on using electrowetting-on-dielectrics (EWOD) to manipulate the droplet. [80-83] While variations and new technologies on EWOD have allowed droplet dispensing to become more high-throughput, [84,85] taking a pool of

`

already generated droplets and dispensing single droplets has not been well developed. The majority of research in droplet spacing and dispensing is primarily focused on devices for droplet sorting with spacing and dispensing incorporated to achieve the sorting technology. [78,86,87] Brouzes *et al*. did demonstrate this spacing process using a multi-valve design with normally closed valves that allows for multiple droplets to be dispensed simultaneously. [88] However, few works have explored spacing devices purely for dispensing single droplets for downstream applications.

Many applications in droplet microfluidics utilize cell culturing [49,61,89] and DNA analysis [59,90]. However, downstream applications involving analyzing cell cultures by DNA often require nanograms to micrograms of DNA. One *E. coli* cell provides 6.9 femtograms of DNA [91], which makes cells from a single droplet very difficult to analyze as most droplets contain at maximum a few thousand cells. Thus, techniques to amplify the DNA from a single droplet are highly desirable. Many DNA amplification techniques exist such as Multiple Displacement Amplification (MDA) [92], Multiple Annealing and Looping Base Amplification Cycles (MALBAC) [93], and Picoplex© single cell Whole Genome Amplification (WGA) [94]. These methods have been previously compared [95] and we chose to use MDA for our system because it is user-friendly and provides a large quantity of DNA [96].

MDA utilizes a unique polymerase called Φ29, which easily and rapidly amplifies an entire genome by using random hexamers to initiate the amplification (Figure 3.1). MDA is able to generate 1-2 μg of DNA from a single cell with genome coverage up to 99% [97]. The ability to generate a large quantity of DNA is useful in many applications where limited DNA quantity restricts analysis that can be conducted. MDA has been

`

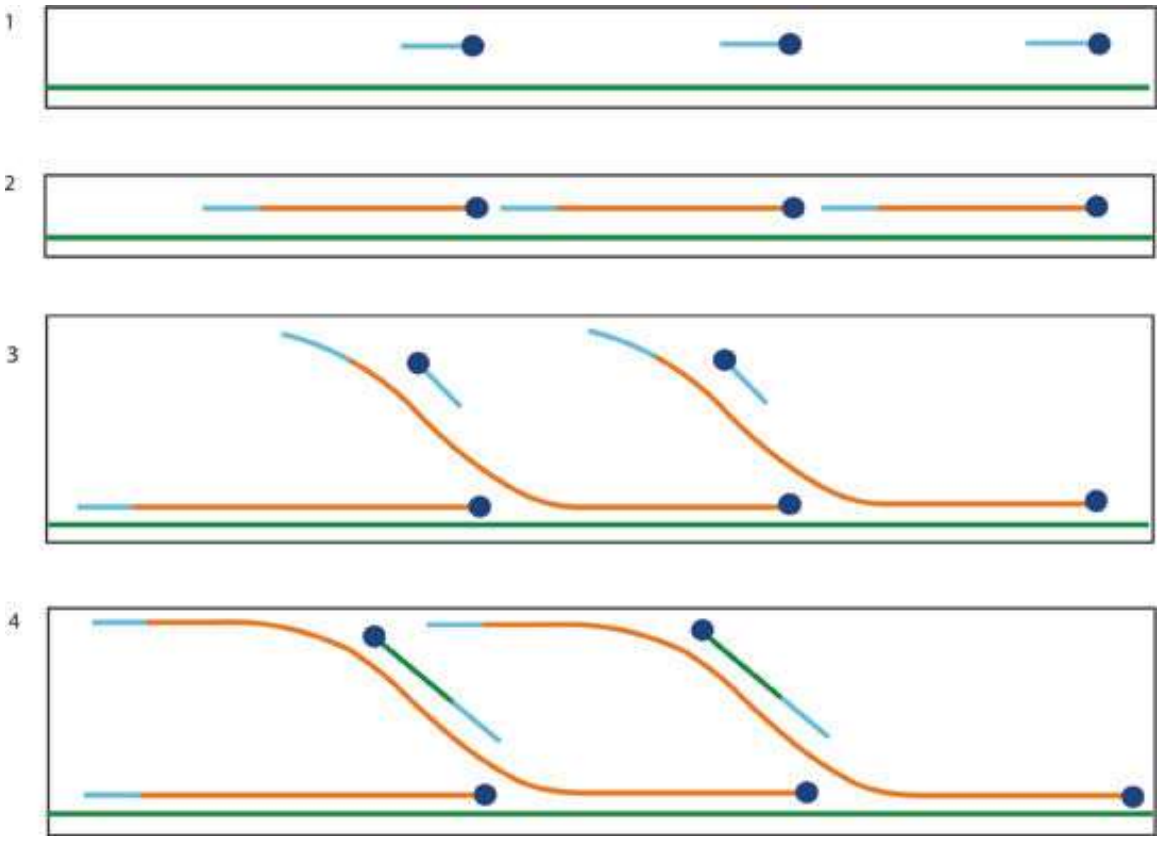

Figure 3.1: Illustration of MDA for DNA amplification. The blue dot (Phi29 polymerase) with a random hexamers (blue line) is bound to the DNA (green line). The polymerase replicates the DNA (orange line) until it reaches the next replicating strand. Another polymerase with hexamers attaches to the extending strand and replicates that strand. This creates a hyper branched structure and results a large amount of DNA amplified from a small initial template.

used to amplify the human genome [98], a single bacterium [99], and microbial communities [100,101]. A major drawback to using MDA is amplification bias whereupon certain regions of the genome are over- and under-amplified caused by preferential priming of specific sequences [102] potentially compromising quantitative analysis [103]. Previous work to reduce this bias have used digital droplet MDA (ddMDA). [102,104,105] In ddMDA, fragments of the genome are separated and encapsulated in droplets to create isolated MDA reactions. The droplets can then be re-pooled and analyzed by sequencing. Other works in microfluidic MDA have used microarrays [106], liquid dispensing [107] or chambers [108] to achieve MDA on small

`

volumes. Our platform differs by using the droplets for cultivation such that MDA is performed downstream on a single droplet containing the cells.

In this chapter, we demonstrate a simple pneumatically operated droplet spacing and dispensing device that separates single droplets from a pool. Our device is capable of spacing droplets at an intermediate throughput. We use this technology to amplify the genome of *E. coli* and verify fidelity of the amplified genome by RT-PCR and whole genome sequencing. In addition, we show successful MDA amplification of genomes from different species in a single droplet.

3.3 Materials and Methods

3.3.1 Droplet Spacing Device Fabrication and Preparation

The photo-mask was designed on L-Edit software and made on a soda-lime glass mask with chrome. SU-8 was spun on a silicon wafer at a height of 50 μm, pre-baked and exposed on the photo-mask. A post-exposure bake was performed, and the SU-8 was then etched to produce the mold for the device. The main device was comprised of poly(dimethylsiloxane) (PDMS) (Sylgard 184). The valve (top) and channel (bottom) layers of the PDMS device were made with a mixture of 10:1 monomer to curing agent. The PDMS was poured on top of the mold and degassed under vacuum to remove air bubbles. The PDMS was solidified by heating at 85 °C. The devices were cut out and holes are punched on the channel layer to make the outlet of the device. The membrane between the valve and channel layer was comprised of PDMS at a ratio of 15:1. The PDMS was degassed, poured on a glass wafer, and spun at 1000 RPM until the thickness of the membrane is 50 μm.[109] The membrane was then heated to 85 °C for 15 minutes to set. The valve layer was bonded to the membrane by oxygen plasma. The outlets for

`

the channel layer were punched out of the bonded device and the two layers were aligned by microscopy. The channel layer was bonded to the other side of the membrane by oxygen plasma.

The Teflon tubing (Cole-Parmer) used to transfer the spaced droplets was treated with Rain-X© by flushing the tubing with Rain-X© solution followed by HFE-7500 (3M) oil. The tube was dried by pushing air through the tubing and allowing it to air-dry overnight.

3.3.2 Microbial Culture

Escherichia coli cells were cultured overnight in LB media at 37 °C for the initial inoculation in droplets. The cells were counted on a hemocytometer and diluted with LB media to an average of 5 cells per droplet (λ=5). Droplets were generated on a PDMS device using HFE-7500 oil with 2% perfluoro-surfactant (RAN Biotechnology) and stored in a micro-centrifuge tube. The droplets containing *E. coli* cells were then cultured overnight at 37 °C.

For the co-culture samples, *Escherichia coli* and *Pseudomonas putida* cells were cultured overnight in LB media at 37 °C for the initial inoculation in droplets. The cells were counted on a hemocytometer and diluted with M9 minimal media to an average of 2 cells per droplet (λ=5). The two diluted cell cultures were then mixed together and droplets were generated in a separate PDMS device. The droplets were stored in both micro-centrifuge tubes and INCYTO C-Chip disposable hemocytometer cultured at 30 °C. Growth was monitored periodically in the C-Chips and the droplets used for the MDA experiments were taken out of the droplets cultured in the micro-centrifuge tubes.

`

3.3.3 Droplet Spacing Operation

Droplets were stored in specially designed 1.5 *mL* micro-centrifuge tube containing two ports housing Teflon tubing and a syringe tip. The droplets were transferred from the micro-centrifuge tube to the device via Teflon tubing by applying pressure with a syringe tip connected to the micro-centrifuge tube. Droplets were introduced into the device and held at the junction by flowing spacing oil while the valve was closed. Initial operation required trial and error testing to determine optimum pressure settings in the droplet and spacing oil channels. After the device reached steady state, 300-µm diameter Teflon tubing was inserted into the outlet channel. Opening the valve and subsequently closing once a single droplet has been released. The device was operated at this state for 1 minute to ensure the droplet had traveled through the entirety of the tubing. The Teflon tubing was then attached to a micro-centrifuge tube and the droplet was collected. Total operating time for dispensing a single droplet was 90 seconds.

3.3.4 Multiple Displacement Amplification

Surfactant destabilizer (3 µl) was added to each droplet in each tube. Phosphate buffered saline (PBS) (4 µl) was added to each tube allowing the aqueous phase containing the bacteria to merge with the solution. Subsequently, the cell lysis solution (4 µl) was added. After a 15-minute incubation period at 65 °C and the addition of a stopping solution (3 µl), the MDA reaction mixture was added to the aqueous phase and the reaction was allowed to proceed for 8 hours at 30 °C. The polymerase was deactivated by heating the solution to 65 °C. The amplified DNA was collected from the

`

mixture by pipetting out the aqueous phase. Refer to the Qiagen Single Cell Repli-G kit for the complete protocol.

3.3.5 RT-PCR Analysis

RT-PCR was performed on seven sites targeting various genes on the *E. coli* genome. These genes are *gadA, rfaJ, fimI, fabA, rpoD, hrpA, and yfgO*. Primer sequences are listed in Table 3.1. Relative concentration was determined by using extracted *E. coli* DNA for developing the standard curve. The extracted genomic DNA was measured via Nanodrop and diluted 10-fold five times sequentially. 5 µL of the DNA from each dilution was added to the RT-PCR tube along with a mixture of 1 µL each of the forward and reverse primers, 4 µL of DNAse/RNAse free water, and 10 µL of SYBR Green RT-PCR solution. The thermocycler was set for a denaturing step at 95°C, annealing at 55°C, and extension at 72°C.

The Ct value was calculated by the RT-PCR program and plotted on a semi-logarithmic scale against the concentration obtained from the Nanodrop. Ct values from the MDA reactions were then interpolated by using the standard curve plot to determine the relative DNA amount. For two species RT-PCR, *gadA* and *rfaJ* gene primers were used to identify *E. coli* and *benA* and *benR* gene primers are used to identify *P. putida*. Primer sequences for the *benA* and *benR* genes are listed in Table 2. Standards curves for the *P. putida* primers were developed similarly to the *E. coli* primers.

3.3.6 Whole Genome Sequencing

Following whole genome amplification, samples were delivered to the University of Idaho IBEST Genomics Resources Core (GRC) facility. GRC staff prepared barcoded Illumina libraries using the IntegenX Apollo 324 PrepX ILM DNA Library kit and

`

custom Illumina compatible BioScientific barcoded adapters. Libraries were amplified with the KAPA library amplification kit, quality controlled on the Advanced Analytical Fragment Analyzer, quantified using the Kapa Illumina library quantification kit, and then sequenced on the Illumina MiSeq using the v3 600 cycle protocol.

Sequenced reads were demultiplexed using bcl2fastq v2.17.1.14, PCR duplicates were removed with Super-Deduper (http://github.com/dstreett/Super-Deduper), overlapped with FLASH2, "-t 20 -m 20 -M 600 -x .05" (available from https://github.com/dstreett/FLASH2, and modified from Magoc and Salzberg [110]), and trimmed for quality using Sickle "-l 200 -q 30 -t sanger"[111]. Cleaned reads were then mapped against the E. coli MG1655 (NC_000913) reference using Bowtie2 with default parameters [112]. Mapping depth was calculated from the resulting BAM files using SAMtools v1.3 [113], and was analyzed and plotted using the R statistical language [114].

3.3.7 RT-PCR on Droplets

E. coli and *P. putida* were inoculated in LB media overnight at 37°C in a rotating incubator. The cultures were diluted to 1000X with DI water and counted on a hemocytometer for determine cell number. For direct RT-PCR on cells verification, the cells were diluted 6 times by a factor of 10. 4 µL of the 10^4, 10^5, 10^6, 10^7 dilutions were put into RT-PCR tubes. RT-PCR steps were performed as described in section 3.3.5. For the standard curve with the addition of the oil and surfactant, 10 µL of the HFE-7500 oil containing 2% surfactant was added to a tube. Then, 4 µL of the aqueous phase was added on top and another 12 µL of water is added. 5 µL of the destabilizer was added and the tubes were centrifuged at 13,000 RPM for 10 seconds. The tubes were incubated

`

at 95°C for 10 minutes for lysis. Then, 8 µL of the aqueous phase was extracted and used for RT-PCR.

For singe droplet RT-PCR, surfactant destabilizer (5 µl) was added to each droplet in each tube after dispensing from the device. Images from each droplet were taken prior to dispensing. DNAse/RNAse free water (12 µl) was added to each tube followed by centrifugation at 13,000 RPM. Then, 8 µL of the aqueous phase was extracted and used for RT-PCR.

3.4 Results and Discussion

3.4.1 Droplet Analysis Platform

Separation of droplet cultured bacteria into individual containers e.g. well plates and tubes were achieved by using a microfluidic device described below. Figure 3.2 depicts the workflow of the single droplet isolation and DNA amplification for analysis. Initially, bacteria can be encapsulated at various numbers in droplets. Adjusting the concentration of the cells can control the number of cells in each droplet. The number of cells in each droplet is distributed based on a Poisson distribution. Both monocultures and co-cultures can be cultivated in each droplet. After culturing, the droplet spacing device can separate individual droplets into tubes for DNA amplification. The droplet is naturally phase separated from the oil phase and after adding surfactant destabilizer, the aqueous droplet naturally merges with the cell lysis solution used to extract the DNA. The extracted DNA can be amplified by the MDA with a series of reagents and incubation steps. The amplified DNA from each droplet can be used for applications such as PCR or sequencing.

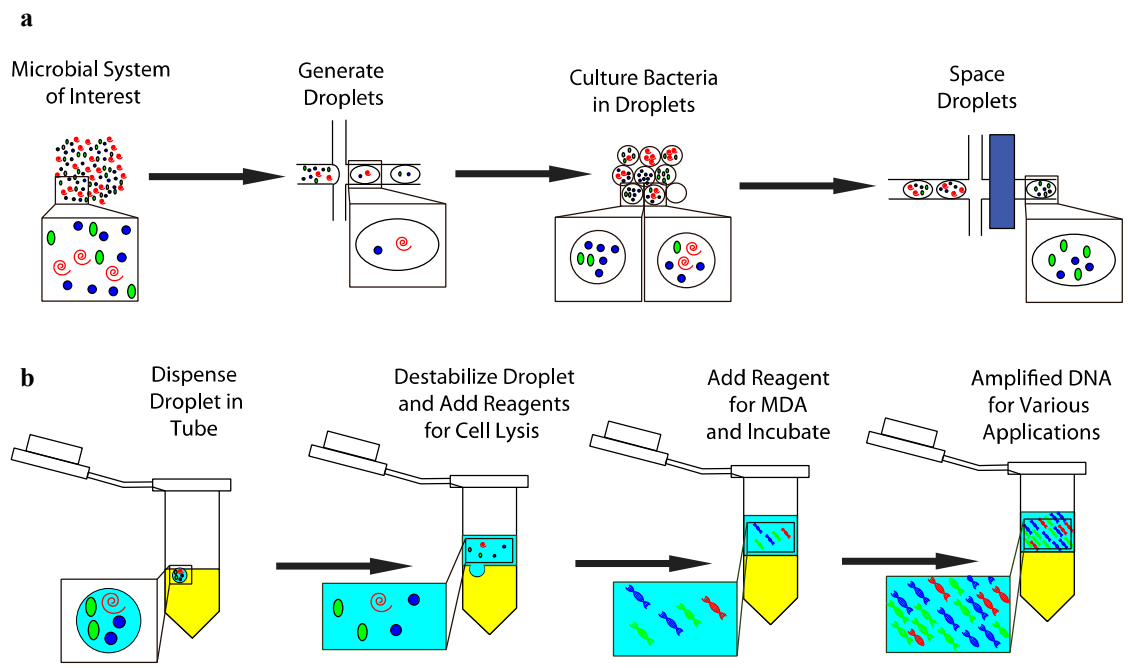

Figure 3.2: Single droplet MDA schematic. a) A bacterial system (either single or multi-species) can be encapsulated in droplets for study using a cross-flow droplet generation device. Bacteria are cultured in the droplets and the spacing/dispensing microfluidic device presented in this paper is used to separate the droplets. B) The droplets are dispensed into tubes. The droplet interface is then destabilized at which point the bacteria are merged with the solution for lysis. The bacteria are subsequently lysed at 65 °C. MDA can be performed in the aqueous phase to amplify the DNA and the resulting DNA can be used for many applications including RT-PCR and next generation sequencing.

3.4.2 Single Droplet Dispensing Validation

The droplet spacing device is a cross-flow droplet generation device with several specific modifications to allow for controlled spacing of the droplets (Figure 3.3a). The valve used to control the device is a normally open valve that partially closes (Figure 3.3a Side View). During operation, droplets are introduced into the device and droplets flow up to the junction while the valve is partially closed (Figure 3.3b). The valve is then opened allowing a droplet to flow past the junction (Figure 3.3c). Upon closing the valve, fluid flow still occurs but presence of the valve membrane partially constricting the channel changes the resistance of the flow and prevents subsequent droplets from entering the cross-flow region of the device (Figure 3.3d).

`

Droplets containing fluorescein were dispensed into a 96-well plate to determine efficiency of the device to space out and dispense individual droplets (Figure 3.3e-f). A total of 48 droplets were dispensed and 83% of the 48 wells used contained a single droplet. Wells containing no droplets arose because droplets were trapped at the connection between the tubing and the device or droplets were stuck onto the wall of the tubing. Securing the tubing as close to the device channel as possible and modifying the tubing with a hydrophobic coating mitigated these issues.

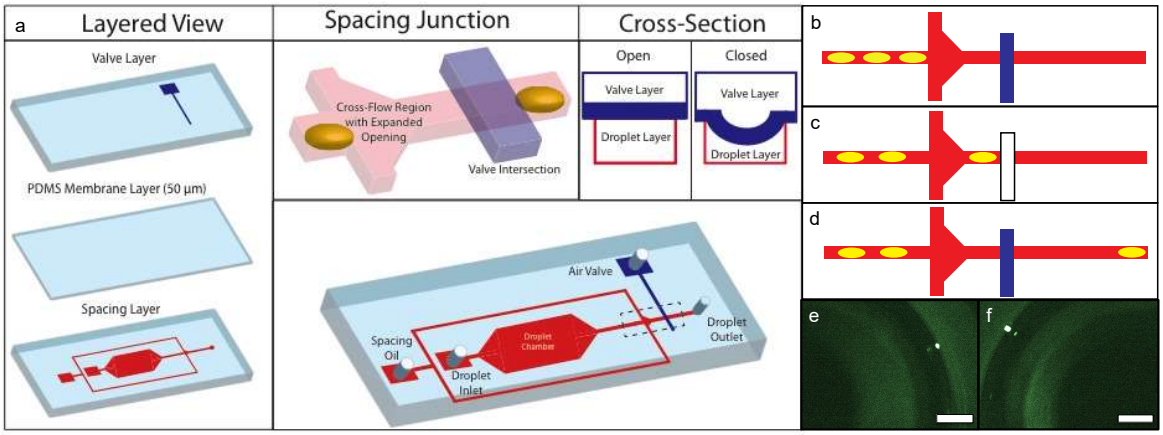

Figure 3.3: (a) Schematic of the droplet spacing device. The cross-flow region has an expanded orifice past the intersection that tapers off into the normal channel dimension to prevent droplet break-up. The channel containing the droplets to be spaced is expanded into a chamber to alleviate high-pressure build-up that can cause droplet merging. The droplet spacing exit ends with a channel rather than a reservoir region like the entrance due to the pressure drop that can cause spaced droplets to be trapped in this region. (b-d) Operation scheme of a droplet being spaced using the device by opening and closing the valve. (e-f) Images of droplets from two different wells after being spaced on a device. Scale bar is 500 µm.

3.4.3 Droplet Cultivation of *E. coli*

Controlling the number of cells for encapsulation during generation is important to ensure the desired number is achieved in a majority of the droplets. To achieve these different cell numbers in droplets, the concentration in the aqueous phase can be diluted. However, even after dilution, the Poisson distribution describes the precise number of cells in each droplet. The distribution is based on the cell density in the sample,

represented by λ. Based on the λ value, the number of cells can be predicted and controlled to achieve the desired cell distribution in droplets.

Droplets containing *E. coli* cells were generated on a flow focusing droplet generation device (Figure 3.4a). The average number of cells per droplet, here referred to as λ, was 5. Droplets are collected in an Eppendorf tube modified by including a syringe tip and Teflon tubing sealed with epoxy at the top of the tub. Droplets flow from the device into the tube via the Teflon tubing and the syringe tip can push the droplets out by applying pressure on the syringe tip (Figure 3.4b). After cultivating overnight, each droplet contained 400-500 cells as determined by microscopy (Figure 3.4c-d).

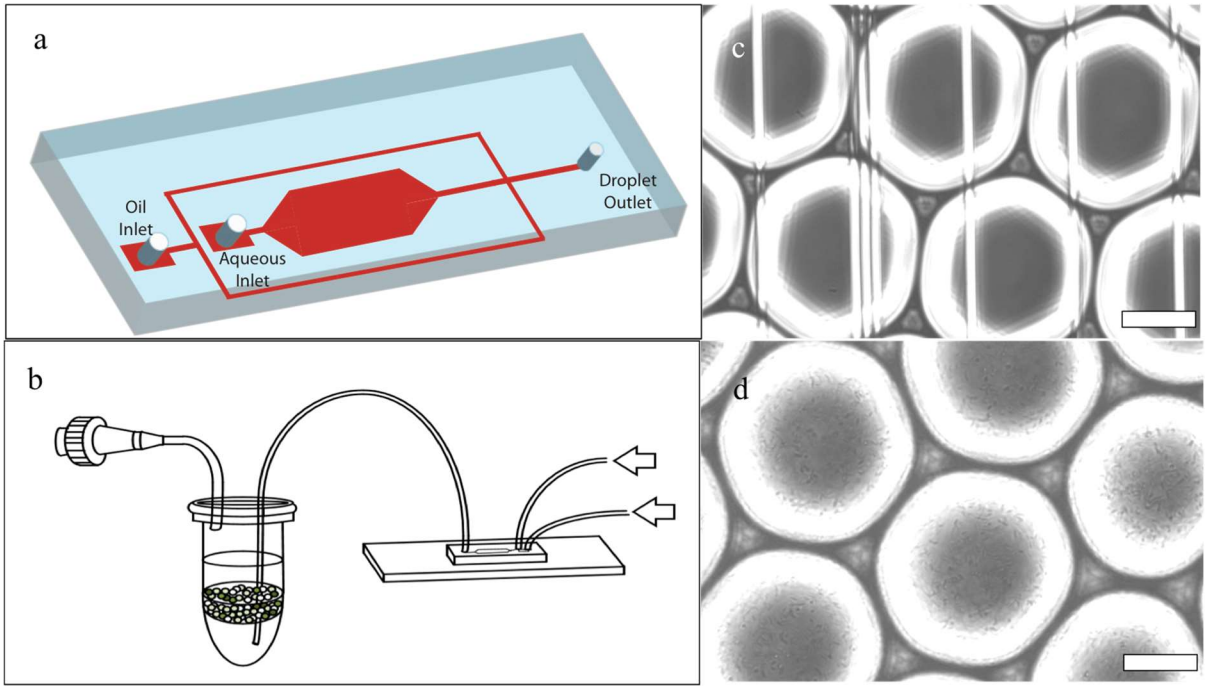

Figure 3.4: (a) Schematic of the droplet generation device. Similar to the droplet spacing device, it is a one layer device with a different flow focusing region to produce the necessary force for producing droplets. (b) Schematic of the Eppendorf tube used for droplet collection and reinjection as well as connection to the droplet generation device. (c) Droplets containing *E. coli* at 0 hour. (d) Droplets containing *E. coli* at 40 hours of growth.

`

3.4.4 Single Droplet Multiple Displacement Amplification

Eight droplets were dispensed into individual tubes (one droplet per tube) and the surfactant-stabilized droplets were broken up, allowing the aqueous and oil phases to separate. After MDA, DNA from each MDA-amplified genome was quantified using a series of 7 RT-PCR primers to determine if there were any major gaps in the genome (Table 1).

Table 3.1: *E. coli* qPCR primer sequences used in this experiment as well as location of each sequence on the genome

Gene	Primer (Forward)	Primer (Reverse)	Length (bp)	Primer Position on Genome (Mbp from origin)
gadA	AATTCCTGCGCCT CGGTCGTGA	TCATACGGCCCCAG TTTGGCGA	104	4.35
fabA	GCTGGGCGTTGGC GAAGTGAAA	CCAGGCCCATAATC AGACGACGGTT	113	1.01
fimI	TACCACGTTGCCC GGCGGAAAT	TGCGCTATCTTCCC CAACCGCA	145	4.54
rfaJ	TGGAGCGGTTGCT GCTGTTGTT	ACGACACCGGAAT TAAAGTACTGCCCA	108	3.80
rpoD	ACAACAGCATCGA CCCGGAACTGG	AGCGTGACTGCGA CCTTTCGCT	104	3.21
yfgO	GTAGCAATATACC GACGAAAACCAC	GTTATTTTAGTTGC CGGATTGGA	181	2.62
hrpA	AACGGTCTTCGCC GTCTACTGT	TTATCCACACCGCA GGAGATACAGT	235	1.49

The 7 genes for which these primers were designed were selected because the genes are distributed across the whole genome (Figure 3.5a). Initial relative DNA amounts were determined from standard curves developed with each primer (Figure 3.5b). All eight droplets containing *E. coli* cells were successfully lysed and the DNA amplified. While each droplet had some variation in the amplified DNA amount, the amounts across all eight droplets were within one order of magnitude of each other. The variation could be a result of the differing number of cells in each droplet and slight differences in input amount for the MDA reaction. In comparison to the negative

`

controls from an MDA reaction on DNAse/RNAse-free water (MDA-Water) and RT-PCR performed directly on DNAse/RNAse-free water (Blank Water), the amount of DNA was many orders of magnitude greater for MDA-amplified DNA. This demonstrates that our spacing system could amplify DNA from a single droplet using MDA without any major loss of the genome. In addition, the amount of DNA amplified is comparable to that of the extracted DNA directly from approximately 10^9 *E. coli* cells.

a

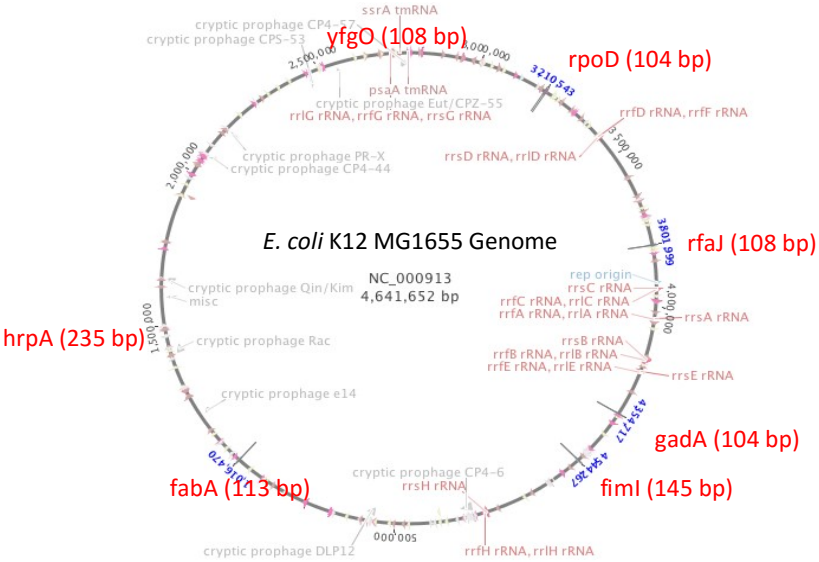

b

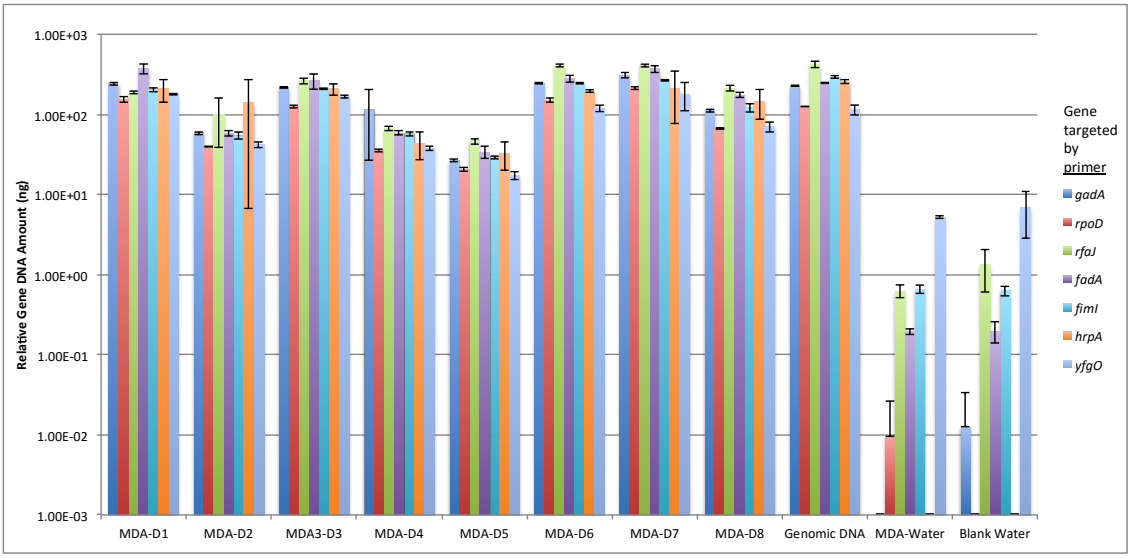

Figure 3.5: (a) Location of the genes on the *E. coli* genome. (b) Relative amount of DNA from MDA reaction. MDA-D1 through D8 represents 8 different droplets containing *E. coli,* MDA-*E. coli* is extracted DNA from cells, MDA-water is MDA-treated DNAse/RNAse-free water, and Blank water is DNAse/RNAse-free water. Seven primers covering the genome are amplified. Relative amount of DNA was calculated by using standard curves for each primer on the positive control. Error bars are standard deviation for replicates of RT-PCR reaction.

`

The whole genomes from droplets 2, 3, and 4 were sequenced and the coverage was mapped and compared to the coverage of the whole genome of DNA extracted directly from *E. coli* cells. These three droplets were selected from the RT-PCR data because they have varying amounts of DNA. Coverage from the three droplets is shown with comparison to the control of the extracted DNA (Figure 3.6). As seen from the previous RT-PCR results, almost the entire genome was amplified as the average percent identity between the 3 samples reached 97.9% while the extracted DNA was at 99.9%. As with most DNA amplification processes, there is an inherent bias to the amplification process, which results in areas of over- and under-amplification. This bias can also be seen with our samples compared to the control. Interestingly, we noted that between the 3 droplet samples, the regions of over- and under-amplification were the same indicating that bias was not random. Previous literature has indicated regions of high GC content could create elevated coverage during sequencing. [115,116] However, mapping and comparing the GC content to coverage shows no clear pattern between bias and GC content. One explanation for the specific bias may be due to the fact that random hexamers used to initiate the MDA reaction may favor specific regions of the genome. The MDA amplified genome did show bias as expected but the entire genome was covered.

3.4.5 Multi-Species Single Droplet MDA

Single species genome analysis in droplets is important, but for many applications, such study of bacterial interactions and co-cultures, multiple genomes must be amplified by MDA. Specifically, each genome must be amplified in a manner that ensures no significant bias to one species in the sample. To that end, we cultured a two-

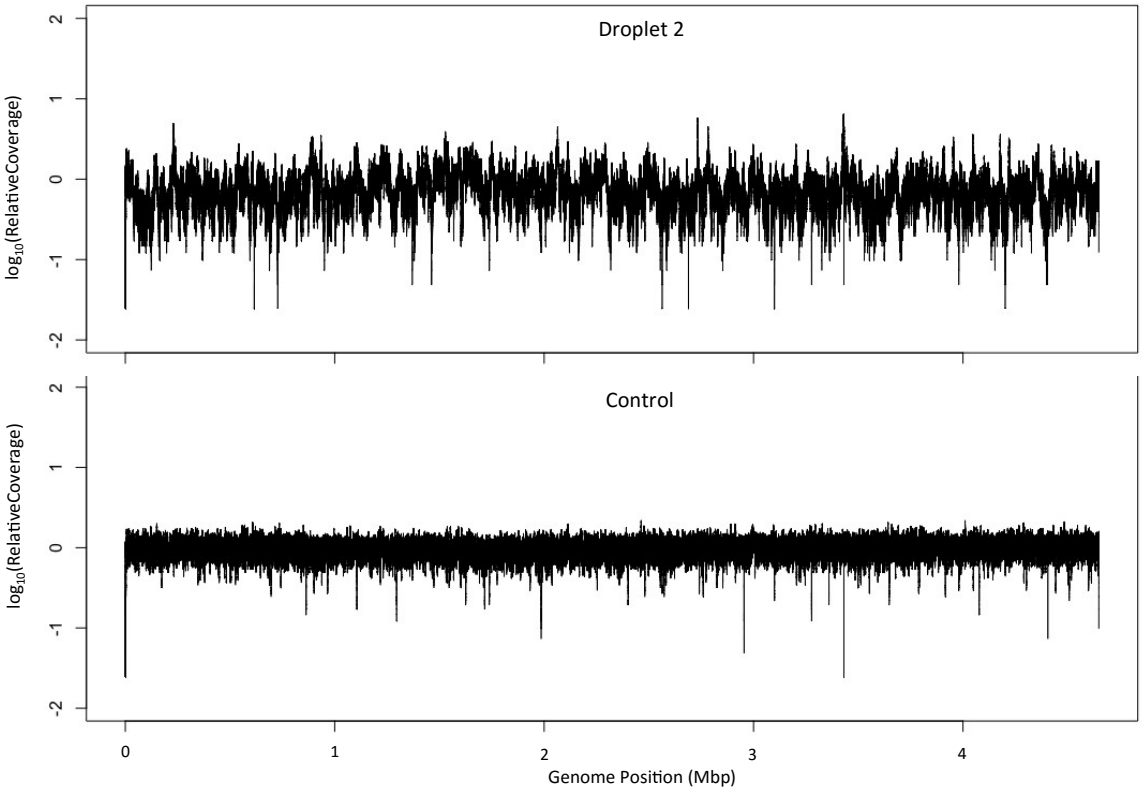

Figure 3.6: Coverage of the genome for MDA amplified DNA from droplets 2 from the previous RT-PCR experiment. The control is extracted genomic DNA from *E. coli.* Coverage is plotted as a relative coverage defined as the coverage at that point normalized to the average coverage from the control sample. Genome coverage across all three amplified samples was similar across the genome with the same patterns emerging.

species system of *E. coli* and *P. putida* in droplets and performed MDA after growth to determine if both species' DNA were successfully amplified.

Table 3.2: *P. putida*-specific primers used for RT-PCR to identify the genome after MDA

Gene	Primer (Forward)	Primer (Reverse)	Length (bp)
benA	GAAGGCAACTGGAAGCTCAC	CCGTGGTCGAAGGAATAGAA	181
benR	GACCCGGTTGACCTGACTTA	CTCATCCAGCCGGTAATGAT	149

After amplification, *benA* and *benR* gene primers were used to identify *P. putida.* These two genes are unique to the organism and are believed to regulate degradation of aromatic acids [117]. In addition, the two primers targeting the genes *rfaJ* and *gadA* were tested and shown to be specific to *E. coli.* Two droplets were dispensed for the MDA reaction (MDA-26-1 and MDA-26-2). During spacing, the droplets were imaged

`

(Figure 3.7a-d) and both species were present in each droplet. As expected for the incubation temperature (30 °C), *P. putida* was the dominant species in each droplet. The RT-PCR results show that the genomes of both species were successfully amplified in each droplet, indicating that the MDA was successfully able to amplify both sets of genomes (Figure 3.7e) regardless of composition. The DNA amount amplified for each species is within one order of magnitude for each droplet. Positive and negative controls of each primer indicate that non-specific primer amplification did not occur.

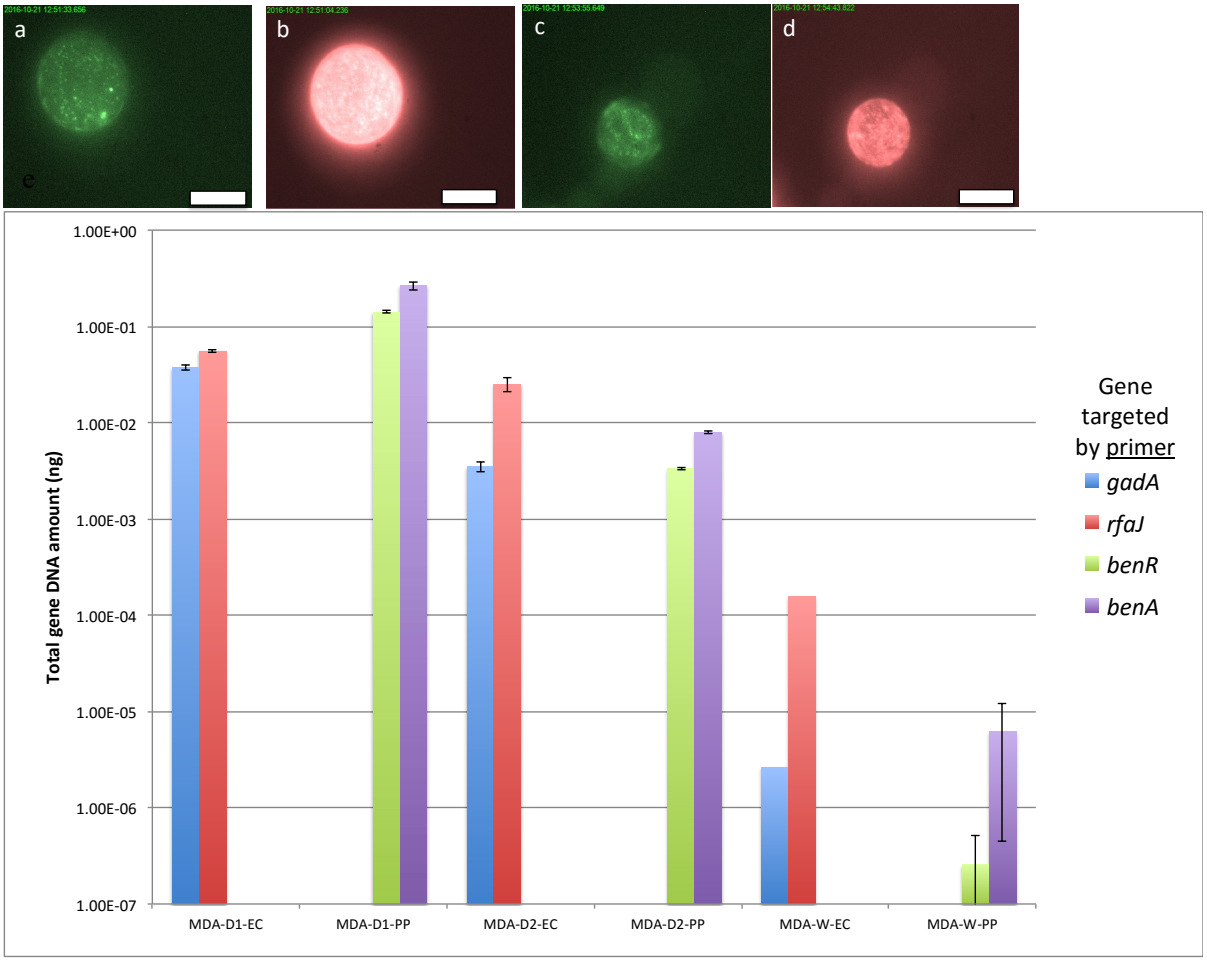

Figure 3.7: (a-d) Fluorescent images of droplet D1 and D2 GFP (a,c) and D1 and D2 mCherry (b,d). Each species was fluorescently labeled: *E. coli* with yellow fluorescent protein and *P. putida* with mCherry. Cultivation occurred at 30 °C for 26 hours. Scale bars are 100 µm. (e) RT-PCR results after cultivation. Inset graph shows the controls, which are genomic extracted DNA to determine if primers are specific to each species. Error bars are standard deviation of replicates performed on the RT-PCR reactions.

`

3.4.6 Single Droplet RT-PCR

MDA is a powerful tool for amplification of DNA, but as demonstrate above, there is a bias introduced from the amplified samples. Quantification from the MDA-amplified samples by RT-PCR can be inaccurate. To perform accurate quantification, RT-PCR must be performed directly on the droplet. However, limit of detection (LoD) is a challenge in as droplets can contain as little as tens of cells. A previous study found the limit of detection from *E. coli* to be $3.5x10^3$ CFU/mL or 3.5 CFU/µL. [118] Based on this information, different concentrations of *E. coli* (decreasing by factor of 10) were used to determine the LoD feasible for quantification of bacteria in droplets.

Initially, RT-PCR was performed directly on *E. coli* and *P. putida* cells with no oil or surfactant. As seen in Figure 3.8a-b, the RT-PCR was successful in quantifying down to 12 cells (0.6 CFU/µL) for *E. coli* and 6 cells (0.3 CFU/µL) for *P. putida* with R-squared values close at 0.999. To determine effects of the oil, surfactant, and destabilizer, the components were added to tube. During this process, the oil and aqueous phase containing the cells separate. As the aqueous phase volume is too small to extract using a pipette, water is added and centrifuged to combine the two aqueous phases. Cell lysis using heat was performed to distribute the DNA evenly in the aqueous solution as centrifugation may have pelleted cells to bottom of the aqueous phase. The aqueous phase is extracted by pipetting and used for RT-PCR. Figure 3.8c-d shows the results of both species with this new protocol that indicates the addition of oil and surfactant has an adverse effect on the accuracy of RT-PCR. The standard deviation increased and fit of the curve significantly decreased. This could be due to several

`

factors ranging from improper lysing, reagent interactions, and error during pipetting to remove the aqueous phase.

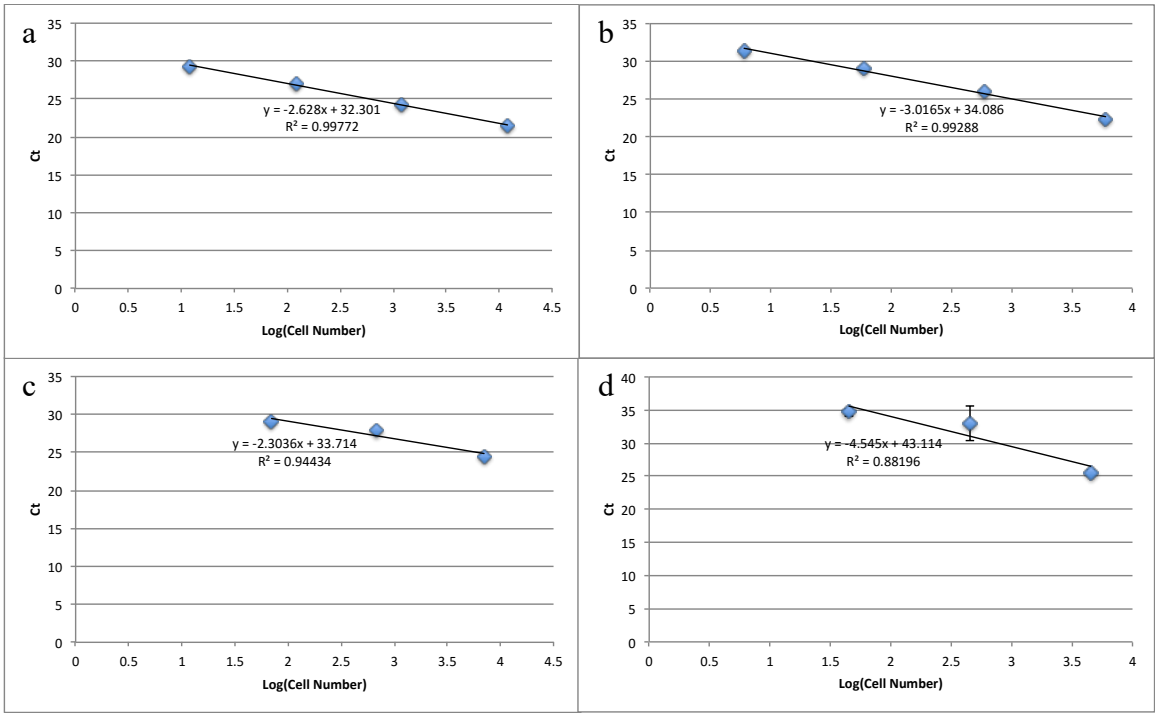

Figure 3.8: (a) Standard curve of *E. coli* cells at decreasing concentrations by a factor of 10 starting at 12,000 cells. Y-axis indicates the Ct value, which is the cycle number at which the fluorescence intensity exceeds the background. (b) Standard of *P. putida* cells at decreasing concentrations by a factor of 10 starting at 6,000 cells. (c) Standard curve of *E. coli* cells at decreasing concentrations by a factor of 10 starting at 7,000 cells with the addition of oil, surfactant, and destabilizer. (d) Standard curve of *P. putida* cells at decreasing concentrations by a factor of 10 starting at 4,500 cells with the addition of oil, surfactant, and destabilizer. Error bars are standard deviation of replicates performed RT-PCR reactions.

We used RT-PCR on droplets containing no cells, *E. coli* only, *P. putida* only, and a mixture of both species. Four droplets of each type was spaced and dispensed. The droplets were destabilized and the protocol described above was applied to perform the RT-PCR. Using the previously developed standard curve, an estimation of cell number was determined (Figure 3.9). As depicted, the RT-PCR results of the blank droplets indicated there were cells in the sample. Signal from a negative control create significant problems for quantification and resulted from the standard curve Ct value varying across samples. Cell numbers for most of the droplets are two magnitudes higher than the blank

`

samples. However, from the resulting droplet culture, the number of cells is two orders of magnitude lower. In addition, several cell containing samples contained cells equal to those calculated as the blank. It is feasible to normalize these results to determine a rough quantification of cell number, but it would be impossible to achieve a precise quantification of each droplet.

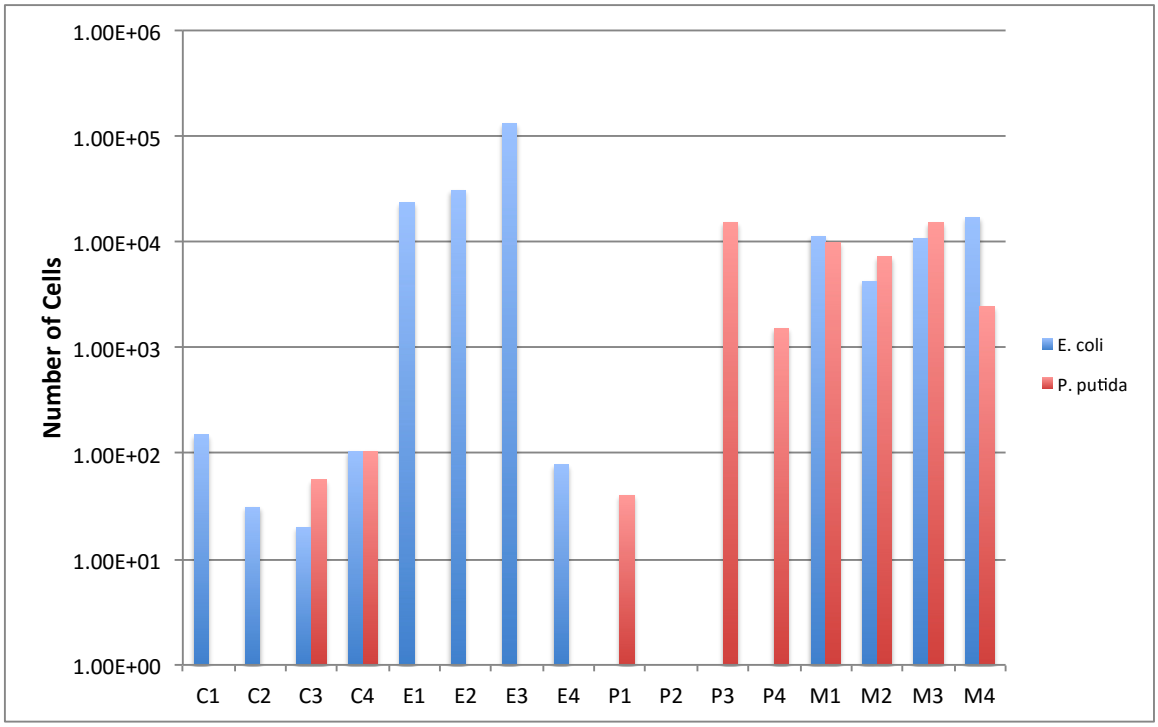

Figure 3.9: Results of the RT-PCR performed on droplets. C1-C4 indicates droplet samples containing no cells. E1-E4 indicates droplets samples containing *E. coli* cells only. P1-P4 indicates droplet samples containing *P. putida* cells only. M1-M4 indicates droplet samples containing both *E. coli* and *P. putida* cells. Number of cells was converted from Ct values using the standard curve.

3.5 Conclusion

Droplet microfluidics' small sample size provides an advantage for a multitude of applications such as high-throughput sample generation and faster reaction times. However, the small sample size becomes disadvantageous when downstream analysis requires larger volumes. Our droplet spacing device is a simple pneumatically operated system that allows for the spacing and dispensing of a single droplet into well plates or

`

tubes. We successfully demonstrated whole genome amplification via MDA on *E. coli* and showed that the genome was successfully amplified using RT-PCR and whole genome sequencing with little loss in coverage. We also performed multi-species MDA on single droplets to prove that all of the species' genomes within a droplet can be amplified regardless of composition. The limitations to this process lie in the MDA-based amplification that can result in bias. In addition, quantification of the droplet content is difficult due to inconsistencies in RT-PCR. The spacing device can be easily applied to other applications such as scale-up of individual droplet cultures and assays such as ELISA or FISH. Future iterations of this device can be modulated to provide automated dispensing for high-throughput usage. The platform we developed to amplify the genome within a droplet could be used to study interactions with bacteria or cells or identify new species.

`

Chapter 4

Droplet Co-Cultivation and Analysis of Gut Microbiome

4.1 Summary

The gut microbial community is an extremely desirable system to study in the human body owing to its role in regulating metabolism and fighting infections. However, due to the complexity of the community (>50 species), it is difficult to understand its functions as many species within the community have yet to be cultivated and characterized. As with all microbial communities, there are many interactions between species that enable some of these unculturables to grow. To that end, we have developed a droplet microfluidic platform for the co-cultivation of anaerobic gut bacteria and subsequent analysis via sequencing. In this work, we studied the effects of media and cell number on the ability to culture subsets of the microbial community and the interactions within each droplet. After culturing bacteria in the droplets, the droplets are spaced and dispensed followed by amplification of the DNA using MDA. Using T-RFLP analysis, we analyzed the microbial diversity in each droplet and determined two samples with low diversity to sequence. Through sequence analysis, we found two distinct "species" within one of the droplet sample. Performing functional analysis, we found

`

complementarity between the two bins in the valine, leucine, and isoleucine amino acid pathways. We have demonstrated a platform for droplet co-cultivation of microbial communities and analyzed the co-cultured samples with next generation sequencing. We were able to hypothesize some mutualistic interactions between the species using this data.

4.2 Introduction

The human microbiome is a complex ever-changing system that has significant impacts on human physiology. The gut microbiome is of particular interest to researchers due to its diversity in comparison to other body sites and to its important role in digestion of nutrients and preventing infections. [119] So many of the bacteria that regulate our health have yet to be discovered. [120] In the gut microbiota, which can include up to a thousand different species [121,122], isolating a single species can be extremely challenging. In addition, many of these unculturable bacteria are unable to grow without necessary partners [123]. Thus, co-cultivation may be the key to cultivating some of these unculturables as well as a deeper understanding of these communities. Along with unknown culture conditions e.g. nutrients, amount of oxygen, etc., these factors present a barrier to a better understanding the human microbiota.

Currently laboratory culture techniques focus on single species cultivation in a low-throughput manner. Droplet microfluidics offers an alternative method by offering high-throughput culture and analysis of complex communities. Previous work in studying gut bacteria in droplets have been primarily focused in two areas: segregation of gut microbiota and direct analysis [51] or culturing of single cells [124]. However, for cultivation of some unculturables, the interaction between species is especially important

`

which necessitates co-culturing. In addition, with so many different possible combinations of bacteria, the co-cultures must be performed in a high-throughput manner.

From previous work, we have developed technology utilizing droplet microfluidics for the co-cultivation of bacteria and analysis of single droplets via next generation sequencing. Combining this technology with the gut microbiota, we developed a platform for co-culturing gut bacteria in droplets under anaerobic conditions. Using PCR and T-RFLP, we screened cultured droplets for targets to perform whole genome sequencing. Selecting two droplets with distinct bacterial species, we analyzed the genomes for interactions between species within the droplet.

4.3 Materials and Methods

4.3.1 Gut Microbe Extraction and Preparation

A fecal sample from a healthy human patient was obtained from Vincent Young's lab at the University of Michigan School of Microbiology. The sample was previously stored at -80°C in a 2 mL cryovial and thawed in an anaerobic chamber to ensure no exposure to oxygen. 1.5 mL of 1X phosphate buffered saline (PBS) was added to the cryovial and the sample was mixed with the PBS using a pipette tip. After mixing, the sample is spun at 1000 rpm to separate fecal debris from the microbes. By extracting the supernatant at 500 μL increments, three aliquots of the sample were made. The samples were stored at -80°C until used. Prior to droplet generation, cell density of the sample was determined by using a hemocytometer. Cells were diluted by 10X and 5 μL of the sample was placed on the hemocytometer. The hemocytometer was placed under a

`

Nikon inverted contrast phase microscope and observed with the 20X objective lens. The cell density was calculated to be $1.9x10^8$ cells/mL.

4.3.2 Droplet Generation in Anaerobic Conditions

The droplet generation device is a modified cross-flow droplet generation device made from PDMS. Photo-masks were designed on L-Edit and made in the Lurie Nano Fabrication Center at the University of Michigan. The SU-8 mold was made by negative etching on a silicon wafer. The silicon wafer was spin coated with SU-8 2035 at a thickness of 50 μm. The wafer was pre-baked at 65°C and then at 95°C. The wafer was then exposed and a post-exposure bake was performed at 95°C. After baking, the wafer was silanized with (tridecafluoro-1,1,2,2,-tetrahydrooctyl)-1-trichlorosilane using a desiccator. PDMS was poured on top of the SU-8 mold, vacuumed to remove air bubbles and heated at 70°C to solidify the polymer. The base for the device was made by pouring PDMS on a blank silanized wafer and baking at 70°C. The devices and bases were then cut to size. To complete the fabrication, the devices were punched with holes to create openings for the channels, and bonded on the PDMS bases via plasma-activated bonding using a corona discharge wand.

The microbial sample extracted from the feces was placed in a Coy© anaerobic chamber stored in a cryovial cool rack. Dilutions were made based on the required cell number in each droplet by the following formula:

$$Volume\ of\ Sample = \frac{Average\ Cells\ per\ Droplet\ (\lambda)}{Droplet\ Volume} * \frac{Total\ Volume}{Sample\ Cell\ Concentration} \quad (4)$$

Three λ values were used for droplet generation: 0 (control), 2 and 10. To dilute the volume and provide the nutrients for growth, four different medias were used: Brain

`

Heart Infusion (BHI) (Becton Dickinson), Gut Microbiota Media (GMM), Schaedler's Media (SM) (Oxoid), and Reinforced Clostridial Media (RCM) (Oxoid). Components for GMM can be found in the Appendix. From these conditions, a total of 12 droplet samples were to be generated on the droplet generation device.

The droplet generation device was placed on a lab compound microscope (Amscope M150C) with a USB connected camera. This allows for visualization of the device during droplet generation while in the anaerobic chamber. Syringes were connected to tubing and syringe tips and placed on a syringe pump (CMA 102 Syringe Pump). The oil phase used was fluorocarbon oil (HFE-7500, 3M) containing 2% perfluoropolyether-polyethyleneglycol surfactant (RAN Biotechnologies). Oil was placed into one syringe and the sample was placed into the other syringe. Flows were adjusted to achieve generation on-chip and observed at 100X magnification. Eppendorf tubes attached with tubing were used to collect the generated droplets. Approximately 500 μL of droplets were collected for each sample and covered with mineral oil to prevent evaporation. The samples were incubated at 37°C in the anaerobic chamber for 1 week.

Droplets were imaged immediately after generation and incubation for 7 days. 10 μL of droplets were taken out of each Eppendorf tube and transferred to the INCYTO C-Chip disposable hemocytometer for imaging. Imaging was done on an inverted phase contrast Nikon microscope using the 20X objective.

4.3.3 Droplet Spacing and Multiple Displacement Amplification

After imaging, droplets are spaced by using the spacing device discussed in Chapter 3. A total of 5 droplets from the BHI cultures and 6 droplets from the SM culture

`

at both cell concentrations were spaced. Before spacing, droplets were imaged to identify each corresponding tube. After spacing, surfactant destabilizer (5 µl) was added to each tube. An additional 4 µL of PBS was added to each tube to increase the volume. Cell lysis solution (3 µL) was added to each tube and the aqueous phase containing the bacteria merged with the lysis solution. After a 10 minute incubation period at 65°C and the addition of a stopping solution (3 µL), the MDA reaction mixture was added to the aqueous phase and the reaction was allowed to proceed for 8 hours at 30 °C. The polymerase was deactivated by heating the solution to 65 °C. The amplified DNA was collected by pipetting out the aqueous phase and the DNA was then diluted 100X before PCR and sequencing.

4.3.4 Partial Community Analysis

The 16S rDNA from the MDA amplified samples was amplified by PCR using the 8F (5'-AGAGTTTGATCCTGGCTCAG-3') and 1492R (5'-CGGTTACCTTGTTACGACTT-3') primers. The 8F primer was tagged with the 6-FAM fluorescent marker for subsequent T-RFLP analysis. After PCR, the product was run on a 0.75% agarose gel via electrophoresis to confirm amplification of the 16S. Subsequently, the products were cleaned up using the Qiagen© PCR Purification Kit. After purification, the samples were digested using New England BioLabs© MSPI enzyme for 2 hours at 37°C. The digested samples were filtered using the Qiagen© Nucleotide Purification Kit. A 96-well plate containing the ROX-1000 size standard dye was obtained from University of Michigan Sequencing Core for the T-RFLP analysis. 3 µL of digested samples were dispensed into each well in duplicates and submitted for T-RFLP to the Core.

`

After T-RFLP, the data was analyzed using Applied Biosystems© Peak Scanner Software v1.0 to obtain fragment length and height. The data was plotted using a script written in R. After identifying each peak manually and compiling in Microsoft Excel, the information was clustered using R.

4.3.5 Whole Genome Sequencing and Analysis

Following whole genome amplification, samples were delivered to the University of Michigan Sequencing Core. Sequencing core staff prepared barcoded Illumina libraries using the IntegenX Apollo 324 PrepX ILM DNA Library kit and custom Illumina compatible BioScientific barcoded adapters. Libraries were amplified with the KAPA library amplification kit, quality controlled on the Advanced Analytical Fragment Analyzer, quantified using the KAPA Illumina library quantification kit, and then sequenced on the Illumina MiSeq using the v3 600 cycle protocol.

To improve quality of the sequence reads, reads for both microdroplet samples underwent dereplication (custom shell script by Sunit Jain, 2011) to reduce computational load in downstream processing, Illumina adapter residual removal by Scythe (v. 0.993) (https://github.com/vsbuffalo/scythe), low quality region removal by Sickle (v. 1.33.6) (https://github.com/ucdavis-bioinformatics/sickle), and interleaving (custom shell script by Sunit Jain, 2012) to associate forward and reverse reads. FASTQC (v. 0.10.1) [125] was used to assess quality of the reads before quality control and after. The assembly software used to generate scaffolds from sequence reads was SPAdes (v. 3.9.0) [126], using the flags “sc” for MDA amplified DNA and “meta” for metagenomic reads. As suggested for a multi-cell data set with longer Illumina paired reads lengths, the iterative k-mer lengths used for assembly were: 21, 33, 55, 77, 99, and 127. The two samples were

`

assembled separately with the same parameters. QUAST (v. 4.3) [127] was used to check assembly quality. There was a large disparity of scaffold coverage sample 83308; while many scaffolds had a low coverage, a large portion had coverage between 208X and 338X, most likely due to the stochastic amplification of MDA. To normalize the coverage of reads across sample 83308 and subsequently improve assembly, bbnorm.sh (v. 37.36) from BBTools (http://jgi.doe.gov/data-and-tools/bbtools/bb-tools-user-guide/bbnorm-guide) was used to remove high coverage reads to target coverage of 50 and remove reads with a coverage less than two. SPAdes assembly and QUAST with the same parameters as before were performed with these normalized reads. BlastN (v. 2.2.29) [128] was utilized to identify any assembled small subunit ribosomal sequences against the Silva SSU (release 128) and NCBI RefSeq-RNA (release 83) databases. Binning of the assembly for both samples was performed by metaBAT (v. 0.32.4) [129]. As suggested, the "very sensitive" option was used for our simple communities, and the absolute minimum contig size for binning was set at 1500 bp. All other parameters were the default parameters. For alternative manual binning and visualization of contigs, scaffolds were also processed through anvi'o (v. 2.3.0), following the metagenomic workflow [130]. Due to MDA amplification, coverage information was not relevant for binning; therefore, read mapping information and the anvi-merge command were not used. As a result, anvi-profile was run with the "--blank-profile" parameter as specified (http://merenlab.org/2016/06/06/working-with-contigs-only/). Manual binning was performed using the automatically generated tree based on tetranucleotide frequency profiles between contig splits in anvi-interactive visualization.

`

Annotation of genes was performed using MG-RAST [131-160]. Analysis was conducted and visualized by the MG-RAST web platform. Reference database used for functional analysis was KEGG.

4.4 Results and Discussion

4.4.1 Droplet Microfluidic Platform for Co-Cultivation of Anaerobes

We have developed a droplet microfluidic platform for the co-cultivation of anaerobic microbial communities. See Figure 4.1a for a flowchart of the process. Extraction of the microbes from the sample is an important first step. As these microfluidic channels are often in the micron range in size, any piece of debris from samples can clog these devices preventing droplet generation. Careful separation of particulates from the microbes must be performed to ensure no debris is in the sample before droplet generation.

After microbial extraction, droplet generation and cultivation is performed. Selection of the λ value based on the Poisson distribution is important for co-cultivation. Factors such as viability and cell clumping can result in incorrect cell density in droplets. Droplet generation must be performed in an anaerobic chamber. Due to the constraints of operating in such a chamber, equipment for generation must be able to be remotely operated. As seen in Figure 4.1b, no microscope with an eyepiece can be used with the chamber so a USB camera is required to monitor generation. Additionally, pressure regulation from an air source cannot be used and a syringe pump must be the source for driving flow in the device.

After cultivation, spacing and dispensing of individual droplets is performed for single droplet analysis. It is possible to achieve bulk droplet analysis in lieu of spacing

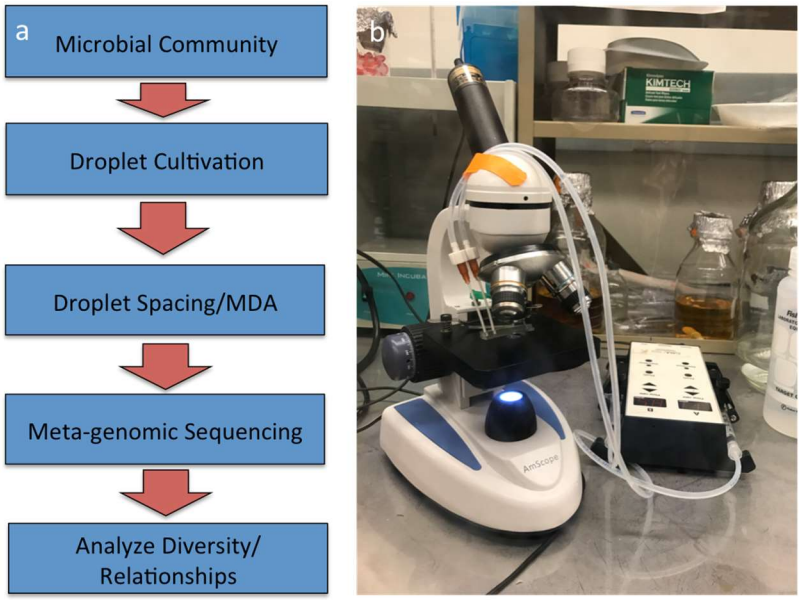

Figure 4.1: (a) Flowchart of platform for analysis of co-cultivated bacteria in droplets. (b) Image of droplet generation set-up in anaerobic chamber.

but individual interactions cannot be observed with this approach. After dispensing, whole genome amplification must be performed for downstream DNA analysis. While our system uses MDA for amplification, other techniques such as MALBAC may be used based on the desired results of the amplification. After amplification, we recommend a preliminary community analysis by PCR, T-RFLP, or other partial community analysis methods. Depending on the desired application, techniques such as PCR are suited for targeted bacteria identification and T-RFLP can be used for community fingerprinting. This allows for better selection for whole genome analysis downstream. Finally, the DNA can be submitted for most sequencing techniques from 16S analysis to whole genome sequencing for *de novo* assembly.

4.4.2 Droplet Co-Culture

Our selection criteria for cells per droplet and media usage were based on the desire to study varying conditions to determine the effects of these parameters on the ability to culture a wide variety of bacteria. Four different media were used: BHI, GMM,

`

SM, and RCM. These media were selected based on a variety of factors. BHI media is a commonly used rich media for cultivating a variety of bacteria. GMM was selected as it was used in a paper [161] for cultivating gut bacteria and it theoretically mimics conditions found in the gut. Schaedler's media was used because it is an extremely rich media, which is specifically designated for anaerobic conditions. Finally, the RCM was used as it favors cultivation of clostridia species, which are commonly found in the gut system. We also selected two different cells per droplet concentration because it was important to ensure the viability of the cells. Viability could be compromised as we handle these cells from sample collection (exposing it to the aerobic condition), extraction, and freezing and thawing cycles. Freezing and thawing could be the biggest issue, as these cells are not suspended in a cryo-preservative. So at $\lambda = 2$, it is highly possible there is no co-culturing occurring as only one cell is viable whereas at $\lambda = 10$, there is a significantly higher probability of co-culturing. However, having too many cells per droplet could also result in too many interactions, making it impossible to study the system. Cultivation temperature was maintained at 37°C corresponding to the human body temperature.

Droplet generation in the chamber can result in variability in droplet size across samples. As operations performed in the chamber are often hindered due to the chamber and thick gloves, instabilities can occur during the generation phase. This can result in larger than expected droplet sizes, which increases the λ value in turn. After generation, droplets were imaged and found to be slightly larger than calculated. However, this ultimately did not affect culturing. For the RCM culture condition, droplets evaporated during cultivation due to insufficient protection from the air. No images are provided, as

`

there were no results after cultivation. For the GMM condition (Figure 4.2), no cells were observed to grow after cultivation. Possible issues include incorrect making of the media due to complexity and incompatibility of the sample to the media. While this media was designed to culture gut bacteria, each natural sample has drastically different compositions and it is possible that the conditions in this media did not suit the culture conditions for the species in the sample. Due to these issues, only the BHI and SM culture conditions were used for further analysis.

After cultivation, both BHI cultures had significant growth in ~20% of the droplets at $\lambda = 2$ and ~ 40% of the droplets at $\lambda = 10$ (Figure 4.3). In addition to growth, there were some morphological differences between each droplet with some droplets containing multiple shapes. Overall, a majority of the droplets contained cocci shaped bacteria. For the GMM cultures, a greater percentage of droplets had significant growth with $\lambda = 2$ at ~30% and $\lambda = 10$ at ~50% (Figure 4.4). The morphological differences were significant in the GMM cultures with almost every shape ranging from cocci to spirilla. More droplets contained different morphologies within the droplet compared to the BHI cultures and growth patterns also varied with some droplets containing large clumped cells while others were evenly distributed. Control droplets containing no cells were imaged to verify no growth occurred. The initial image analysis indicated that our droplet co-cultivation platform was successful in culturing distinct bacterial systems.

4.4.3 T-RFLP Analysis for Sample Selection

Droplets were dispensed from each sample: 5 droplets each from BHI samples and 6 droplets each from SM samples for MDA. After MDA, the 16S gene was PCR amplified using the 8F and 1492R primers. PCR amplification is used for T-RFLP

`

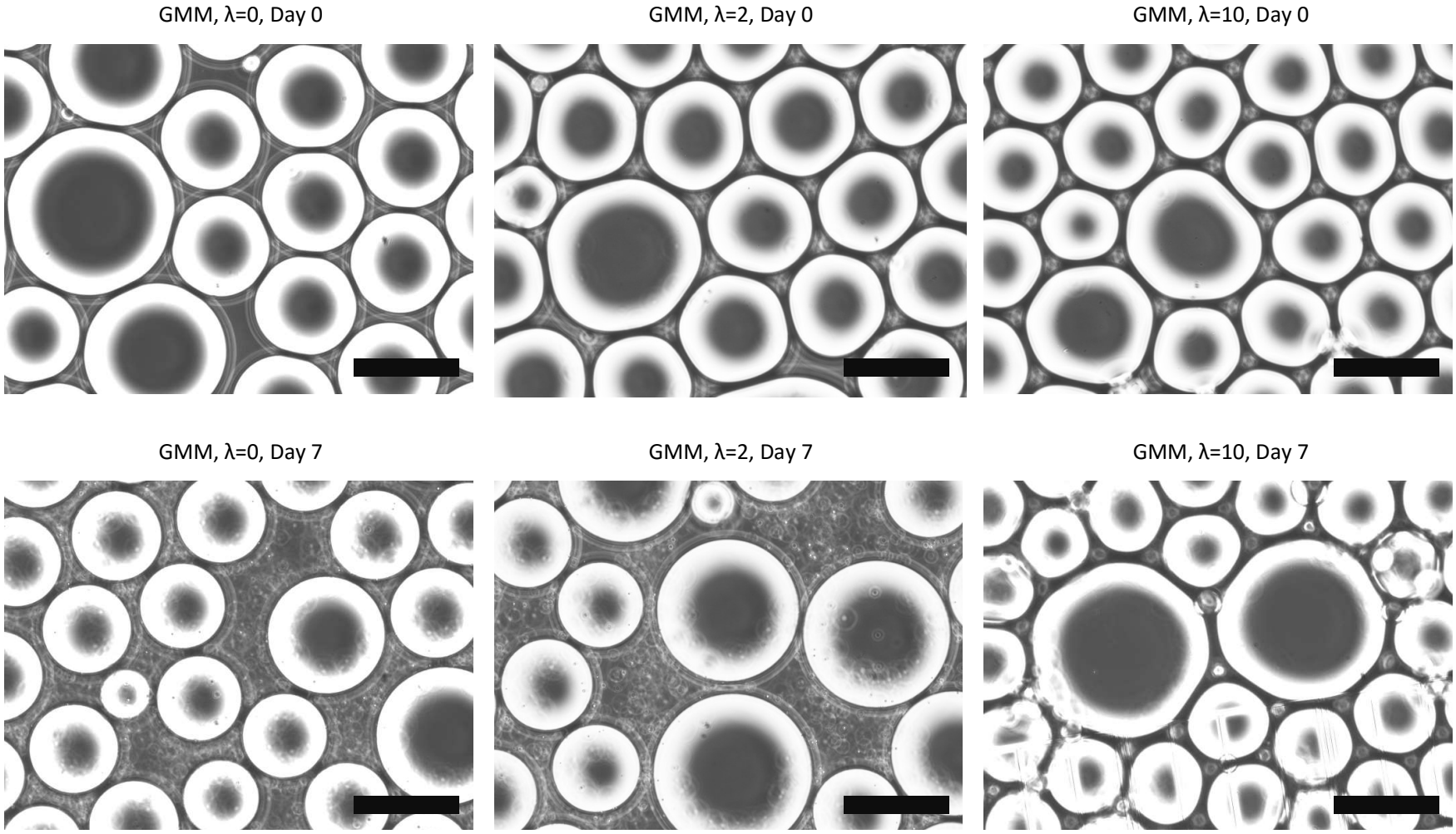

Figure 4.2: Cultivation of gut microbial community using Gut Microbiota Media (GMM) at 2 different cell concentration. Also included is the negative control at 0 cells/droplet. No observable cells grew after 7 days. Scale bar represents 100 µm.

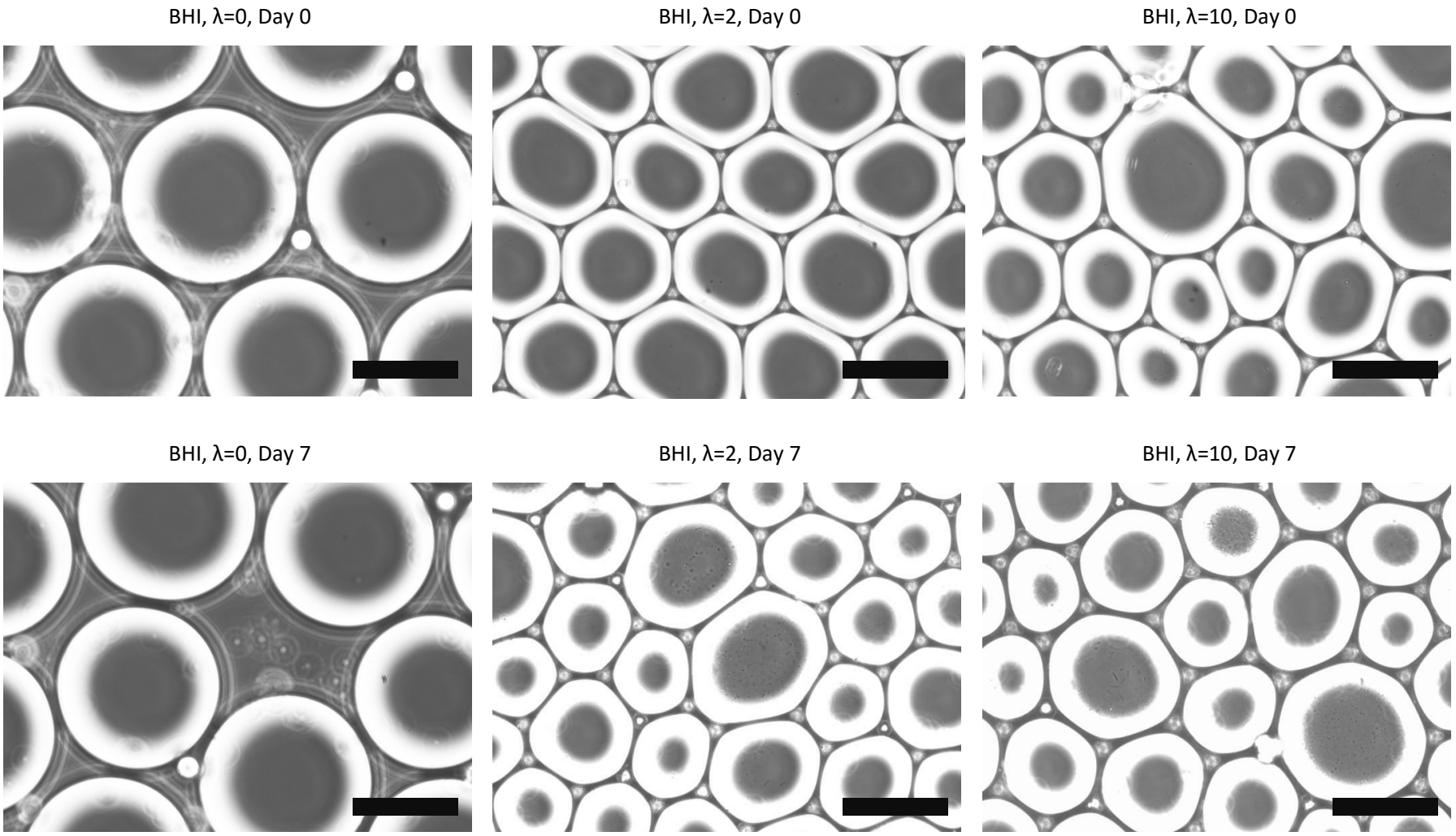

Figure 4.3: Cultivation of gut microbial community using Brain Heart Infusion (BHI) media at 2 different cell concentration. Also included is the negative control at 0 cells/droplet. Growth was observed after 7 days with some noticeable differnce in cell morphology. Scale bar represents 100 µm.

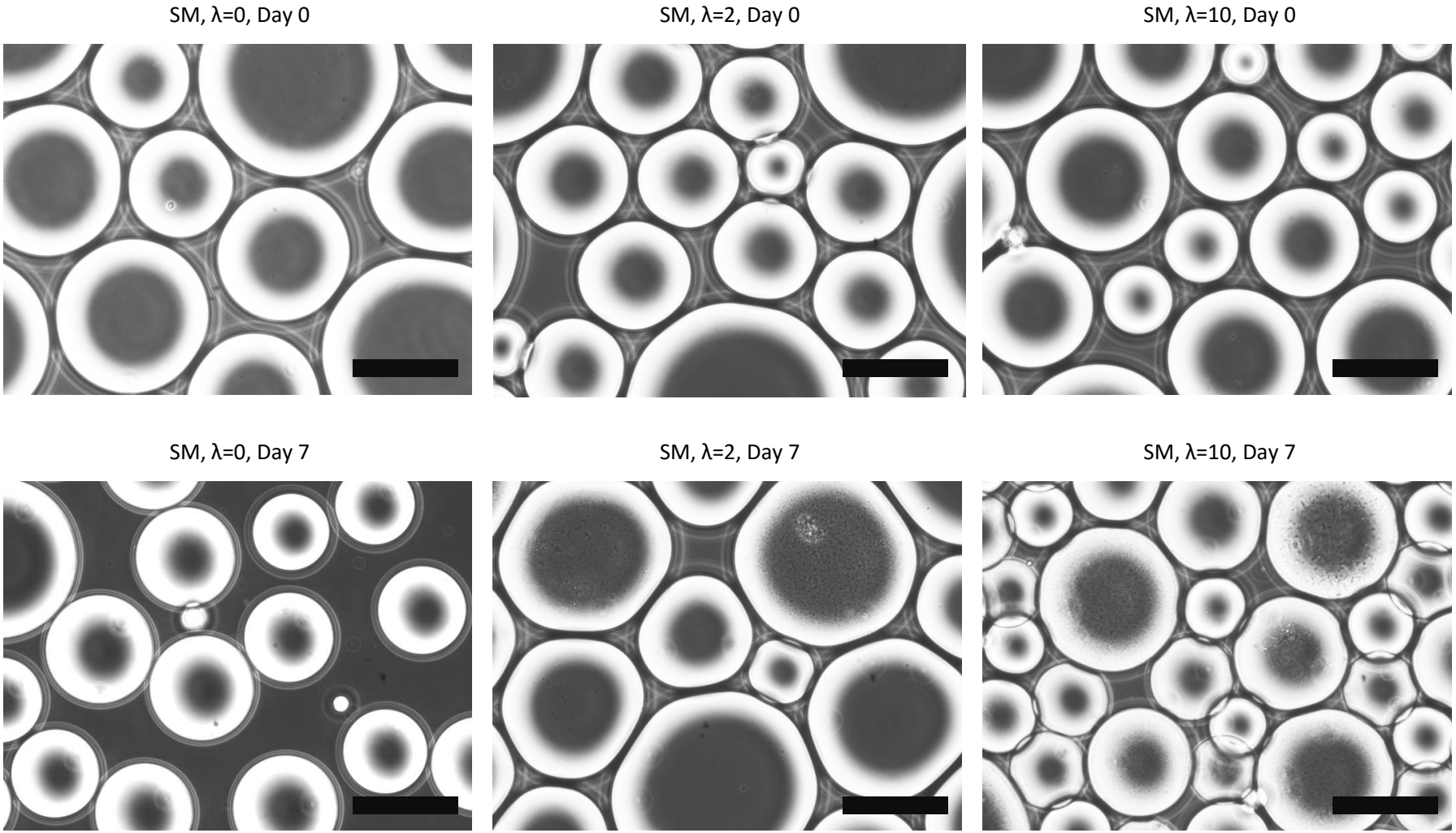

Figure 4.4: Cultivation of gut microbial community using Schaedler's Media (SM) at 2 different cell concentration. Also included is the negative control at 0 cells/droplet. Growth was observed after 7 days with some noticeable differnce in cell morphology. Scale bar represents 100 µm.

preparation and verification of DNA in samples. After PCR, the product length was verified by gel electrophoresis (Figure 4.5). *E. coli* DNA were used as a positive control. The resulting amplicon was the expected size (~1500 bp). After processing and submitting the samples for T-RFLP, the peak data was analyzed. Noise removal and normalization was conducted by removing any peak height less than 1% of the total peak height. Subsequently, the peaks and fragment lengths were plotted to find samples for

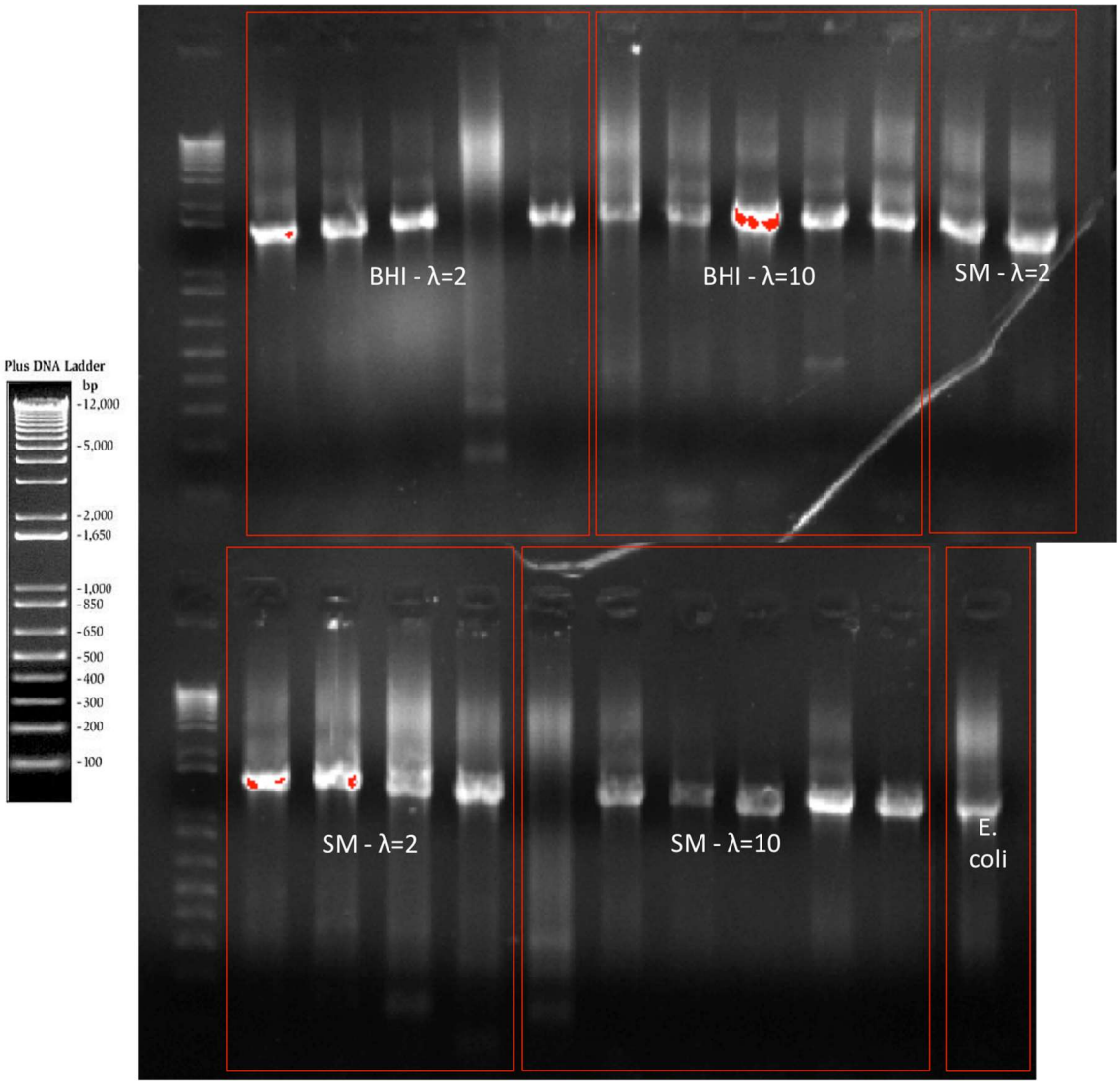

Figure 4.5: Results of the gel electrophoresis on the MDA amplified samples from the droplets. A total of 10 from BHI cultivated samples and 12 from SM cultivated samples were amplified. Each lane in each category corresponds sequentially to each sample in the category. Almost every sample contained amplified bacterial DNA.

sequence submission.

For BHI cultivated samples, there was some diversity between the different droplets. More surprisingly, many of the samples contained 5 or more peaks. A few peaks were present in many of the samples: 153, 164, 282, and 554. These peaks indicate species highly present in the sample, meaning that the BHI culture condtions was favorable for the growth of these species. For SM cultivated samples, there was greater diversity compared to the BHI samples. Additionally, most of the peaks were not shared by the BHI samples. The most ubiquitous peaks were 81, 89, 130, and 164. It is interesting to note peak 164 was reoccurring in both BHI and SM cultivated samples denoting a prevalent and robust species. As expected, there were less species for $\lambda = 2$ than $\lambda = 10$ for both culture media, but it was more apparent in the SM cultivated samples.

The primary criterion for sample selection for whole genome analysis is complexity of the community in the droplet. Any droplet containing more than 5 species would be very difficult to elucidate any bacterial relationships from. There would be too many interactions to decipher based purely on genomic data and isolation of specific interactions would be next to impossible. In addition, only two samples were going o be selected and as such, it would be ideal for both samples to contain different species. To select the most viable samples for analysis based on these two criteria, a binary hierarchical clustering was performed on all the samples to determine similarity (Figure 4.6). Peak height was not factored into the clustering. Based on the clustering analysis performed, three clusters were identified for similarity. Of the three clusters, two contained samples with 3-4 peaks of interest: Sample SM-2-2 and SM-2-4 (Figure 4.7).

The samples contained one shared peak and had sufficient quantities of each species for adequate coverage for whole genome analysis. To determine if there is sufficient coverage for whole genome assembly, the major peak height from each fragment was calculated as a percentage of the total. This percentage is used to convert to coverage using the following formula:

$$C = \frac{x * n}{L} \tag{5}$$

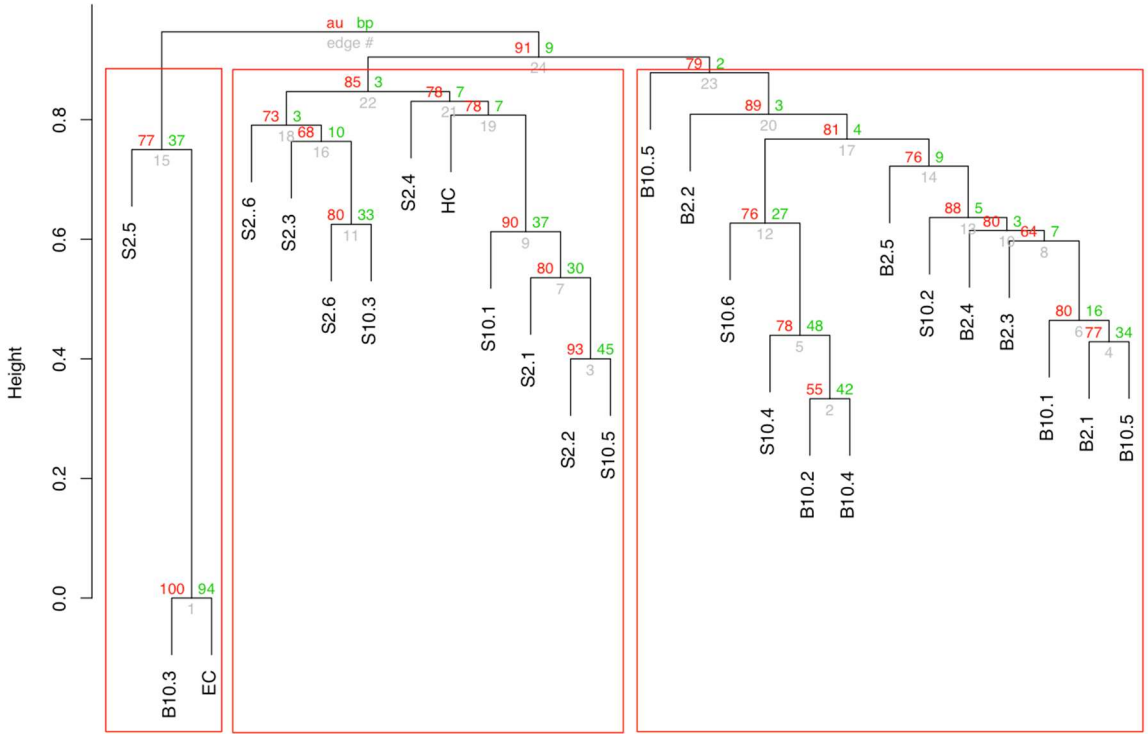

Figure 4.6: Hierarchical clustering using binary values on T-RFLP peaks in each droplet sample. B and S represent the media used. The number following is the λ value. The number after the period represents the sample number (1-5 for BHI and 1-6 for SM). Red boxes are the groupings after clustering.

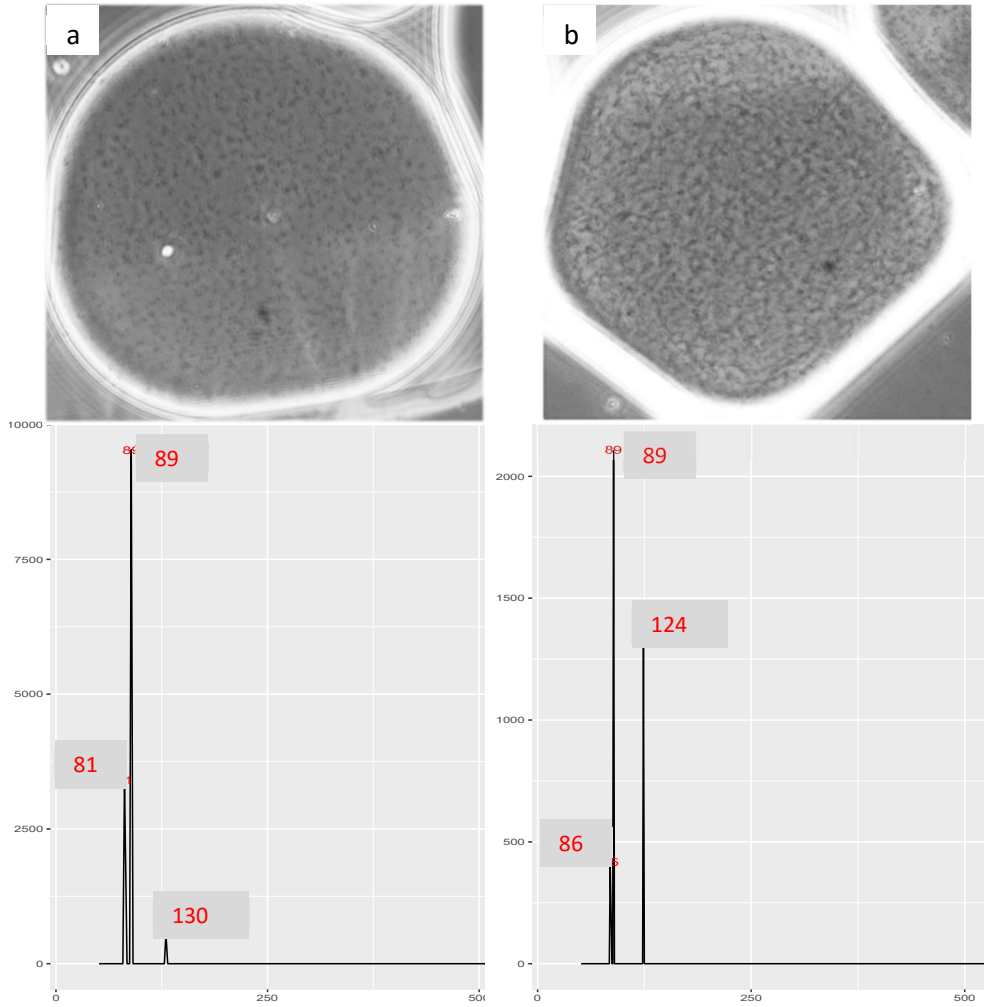

Figure 4.7: (a) Image droplet S2-2 and T-RFLP profile. (b) Image of droplet S2-4 and T-RFLP profile.

where C is the coverage, x is the fraction of the species, n is the number of reads, and L is the length of the genome. Assuming the sequencer is the Illumina MiSeq at 300 bp paired end reads and an average genome size of 4 Mbp [162], the coverage is calculated for each peak in both samples. Additionally, for accurate *de novo* assembly, coverage needs to be 50-100X [163]. We found that for both samples submitted for sequencing, all species should be sufficiently covered for accurate assembly (Table 4.1).

Table 4.1: Peaks and coverage of each peak for the two samples. NP denotes no peak meaning there was no signal in that sample.

Peak	SM 2-2 Coverage	SM 2-4 Coverage
81	759	NP
86	NP	82
89	2118	411
124	NP	257
131	123	NP

4.4.4 Whole Genome Analysis of Droplet Culture

After Illumina sequencing, the sequences of the two samples were processed by a protocol developed in Gregory Dick's lab at the University of Michigan. During quality control, adapters and trimming reduced the number of reads from each sequence sample. Approximately 3% of the total reads from S2-2 and 10% of the total reads from S2-4 were removed. After quality control, contigs were assembled using MetaSPAdes program based on work by Vollmers *et al.* [164] that indicate it is the most suitable program for low diversity MDA amplified samples. These contigs are analyzed for coverage to determine how many times each show up in the sample. The coverage for samples S2-2 was uniform with the expected normal distribution with an N50 value of 8420 (Figure 4.8a). The N50 value indicates the weighted media statistic such that 50% of all the contigs in the sample are that length or larger. The coverage for sample S2-4 had one region with normal distribution and an extremely low coverage region with an N50 value of 3259. The coverage was normalized using BBNorm in sample S2-4 lowered the higher coverage region to 30X, but the low coverage region remained at 1-3X (Figure 4.8b). The resulting N50 value was 39551, indicating an abnormally large N50 value but the source could not be determined.

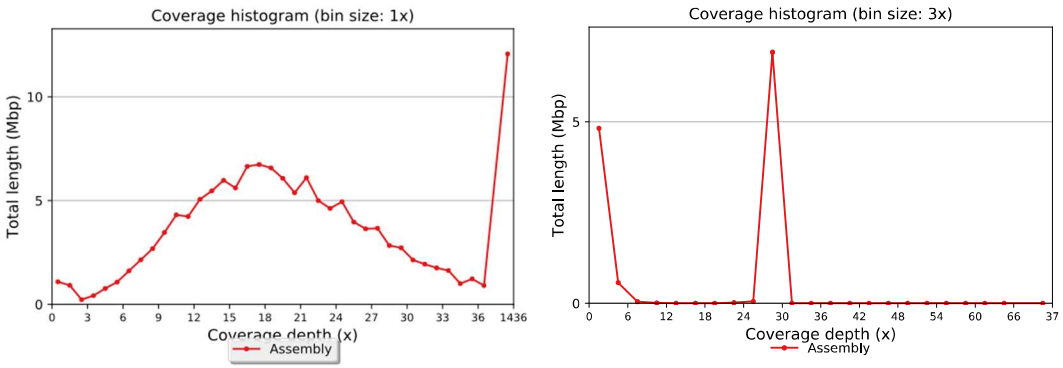

Figure 4.8: (a) Coverage of S2-2 after assembly. Increased peak towards end of graph is due to program combining all contigs beyond coverage of 37 together. (b) Coverage of S2-4 after assembly and normalization.

To determine which contigs belong to which species, these reads are separated into distinct clusters or bins. Initially, ANVI'O is used for manual binning based on GC content and tetranucleotide frequency (TNF). Differential coverage can also be used for binning, but since coverage for some contigs is extremely low in S2-4 it is not used for this study. After binning, S2-2 contigs were separated two bins while S2-4 contigs were separated into initially into two bins (Figure 4.9). Based on the open reading frame (ORF), completeness of each bin and redundancy (multiple copies of the same gene potentially belonging to another species) can be calculated for each bin. For Bin 1 of S2-2, the completeness and redundancy could not be calculated as sequence analysis indicates the bin is eukaryotic. For Bin 2 of S2-2, analysis indicates it is a bacterial species with 98.6% completeness and 1.4% redundancy. Initially, S2-4 contained two bins with Bin 1 indicating a *Bacteroides* genome but with a redundancy of 57.6%. However, further refinement broke that bin into 3 bins with a *Bacteroides* bin (Bin 1) at 99.3% completeness and 4.3% redundancy. The two remaining bins and *Escherichia* bin were incomplete. Binning was repeated using metaBAT, an automated binning tool. Bin 1 for S2-2 contained significant redundancy at 88.53% but as expected, this software is not suitable for eukaryotic DNA analysis (Figure 3.9a). Bin 2 for S2-2 achieved 95.7%

completeness and 0.0% redundancy (4.9c). For S2-4, the samples were normalized prior to binning. Bin 1 at 97.96% completeness and 4.08% redundancy; Bin 2 achieved 11.54% completeness and 3.45% contamination (Figure 4.9d). A third bin was generated, but the bin was too small for analysis.

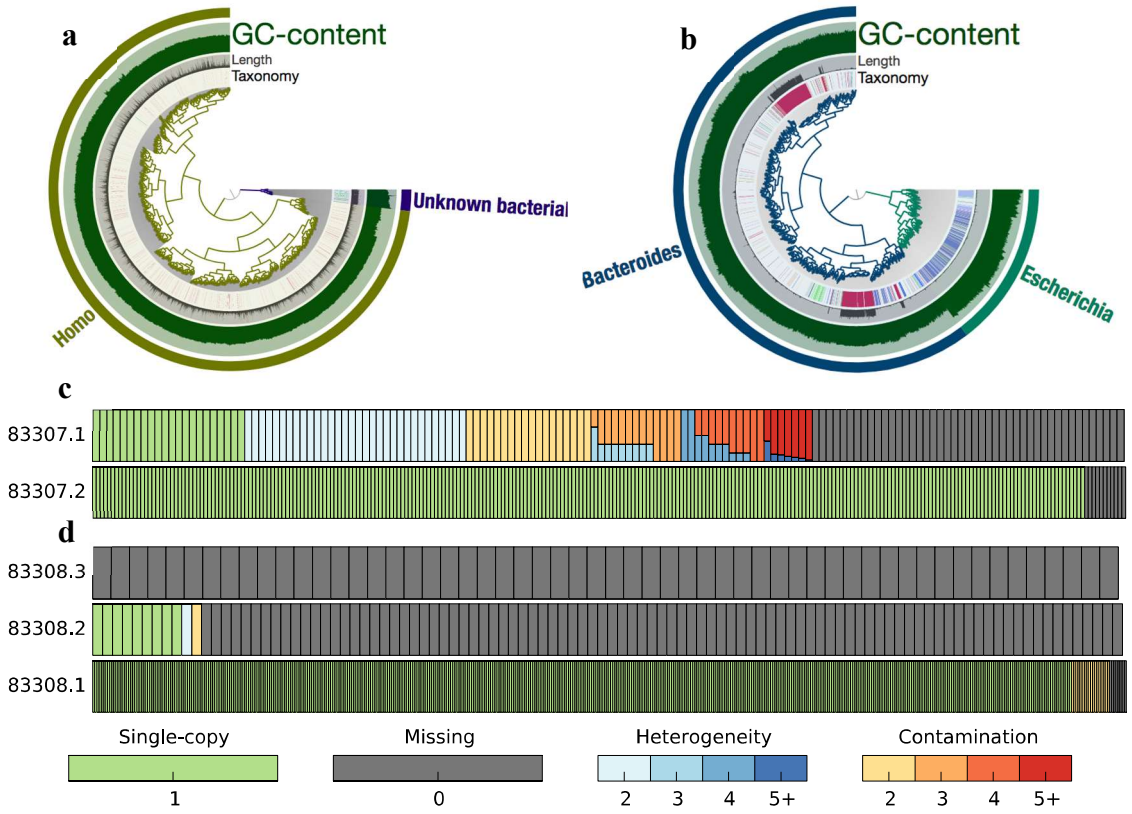

Figure 4.9: (a) Visualization of bins from S2-2 using anvi'o. (b) Visualization of bins from S2-4 using anvi'o. Second ring represents GC content, third ring represents the length of each contig, fourth ring represents the taxonomy. (c) Visualization of the Bin 1 (83307.1) and Bin 2 (83307.2) from S2-2 using metaBAT. (d) Visualization of Bin 1 (83308.1), Bin 2 (83308.2) and Bin 3 (83308.3) from S2-4 using metaBAT.

Bins from both samples were analyzed using MG-RAST and identity of each bin was confirmed. As S2-2 has a eukaryotic bin, analysis for S2-2 could not yield sufficient functional relationships since the software cannot analyze eukaryotes. For S2-4, one of the bins had too few contigs to be processed. The first and second bins were analyzed for identity and functionality. The first bin consists primarily of *Bacteroides* genes and

achieved up to 98% genome completeness. The second bin is less complete, but there are significantly more genes for *Parabacteroides* present in the second sample. Based on this information and due to the similarity of the *Bacteroides* and *Parabacteroides* species [165], it is possible the binning process could not differentiate between the two species' genomes. However, performing functional analysis, there are some correlations between the pathways found in the two bins (Figure 4.10). In amino acid metabolism, Bin 1 contained genes for valine, leucine, and isoleucine biosynthesis pathways while Bin 2 contained genes for valine, leucine, and isoleucine degradation. Bin 1 did contain a few genes for degradation but Bin 2 contained no genes for biosynthesis. Similarly, Bin 1 contains genes for lysine biosynthesis while Bin 2 contains genes for lysine degradation. This correlation is slightly weaker as the pathways for lysine degradation did occur in some capacity in Bin 1. Beyond amino acid metabolism, another interesting pathway highlighted is glycan metabolism. Bin 1 and Bin 2 both contain genes for peptidoglycan biosynthesis, but Bin 1 contains genes for mannosidase and fucosidase degradation while Bin 2 contains genes for glycosaminoglycan degradation. As many *Bacteroides* species are known for degradation of polysaccharides and glycan that the human host cannot degrade [166], it is possible this task is divided among different species. Overall, many of the genes found in Bin 1 are not present in Bin 2. This could be due to the incompleteness of the genome. However, interestingly, there are several genes from Bin 2 not present in Bin 1. Due to the completeness of Bin 1, it is unlikely this is due to incorrect binning. This indicates there is some mutualistic relationship between the two species.

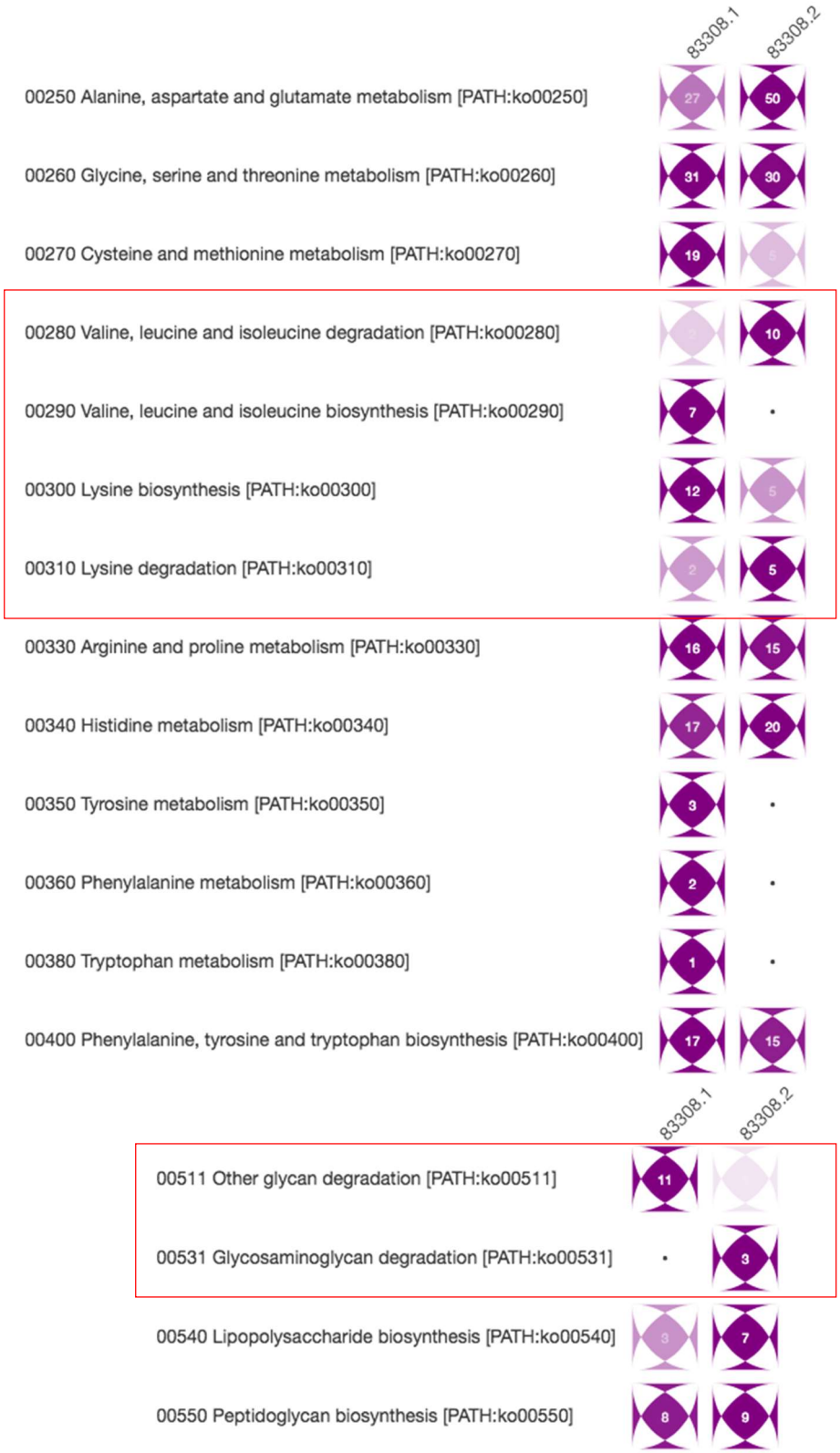

Figure 4.10: Functional analysis of amino acid and glycan pathways for degradataion and biosynthesis. 83308.1 is Bin 1 and 83308.2 is Bin2. Values in diamonds indicate number of genes present in each bin. Red boxes indicate pathways where there is potential complementarity between the two bins.

4.5 Conclusion

We have demonstrated a platform for droplet enabled anaerobic natural microbial community co-cultivation and analysis. The bacteria from the community can be separated into subsets within the droplets. The droplets can be cultured in large scale together and separated using the spacing and dispensing device described in the last chapter. Droplets were analyzed by amplifying the DNA and were screened by using T-RFLP. The samples were sequenced and we were able to determine some synergistic interactions in the amino pathways between the two major species in the droplet. This platform is a powerful tool for studying many different microbial communities to elucidate relationships between different species by compartmentalizing them in droplets. In addition, cultivation and imaging provide important information that sequencing cannot, such as morphology and special/temporal growth. The technology can be modified to be high-throughput by automating the spacing/dispensing process. We believe this tool is applicable for studying bacterial as well as host interactions for many systems.

4.6 Appendix

Table 4.2: Gut microbiota media components

Gut Micrbiota Media		
Component	Amount/L	Concentration
Tryptone peptone	2 g	0.2%
Yeast extract	1 g	0.1%
D-glucose	0.4 g	2.2 mM
L-cysteine	0.5 g	3.2 mM
Cellobiose	1 g	2.9 mM
Maltose	1 g	2.8 mM
Fructose	1 g	2.2 mM
Meat extract	5 g	0.5%
Potassium phosphate monobasic	100 mL (1M stock solution at pH 7.2)	100 mM
Magnesium sulfate heptahydrate	0.002 g	0.008 mM
Sodium carbonate	0.4 g	4.8 mM
Sodium chloride	0.08 g	1.37 mM
Calcium chloride	1 mL (0.8 g/100 mL stock)	0.80%
Vitamin K (menadione)	1 mL (1 mg/mL stock solution)	5.8 mM

Iron sulfate	1 mL (0.4 mg stock solution)	1.44 mM
Histidine hematin solution	1 mL (1.2 mg hematin/mL in 0.2M histidine	0.1%
Tween 80	2 mL (25% stock solution)	0.05%
ATCC vitamin mix	10 mL	1%
ATCC tracer mineral mix	10 mL	1%
Acetic acid	1.7 mL	30 mM
Isovaleric acid	0.1 mL	1 mM
Propionic acid	2 mL	8 mM
Butyric acid	2 mL	4 mM
Resazurin	4 mL (0.25 mg/mL stock solution)	4 mM

Chapter 5

Droplet-Enabled Cultivation of Endosymbiotic Bacteria from Tunicate

5.1 Summary

E. frumentensis is an endosymbiotic bacterium found in the marine animal tunicate that can produce a valuable compound for treating cancer. However, attempts to culture this bacterium have failed, as culture conditions are complex. We developed a method for extraction of the bacteria from within the tunicate cells. Using the cell content itself, we created a media for culturing in droplets. After cultivation, we found significant growth within the droplets. However, upon further analysis using T-RFLP, the bacteria cultured were not the targeted endosymbiont. While the platform remains viable, further work to understand the culture conditions for the bacteria are needed to successfully isolate it.

5.2 Introduction

Microbial communities beyond human microbiota are of great interest as they may offer new species of bacteria capable of improving agriculture [167,168], providing

valuable commodity chemicals [169], and treating contamination [170,171]. Previous studies [172,173] have found that the marine animal *Ecteinascidia turbinata* or tunicate produces low quantities of the compound Ecteinascidin-743 (ET-743), shown in Figure 5.1a and 5.1b. ET-743 is a compound used to treat ovarian cancer and soft tissue sarcoma. [174] Yields obtained from extraction of the tunicate are too low for commercial usage. The current methods of producing the drug through semi-synthetic means from fermentation-derived cyanosafracin B in 17 chemical steps is expensive. [7] Previous work [175] has found an endosymbiotic bacteria dubbed γ-proteobacteria *Candidatus Endoecteinascidia frumentensis* prevalent in nearly all *Ecteinascidia turbinata* samples. Further studies by Rath et al. [7] have identified *Candidatus Endoecteinascidia frumentensis* as the producer of ET-743 in the tunicate.

Work to focus on isolation of *E. frumentensis* for commercial usage has primarily focused on in vivo analysis and meta-genomic/meta-proteomic studies. In a previous study by Moss et al., FISH with *E. frumentensis* specific probe binding to the 16S rRNA was used to locate the regions where the bacteria reside within the tunicate cells [176]. More recently, meta-genomic work from the Sherman Lab at the University of Michigan has successfully sequenced the genome and mapped the metabolic pathway (Figure 5.1c) of *E. frumentensis* [7,8]. However, isolation of the bacteria and successful cultivation has yet to be achieved.

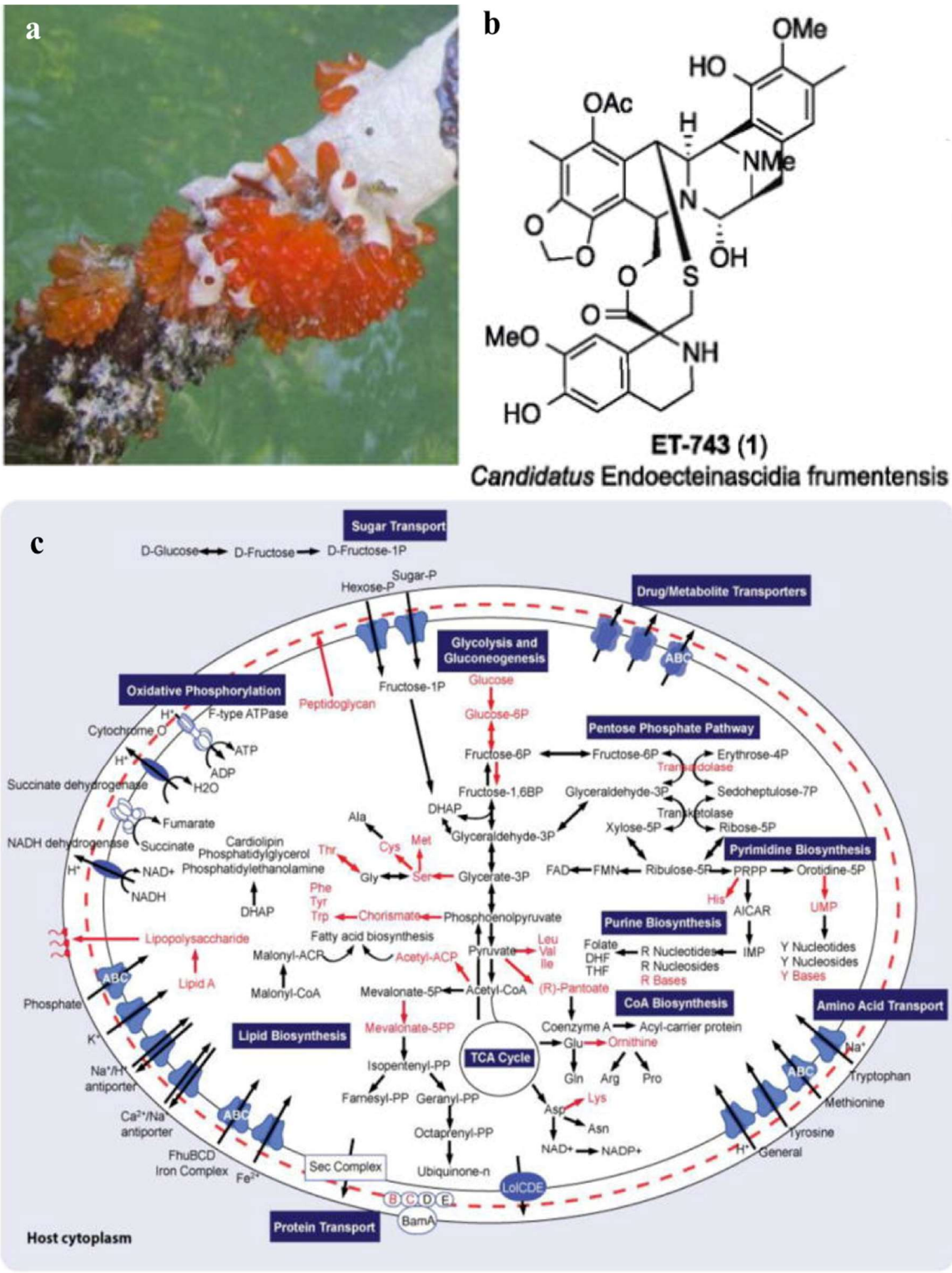

Figure 5.1: (a) Image of tunicate in its natural habitat. They are typically found growing on mangrove trees in the waters of the Caribbean Sea. (b) Molecular structure of ET-743. Similar to saframycin-B, current methods of production involve a complex 17-step reaction. (c) Metabolic map of *E. frumentensis* based on genome sequencing and assembly. Missing pathways are shown in red. As an endosymbiont, many of the commonly found pathways are missing as the host provides many of the intermediates and amino acids the bacteria needs. Figures a & b adapted from [7] and figure c adapted from [8].

Our developed microfluidic platform for gut microbiome cultivation can be

reconfigured for cultivation of this endosymbiotic bacterium. In order to extract the bacteria from within the tunicate cells, we developed a method modified from a previous paper for extraction of *Coxiella burnetii* [177], another endosymbiont. We also used droplet microfluidics to isolate single cells within each droplet and cultured the bacteria. Finally, using T-RFLP, we analyzed the cultured bacteria for *E. frumentensis*.

5.3 Materials and Methods

5.3.1 E. frumentensis Extraction

Frozen tunicate was thawed from -80°C at room temperature for 2 hours. After thawing, sterilized scissors were used to cut a quarter of the tunicate. Tunicate tissue was placed in a sterilized blender, 50 mL of DI water was added, and blended five times under the pulse setting. Everything was collected and filtered with multiple 20-µm Steriflip filter units (Millipore Sigma©). The trapped tissue on the filter was transferred to 1.5 mL micro-centrifuge tubes at approximately 0.5 g per aliquot.

For chemical lysis, the SPD buffer is used. The SPD buffer was made by mixing a solution with 1 mg/mL of digitonin, 250 mM sucrose and 1 mL of PBS. Additional concentrations were made by diluting this stock solution. 1 mL of the SPD buffer was added to each tube as desired and the tubes were incubated at room temperature for 30 minutes. Every 10 minutes, the solution was remixed by vortexing. For lysis by sonication, 1 mL of ddH_2O was added to each tube. The tube was placed in a water bath sonicator for 10 minutes. After lysis, all tubes were centrifuged at 1000 rpm to for 5 minutes and the supernatant was pipetted out as it contained the bacteria.

5.3.2 Culture Media

Tryptic soy broth (TSB) media was made by adding premade TSB powder to DI water. Additionally, 29 mM of fructose 1,6 bi-phosphate was added before autoclaving at the L20 cycle. Reinforced fructose media (RFM) was made by adding 0.5 g/L of potassium phosphase monobasic, 0.095 g/L magnesium chloride, 0.0015 g/L iron sulfate anhydrous, 7.28 g/L sodium chloride, 62.5 mL/L RPMI media, 5.0 g/L casamino acids, 5 mL horse serum, and 5.22 g/L fructose to water. After mixing, the media was sterilized by filtering through a 0.22-µm steri-filter.

Cell extract media (CEM) was made by taking tissue from the tunicate after blending to extract out nutrients. The tissue was placed in a 10 mL glass bottle containing a single glass bead and 1 mL of DI water was added. The sample was sonicated for 20 minutes in a water bath sonicator. Then, the sample was filtered through a 0.22-µm filter.

5.3.3 Droplet Cultivation

The bacterial extraction was counted by a hemocytometer to determine the cell density for droplet generation. After counting, the bacteria were diluted down to $\lambda = 2$, 10, and 50 cells per droplet along with $\lambda = 0$ to serve as the control. Droplets were generated on flow focusing generation device made of PDMS. In the aqueous channel, the media with various cell concentrations was introduced into the device by a syringe tip attached to Teflon tubing. In the oil channel, HFE-7500 perfluorinated oil (3M) mixed with 2% perfluoropolyether-polyethyleneglycol surfactant (RAN Biotechnology) was added by the same method. The liquids were driven in the channel by pneumatic pressure controlled via LabVIEW. Droplets were generated by adjusting the two

pressures in the oil and aqueous channels until droplets formed at a steady rate. Generation was monitored on an inverted phase contrast Nikon microscope on the 4X objective. Generated droplets were transferred via 500-µm diameter Teflon tubing connected to Eppendorf tubes. Approximately 500 µL of droplets were collected for each sample and covered with mineral oil to prevent evaporation. The samples were incubated at 28°C for 5 days. Additionally, 10 µL of droplets were dispensed into an INCYTO C-Chip disposable hemocytometer for imaging. After imaging, the openings to the hemocytometer were sealed with Epoxy, and the samples were incubated for 5 days. Imaging was done on an inverted phase contrast Nikon microscope on the 20X objective.

5.3.4 PCR and T-RFLP Analysis of Droplet Cultured Bacteria

Droplets from the incubation in the hemocytometer were collected by peeling off the epoxy glue with a razor blade, opening up the hemocytometer, and withdrawing the droplets using a pipette. Droplets were destabilized using 5 µL of 1*H*,1*H*,2*H*,2*H*-perfluoro-1-octanol (Sigma Aldrich). The DNA from the cells was extracted using the Qiagen DNEasy Blood and Tissue Kit.

PCR primers for amplification of the 16S rDNA were designed on 3 Prime. Primers were ordered from Integrated DNA Technology. Primers 8F (5'-AGAGTTTGATCCTGGCTCAG-3') and 1492R (5'-CGGTTACCTTGTTACGACTT-3') were used for PCR amplification of the whole 16S rDNA. The 8F primer had a 6-FAM fluorescence marker attached. Primers specific to *E. frumentensis* were Specific Forward (5'-TGGTTAAGAGCTGATATATTTGACG-3') and Specific Reverse (5'-CACCGGAAATTCCTCTACCC-3'). PCR amplification was conducted with the droplet samples, extracted tunicate DNA for a positive control, and *E. coli* DNA for a negative

control. After amplification, results were verified by gel electrophoresis with a 0.75% agarose gel. The PCR products were cleaned up using the Qiagen© PCR Purification Kit. Target specific PCR products were submitted for Sanger sequencing at the University of Michigan Sequencing Core. Sequencing data was compiled on Geneious© 8 by combining the forward and reverse reads for each sample. Then, the resulting sequence was aligned to a reference for similarity.

For T-RFLP analysis, the 16S amplified samples, extracted tunicate DNA sample, and *E. coli* DNA control were digested using New England BioLabs© MSPI and RSAI enzymes for 2 hours at 37°C. The digested samples were filtered using Qiagen© Nucleotide Purification Kit. A 96-well plate containing the ROX-1000 size standard dye was obtained from University of Michigan Sequencing Core for the T-RFLP analysis. 3 µL of digested samples were dispensed into each well in duplicates and submitted for T-RFLP to the Core. After T-RFLP, the data was analyzed using Applied Biosystems© Peak Scanner Software v1.0 to obtain fragment length and height. The data was plotted using a script written in R.

5.4 Result and Discussion

5.4.1 Endosymbiont Extraction and Analysis

Endosymbiotic bacteria are difficult to extract owing to their location within their hosts. The challenge lies in finding a technique for successful lysis of the eukaryotic cell membrane while maintaining viability of the bacteria within the cell. Thus, this "Goldilocks" conundrum (not too harsh, not too gentle) requires testing and verification to determine the best method. Utilizing two methods, chemical and sonication, we found

both methods could successfully lyse the eukaryotic cell wall to varying degrees of success.

The precursor to the lysis using these two techniques is a mechanical disruption using a blender. The solution is filtered to remove any cells that remain in the supernatant as previous experiments conducted by Jihyang Park have demonstrated that extracellular bacteria in the sample can grow robustly in droplets. We then used a chemical lysis agent called digitonin, known to be a gentle detergent, and water bath sonication to lyse the cells. After lysis, centrifugation at low speed removes any cellular particulates, which reduces DNA from the cells in the sample, as well as prevent clogging in the microfluidic device. The bacteria extracted were analyzed with T-RFLP to determine extraction of the *E. frumentensis* and best suitable extraction method. A schematic of this process is shown in Figure 5.2. T-RFLP is used for two reasons: (1) identification of *E. frumentensis* and (2) fingerprinting of other species in the sample. Since the peak height of *E. frumentensis* is known (503 bp), T-RFLP will confirm the presence of the target and quantify the amount of the target in the sample. Three extraction locations were used: 1st supernatant, 3rd supernatant, and precipitate. The 1st and 3rd supernatant indicates the number of times the extraction was performed. After centrifugation, the supernatant was removed and the extraction method was applied again to the precipitate. In addition to these locations, 4 extraction methodologies were applied: 0.2 M digitonin, 1.0 M digitonin, 2-minute sonication, and 10-minute sonication.

We performed T-RFLP on the 1st supernatant for the 4 extraction conditions. All 4 conditions successfully extracted the target bacteria at varying quantities. The 0.2 M digitonin concentration performed the best (Figure 5.3), representing 13% of the bacterial

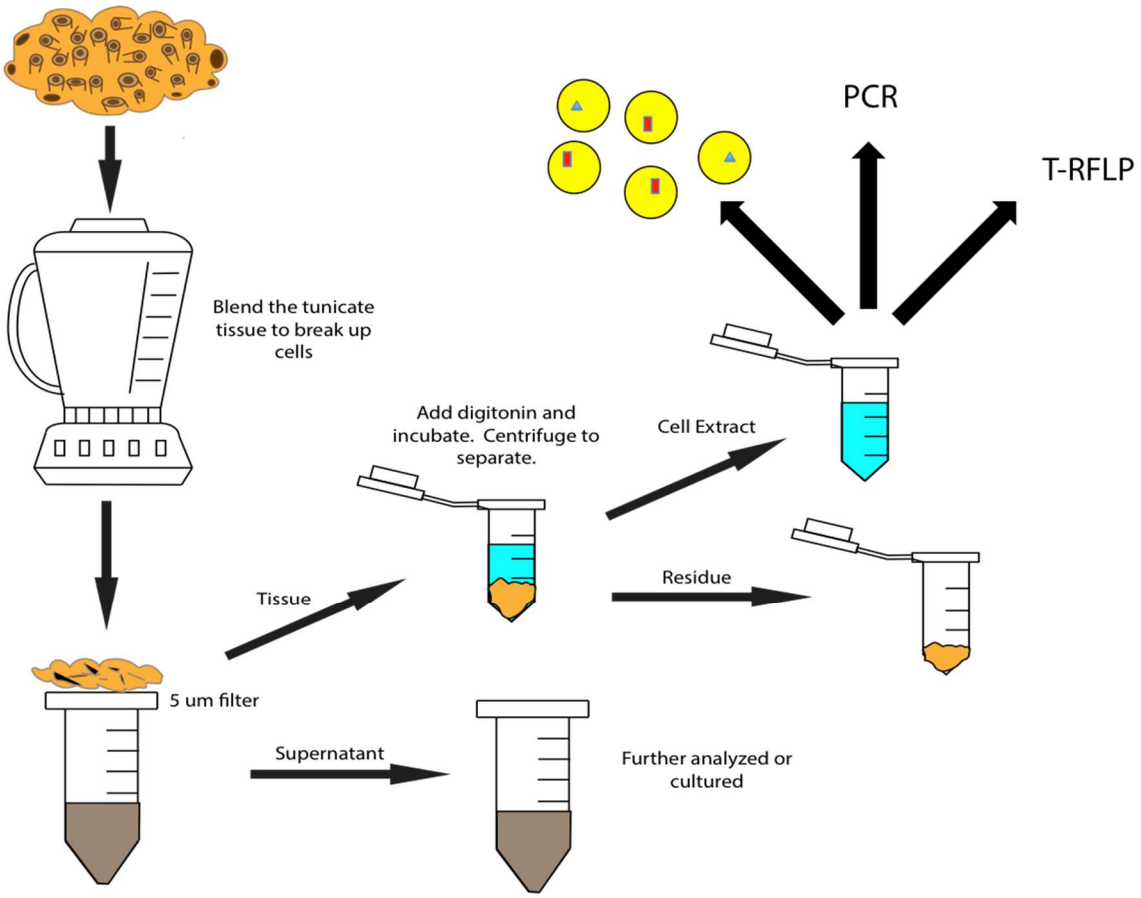

Figure 5.2: Process for extraction of *E. frumentensis* from tunicate cells. Whole tissue is broken up using a blender. The tissue is filtered out from the extracellular bacteria. The cells are lysed and centrifugation separated the bacteria from the rest of the tissue. The bacteria can then used for culturing or analysis.

sample. It is important to note that higher concentrations of digitonin and longer sonication times actually resulted in lower extraction efficiency of the target. One potential explanation for this phenomenon is that too harsh of an extraction can result in the lysis of the bacteria as well. Other peaks in the sample indicate other bacterial species are present as a result of insufficient separation from the extracellular bacteria or the presence of other endosymbionts in the sample. 3rd supernatant samples contained no *E. frumentensis* likely due to extraction of the majority of the target in the 1st and 2nd extractions. The precipitate still contained a large portion of the target with the highest concentration in the 0.2 M condition at 20.6%. This indicates the extraction conditions

provided were insufficient to lyse all of the cells. Combined with the data from the 3rd supernatant, additional lysis steps do not increase the number of cells lysed and the remaining bacteria are retained in the cells. Based on this information, we recommend using the 0.2 M digitonin as the lysis procedure going forward for extraction of endosymbionts in tunicate cells.

5.4.2 Droplet Cultivation and Analysis

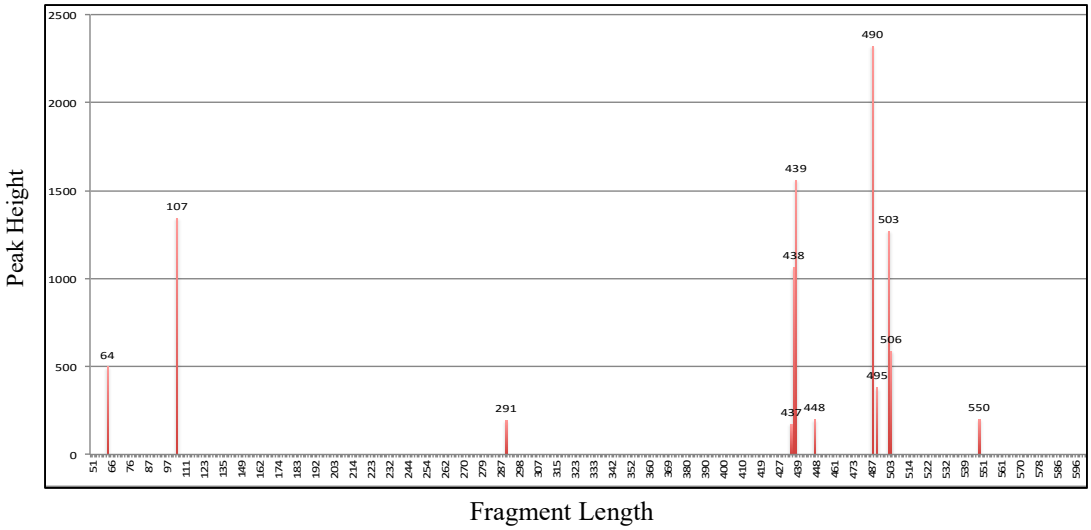

Figure 5.3: T-RFLP results using the most optimized extraction protocol at 0.2 M digitonin.

Three different media were utilized for the cultivation of *E. frumentensis*: Tryptic Soy Broth (TSB), Fructose Reinforced Media (FRM), and CEM (Cell Extract Media). Because the conditions inside the host cells are unknown, media usage is one of the biggest unknown factors in successful cultivation of the targeted bacteria. TSB was selected as a rich media owing to its generic usage in many bacterial cultures. FRM is a modified media from the cultivation of *Coxiella burnetii*, another γ-proteobacteria endosymbiont. Typically, *C. burnetii* is cultivated in an citrate rich environment as its a pathogenic bacteria responsible for Q fever [178]. Analysis of *E. frumentensis*'

metabolic pathway shows that it cannot properly utilize glucose as a carbon source. Thus, we added Fructose 1,6 bi-phosphate as a replacement for the needed carbon source to modify the media resulting in the fructose reinforced media. Finally, endosymbionts often rely on other components besides nutrients from their hosts such as signaling molecules; we produced a media using the cell extract from the tunicate to mimic the host environment. The extraction process was performed in a water bath sonicator using a glass bead for disruption [179]. Subsequently, the mixture is filtered through a 0.22 μm filter to ensure no cells remain in the media. While the media is more diluted compared to the inside of the host cells, the theoretical components are there for cultivation. Other culture conditions are aerobic incubation, assuming the host cell provides sufficient oxygen to the bacteria, and incubation temperature at 28°C. The natural environment of the tunicates used is the Caribbean Sea, which has an average water temperature around 28°C [180].

Besides media, we also selected 3 different λ values for cultivation since the viability of these bacteria after cultivation was unknown. The λ values were 2, 10, and 50 as well as 0 for the negative control. Cultivation was performed with the droplets stored in both tubes and C-Chips. After cultivation, droplets from both storage methods were imaged. In the C-Chip samples, considerable growth occurred in all cell concentrations for the CEM after 5 days except for the negative control (Figure 5.4). For both the TSB and RFM samples, no growth was observed in the droplets. However, for the droplets cultured in the tube, no growth for all three media were observed after 5 days. The cause for this lack of growth could be due to factors such as insufficient oxygen provided to the cells. After cultivation in droplets, the bacteria from the CEM

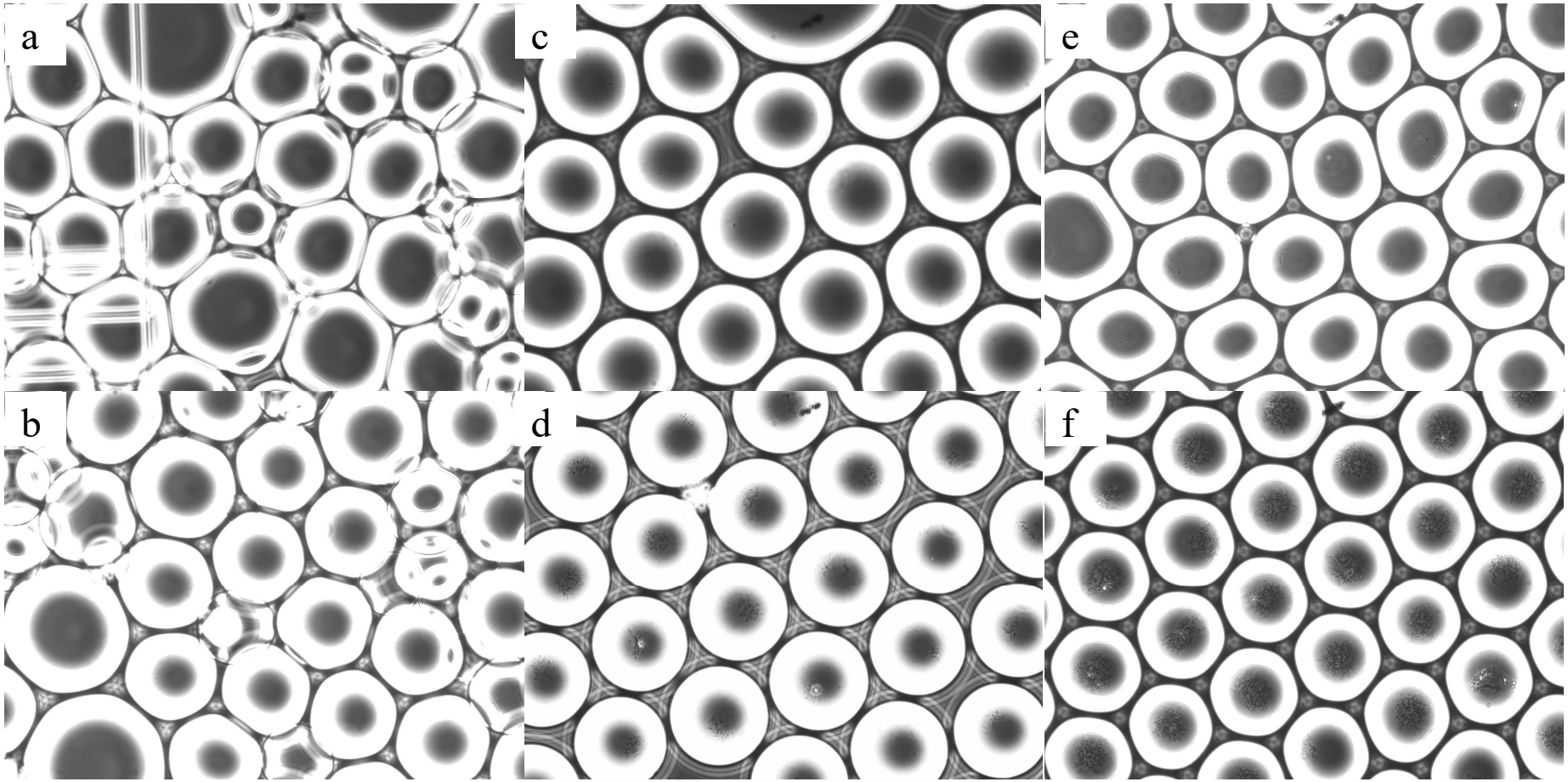

Figure 5.4: Droplet cultures of bacteria extracted from tunicate cells using Cell Extracted Media (CEM). (a) 0 cells at 0 days (b) 0 cells at 5 days (c) 2 cells at 0 days (d) 2 cells at 5 days (e) 50 cells at 0 days (f) 50 cells at 5 days.

were transferred to an Eppendorf tube containing 1 mL of the CEM for scale-up. The resulting scaled-up culture was imaged (Figure 5.5).

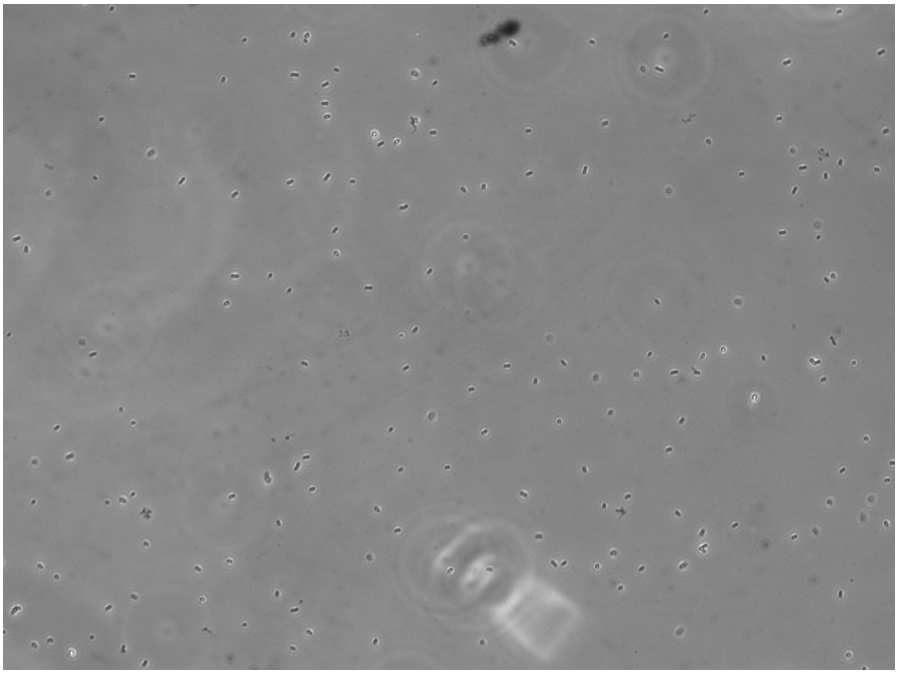

Figure 5.5: Cells cultured in CEM from the droplets. Images taken with a 10X objective lens.

5.4.3 PCR and T-RFLP Analysis of Droplet Culture

PCR and T-RFLP were used to probe the 16S rDNA of the cultures cultivated to determine if the cultures contained *E. frumentensis*. PCR using primers specific to the target were designed by taking the 16S of all the known bacterial species in the tunicate sample. The sequences were aligned and highly mismatched regions were used to design the forward and reverse primers, ensuring specificity to the *E. frumentensis.* The primers were verified by amplifying on the extracted tunicate DNA. Subsequently, the amplicon from the control was sequenced via Sanger sequencing and aligned to the expected amplicon sequence. The resulting alignment was 99.6% verifying the primer was successful at amplifying the *E. frumentensis* 16S. T-RFLP was similarly performed on

the extracted tunicate DNA and demonstrated a high abundance of the *E. frumentensis* target at the 503 peak.

PCR and T-RFLP analysis were performed on the extracted samples before cultivation. Samples from the supernatant, cell extract and the residue were analyzed. DNA extraction was performed with two different extraction kits: Promega© and Qiagen©. The Promega© kit uses isopropanol to precipitate the DNA while the Qiagen kit uses a filter to separate the DNA. PCR amplification with the 16S and species-specific primers was performed. Results from amplification using gel electrophoresis suggest either insufficient DNA or inhibition during PCR in the 16S as the cell extract samples did not amplify. However, species-specific amplification occurred in all sites indicating presence of the target. T-RFLP was conducted on the samples with 16S amplification. Based on the results seen in Figure 5.6a, amplification of the target at peak 503 is seen in the Qiagen© kit extracted samples on the supernatant samples. However, using the Promega© kit samples, the 503 peak was not observed. Also note the fluorescence peaks from each, there is a significantly higher signal from the Promega© kits. This could indicate the extraction process differs for the two kits that resulted in a higher amount of one species in the sample to release its DNA. Thus, the signal from the other species does not show up in the T-RFLP plot, as it is significantly lower. For the cell extract sample, there was insufficient signal for any analysis. In the residue samples, only the Promega samples were amplified successfully. In Figure 5.6b, the peak 503 is one of the lower peaks indicating a small presence of the target. In all of the samples, peak 492 was seen as the predominant peak in all of the samples. This peak could not be identified, as the whole 16S of all the species in the tunicate was not sequenced

previously. Compared to the controlled DNA, we find there is significant amplification of the target in this sample. One explanation for this phenomenon is different tunicates were used for samples and control.

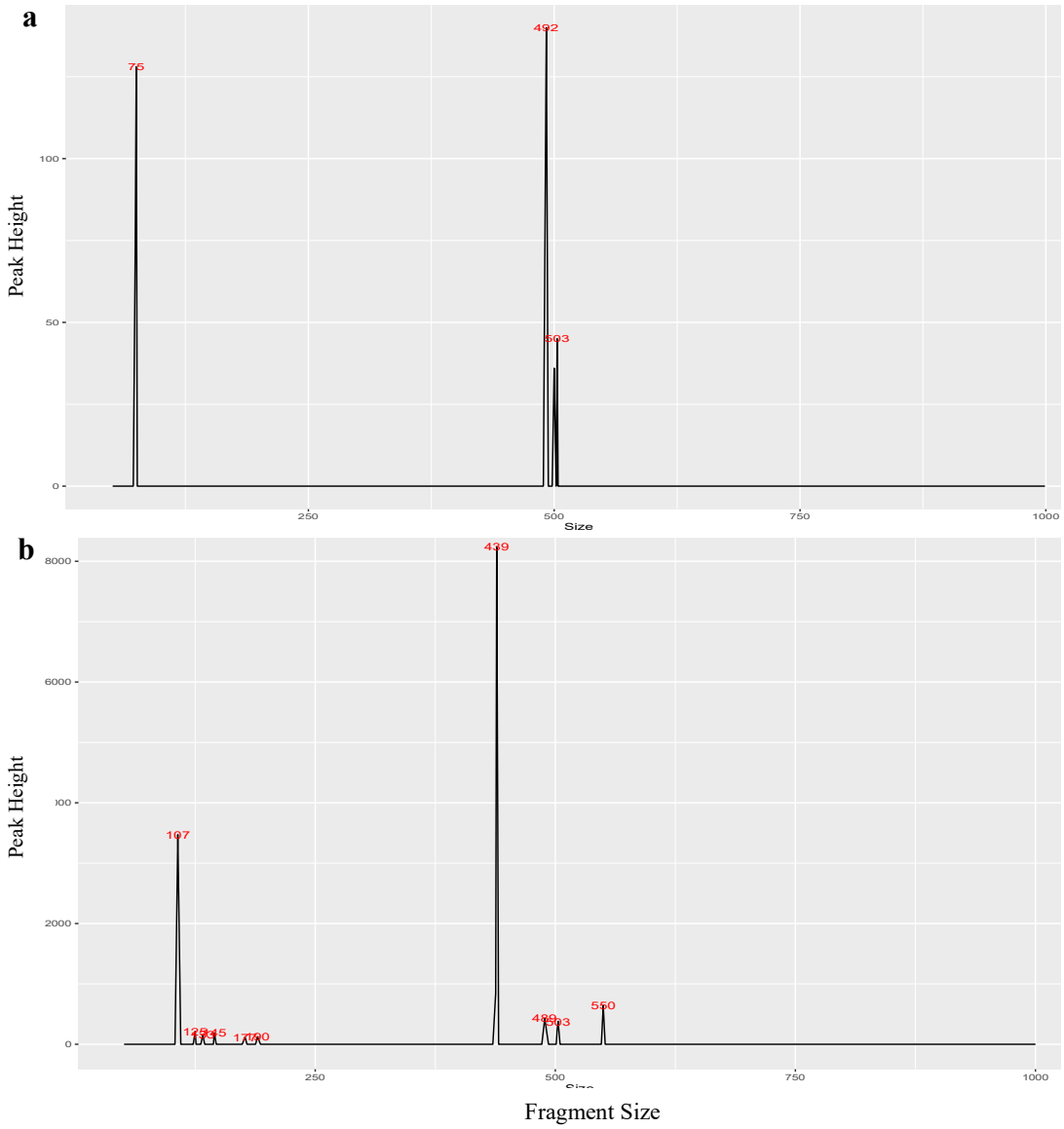

Figure 5.6: (a) T-RFLP results of cells from the supernatant using the Qiagen DNA extraction kit. (b) T-RFLP results of cells from the residue using the Promega DNA extraction kit.

Analysis of the droplets and scaled-up culture was conducted similarly using PCR and T-RFLP. Two volumes of the extracted DNA were used: 0.5 µL and 15 µL. After

amplification of the droplet culture and scaled-up culture, gel electrophoresis of the amplicons showed no amplification of the 16S using either kit except for a faint band with 15 µL using the Qiagen kit on droplets. Species-specific primer did amplify for the majority of the samples, but non-specific amplification also occurred for the blank sample. Sanger sequencing was performed on the species-specific amplicons from the droplet, but the resulting sequencing results showed no reads for the samples submitted and ones with reads could not be aligned in respect to the forward and reverse reads. Samples submitted to T-RFLP indicated most the samples contained peaks at 103 and 109, but no target (Figure 5.7). Ultimately, the results of the analysis indicated the bacteria cultured in the droplets were not the targets.

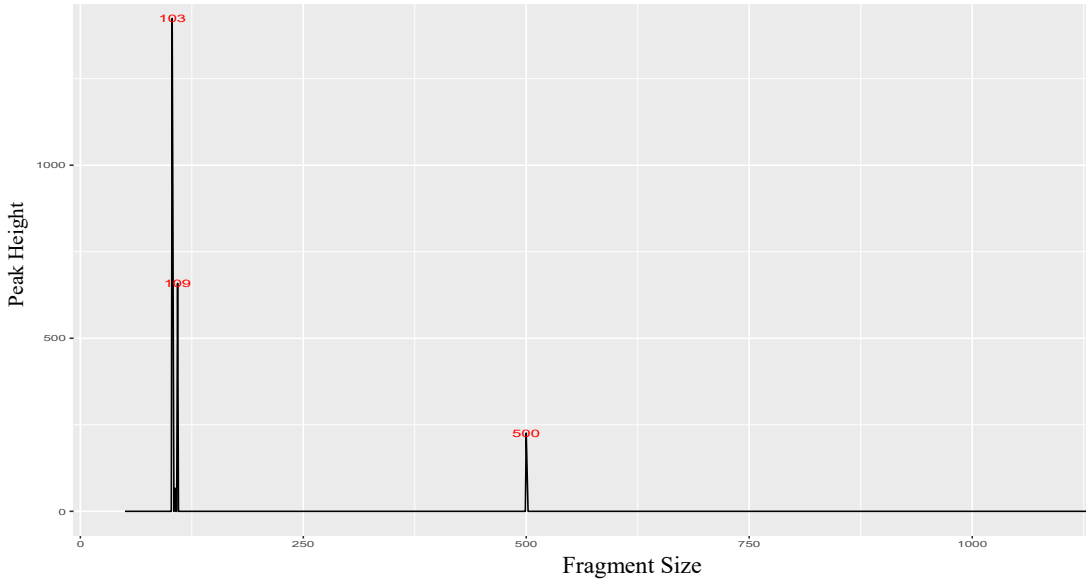

Figure 5.7: T-RFLP results from bacteria initially cultured in droplets then transferred to a tube culture for scale-up. The culture is grown in CEM.

5.5 Conclusion

We have demonstrated work towards culturing endosymbiotic bacteria from a marine animal. While we were not successful in culturing the target, progress has been made in understanding this bacteria. It is clear based on the analysis via PCR and T-

RFLP that this target is present in the samples. The extraction method we demonstrated was successful in lysing the tunicate cells and extracting the target. However, repeating the process on a different tunicate resulted in much lower abundance of the target suggesting the density of the species is variable across samples. Using a unique process, we devised a media using the extract of the tunicate cells and we cultured a bacterial species using this media. PCR and T-RFLP analysis indicate that this species is not the *E. frumentensis.* Endosymbiotic bacteria are extremely complex and their cultivation conditions are not well understood. Further work is needed to understand these conditions for *E. frumentensis* to successfully be cultured outside of its host.

Chapter 6

Conclusion and Future Work

6.1 Conclusion

The work of this thesis aimed to continue the advancement of droplet microfluidic technology and its usage in studying microbial communities. How we look at microbes in the human body and their role in governing our health has evolved significantly in the last decade. However, there are still significant gaps in knowledge in our understanding in the human microbiome, due in large part to the number of species yet to be cultured and analyzed within these communities. Traditional laboratory techniques using pure species cultivation does not account for the interactions in communities that are necessary for many species to grow and thrive. Droplet microfluidics offers the tools needed for culturing and studying these "unculturables" as it provides high-throughput sample generation and offers the compartmentalization of subsets within the community to study interactions. Similarly, downstream analysis technology allows these samples to be analyzed at a rapid pace. However, development for manipulation of the droplets and overcoming small sample sizes for future laboratory analysis are still needed.

In our first aim, we demonstrated the development and proof-of-concept for a simple droplet content separation device. Using only pneumatic lines, we were able to separate a desired target (microparticles) from the droplet using functionalized beads. The target is subsequently recaptured on-chip and we analyzed the efficacy of the device by determining yield and specific recovery at different concentrations of the target versus impurities. Yield increased as the number of targets in the sample decreased while conversely specific recovery increased as the number of targets in the sample increased.

Spacing and dispensing of single droplets is another important application, especially in the context of studying microbial cultures. We developed a two layer pneumatically operated device for dispensing single droplets from a bulk collection into tubes. Then, to tackle the issue of limited cell content for analysis, we performed MDA to amplify the DNA and demonstrated successful amplification of both single and multiple species DNA via RT-PCR. We also worked on quantification of these droplets using direct RT-PCR.

Finally, to demonstrate some applications of the droplet technology we developed, we developed a platform for co-cultivation of bacteria from the human gut. This platform involves co-cultivation in droplets followed by DNA amplification via MDA and analysis using both T-RFLP and next generation sequencing. After sequencing analysis, we identified some complementarity of amino acid pathways between two species in a single droplet based on the genes each species lacks.

We also applied a similar system for cultivation of an endosymbiotic bacterium *E. frumentensis.* To extract the bacteria, we developed a technique for breaking the cell membrane while retaining viability of the target bacteria. While we were successful in

extracting the bacteria from within the cells, cultivation proved difficult due to the complex conditions in which these bacteria grow.

6.2 Future Work

6.2.1 Droplet Separation/Droplet Spacing and Dispensing

Significant progress has been made in both technologies for droplet manipulation in terms of separation and dispensing. However, there are improvements for enhancing the technology for future applicability. For the droplet content separation system in Chapter 3, automation is an important next step to allow for the system to achieve high-throughput operation. This can be achieved by adding sensors on the device to detect viscosity changes demonstrated in Figure 6.1a. The device detects the droplet interface as it enters the post region and the programming for the pressure regulation stops the flow of the subsequent droplets from entering the post region. Then, once the droplet passes through the posts, the viscosity changes signal for the device to generate a new droplet for re-encapsulation. After a programmed period of time, the new droplet containing the target can be removed. This could significantly speed up rates to allow for separation of thousands of droplets. Additional channels can be added for easier retrieval of the re-encapsulated droplets as the current design does require retrieval to be done through the droplet inlet channel. Increasing flowrates in the channel could further decrease device operation time. As the balance of pressures in the channel is important, varying these pressures to optimize the capture and re-encapsulation time is needed.

In addition, the surface functionalization needs to be extended beyond micro-particles. Capture of other targets such as bacteria, cells and DNA would be highly desirable to bring this technology to wider applicability. For example, single species

separation can be performed with this device in complex communities by encapsulating subsets of the community within a droplet. Using an antibody specific to the target, the bacteria of interest could be captured and separated from the rest of the community. This target can be easily retrieved from the device for analysis or further culturing. Another application is the separation of DNA probes for performing FISH. Since FISH uses a fluorescent DNA probe, washing must be performed to remove unbound probes. Thus, by attaching a biotin molecule it is possible to capture unbound probes from the droplet and separating the probes from the cells. The cells can be captured downstream or re-encapsulated by redesigning the device. This concept can also be applied to any process that requires washing like ELISA.

Droplet spacing and dispensing from Chapter 4 can also benefit from automation by detection software such as LabVIEW. Droplet imaging detection controls the valve for spacing and enables automatic spacing and dispensing of droplets. When the imaging detects a droplet approach the spacing junction, the valve can be programmed to be open. Once that droplet is no longer detected by the imaging, the valve closes again. A certain amount of time is allotted before the next droplet can be spaced to ensure sufficient time to allow the first droplet to be dispensed. Automation could be further enhanced by including attaching the droplet dispensing tubing to an X-Y-Z positioner (Figure 6.1b) for automated dispensing into well-plates. Currently, each droplet dispensation is allotted a certain amount of time to ensure ample time for the droplet to transfer from the device to the tube. Based on this time interval, the positioner could be programmed to move after each allotted time.

This pneumatic system could even be reconfigured to achieve sorting by adding another channel to form a Y-junction. The valve is placed on one side of the junction that is shorter in length compared to the other junction. When the valve is open, the resistance in that channel is lower allowing a droplet to flow into that channel. When the valve is closed, the resistance is higher than the other channel forcing the droplet to move to the other channel. Using this technique, droplets can be sorted.

Future advancements in DNA amplification to reduce bias could enable quantification of cell numbers in a droplet and obtain more accurate genomes for sequencing. This would provide a powerful tool for future applications as both amplification of small sample sizes and quantification of those samples could be achieved. In the meantime, troubleshooting and optimization of the qPCR step by reducing errors from aqueous separation and improved DNA extraction could enable accurate quantification of the cells in the droplet.

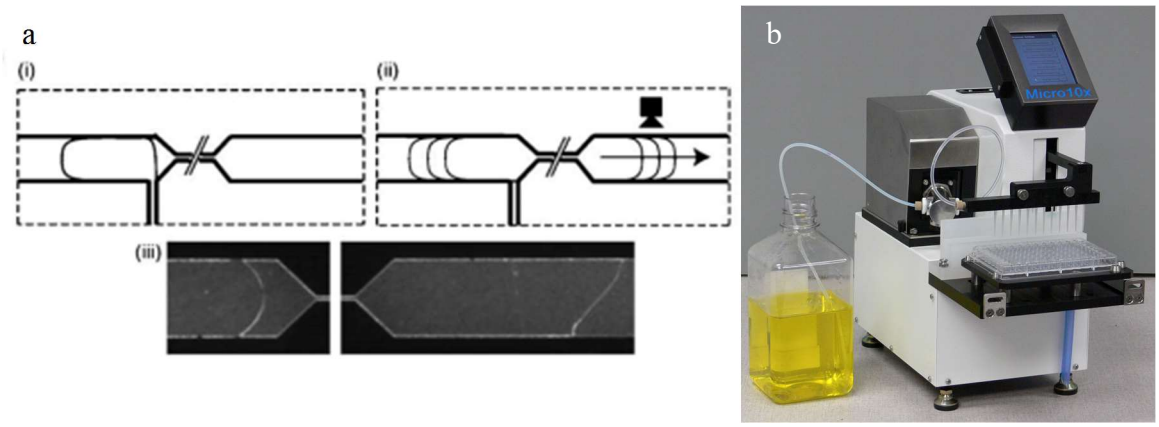

Figure 6.1: (a) Example of a microfluidic droplet viscometer that senses the interface between two phases.[9] (b) Commercial X-Y-Z system for automated dispensing into a 96 well-plate from Hudson Robotics©.

6.2.2 Application of Droplet Cultivation and Analysis for Culturing Novel Bacteria

With our droplet co-cultivation platform, many of the challenges came from the sequencing analysis of the droplet. Better resolution sequencing such as Illumina Hi-Seq and PacBio could resolve the issues with low coverage and enable better binning of the meta-genomic data. In addition, the usage of a different DNA amplification technique could allow for better quality DNA since low coverage for one species is often a result of the bias from MDA. Techniques such as MAL-BAC could be easily adapted to this platform for improving coverage uniformity as this process can be conducted off-chip. Technological improvements such as consistent droplet generation in the anaerobic chamber would improve consistency in droplet cultures. Setting up a process to ensure the device remains bound to the microscope would improve consistency of generation. A better set-up for pressure controls in the chamber with a more precise syringe pump would ensure more monodisperse droplets caused by hysteresis effects during generation. While the resulting sequences yielded in poor genome completion for some of the bins, better sequencing results in the future could provide more accurate functional information for identifying complementarity. Other software for quality control and assembly should be considered as loss of reads can cause significant problems downstream with incomplete genomes.

Media and oxygen conditions are extremely important facets to culturing and in this work, only four media were used and one oxygen condition. In future work, other media such as minimal, species specific, or real environmental media (from the gut) could enable different diversity cultures. Oxygen conditions should also be varied, as there are bacteria in the gut that are micro-aerobic or even facultative anaerobes. This

system could easily be applied to many other body sites with easily attainable environmental media. We previously demonstrate cultivation of microbial communities obtained from plaque samples using concentrated saliva (Figure 6.2). We were able to amplify the cultures from droplets, but the process was not refined during single droplet dispensing. It would be insightful to split a droplet and perform the culture scale-up and MDA amplification to compare the resulting cultures. This could tell us the effects of MDA on real culture samples and ascertain how similar the scaled-up culture is compared to the MDA amplified DNA. In addition, scale-up can also be performed by biofilm forming devices and studying the differences between the planktonic culture and biofilm cultures could provide information on this effect.

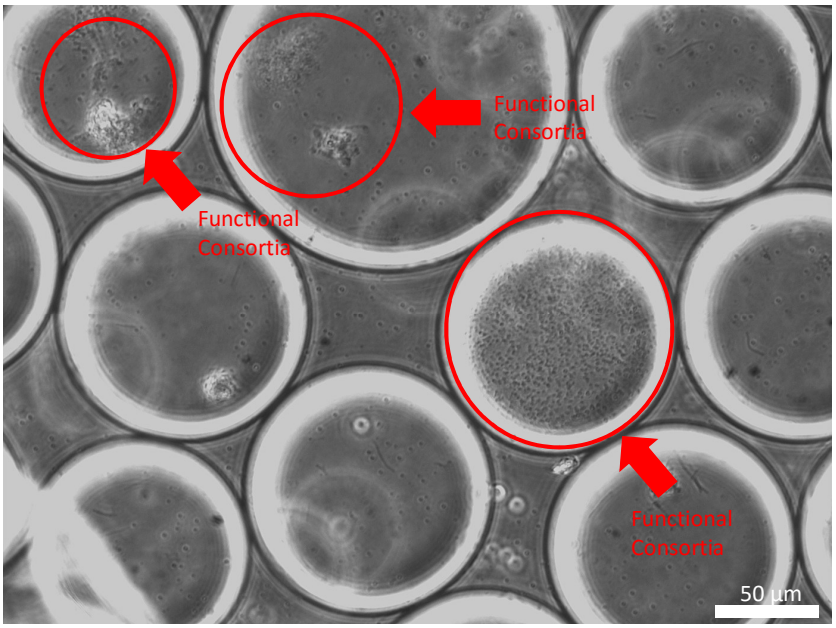

Figure 6.2: Cultivation of bacteria extracted from human plaque. The cultivation media is 10X concentrated saliva. Bacteria were cultured for 4 days.

Finally, *E. frumentensis* cultivation could benefit from improvements on the bacterial extraction. While our analysis verified existence of the target in the sample, viability remains a question. A live-dead stain analysis would allow for confirmation of

the bacteria. It would be beneficial to verify live-dead staining by identifying some mark genes for viability of the bacteria. With our extraction method analysis, there are still many bacteria that did not get released from the cells. Further optimization of the extraction methodology would be helpful for future culturing. Varying the digitonin concentrations further and trying some alternative lysis buffers could help extract more of the microbes from the tunicate. In addition, the usage of sonication did result in extraction of the target. However, no further work to culture the microbes from this extraction method was done. Cultivation of bacteria from this extraction method could provide insight into viability of the cells compared to the digitonin. Further work on understanding culture conditions are needed, as the host environment is still largely unknown. Studying the metabolites within the host cell could provide the needed answers for culture conditions such as signaling molecules or intermediates. This analysis could be performed by mass spectrometry or HPLC. Finally, if cultivation cannot be achieved, insertion of genes for ET-743 production into another species should be considered.

BIBLIOGRAPHY

1. Wang S, Sung K-J, Lin XN, Burns MA (2017) Bead mediated separation of microparticles in droplets. PLOS ONE 12: e0173479.
2. ThermoFisher (2017).
3. Lasken RS, McLean JS (2014) Recent advances in genomic DNA sequencing of microbial species from single cells. Nat Rev Genet 15: 577-584.
4. Turnbaugh PJ, Ley RE, Hamady M, Fraser-Liggett C, Knight R, Gordon JI (2007) The human microbiome project: exploring the microbial part of ourselves in a changing world. Nature 449: 804-810.
5. Rastogi G, Sani RK (2011) Molecular Techniques to Assess Microbial Community Structure, Function, and Dynamics in the Environment. New York, NY: Springer New York. pp. 29.
6. Escobar-Zepeda A, Vera-Ponce de León A, Sanchez-Flores A (2015) The Road to Metagenomics: From Microbiology to DNA Sequencing Technologies and Bioinformatics. Frontiers in Genetics 6.
7. Rath CM, Janto B, Earl J, Ahmed A, Hu FZ, Hiller L, et al. (2011) Meta-omic characterization of the marine invertebrate microbial consortium that produces the chemotherapeutic natural product ET-743. ACS chemical biology 6: 1244-1256.
8. Schofield MM, Jain S, Porat D, Dick GJ, Sherman DH (2015) Identification and analysis of the bacterial endosymbiont specialized for production of the chemotherapeutic natural product ET-743. Environ Microbiol 17: 3964-3975.
9. Livak-Dahl E, Lee J, Burns MA (2013) Nanoliter droplet viscometer with additive-free operation. Lab Chip 13: 297-301.
10. Konopka A (2009) What is microbial community ecology? The ISME Journal 3: 1223.
11. Ding T, Schloss PD (2014) Dynamics and associations of microbial community types across the human body. Nature 509: 357-360.
12. Sender R, Fuchs S, Milo R (2016) Revised estimates for the number of human and bacteria cells in the body. bioRxiv.
13. Amann RI, Ludwig W, Schleifer K-H (1995) Phylogenetic identification and in situ detection of individual microbial cells without cultivation. Microbiological reviews 59: 143-169.

14. Head I, Saunders J, Pickup R (1998) Microbial evolution, diversity, and ecology: a decade of ribosomal RNA analysis of uncultivated microorganisms. Microbial ecology 35: 1-21.
15. Rappé MS, Giovannoni SJ (2003) The uncultured microbial majority. Annual Reviews in Microbiology 57: 369-394.
16. Bartram AK, Lynch MD, Stearns JC, Moreno-Hagelsieb G, Neufeld JD (2011) Generation of multimillion-sequence 16S rRNA gene libraries from complex microbial communities by assembling paired-end illumina reads. Appl Environ Microbiol 77: 3846-3852.
17. Wolin M, Miller T, Stewart C (1997) Microbe-microbe interactions. The rumen microbial ecosystem: Springer. pp. 467-491.
18. Ventola CL (2015) The Antibiotic Resistance Crisis: Part 1: Causes and Threats. Pharmacy and Therapeutics 40: 277-283.
19. Al-Awadhi H, Dashti N, Khanafer M, Al-Mailem D, Ali N, Radwan S (2013) Bias problems in culture-independent analysis of environmental bacterial communities: a representative study on hydrocarbonoclastic bacteria. SpringerPlus 2: 369.
20. Eisenhauer N, Scheu S, Jousset A (2012) Bacterial Diversity Stabilizes Community Productivity. PLOS ONE 7: e34517.
21. MacLean D, Jones JD, Studholme DJ (2009) Application of'next-generation'sequencing technologies to microbial genetics. Nature reviews Microbiology 7: 287.
22. Metzker ML (2010) Sequencing technologies--the next generation. Nature reviews Genetics 11: 31.
23. Handelsman J (2004) Metagenomics: application of genomics to uncultured microorganisms. Microbiology and molecular biology reviews 68: 669-685.
24. Wilmes P, Bond PL (2006) Metaproteomics: studying functional gene expression in microbial ecosystems. Trends in microbiology 14: 92-97.
25. Woo PCY, Lau SKP, Teng JLL, Tse H, Yuen KY (2008) Then and now: use of 16S rDNA gene sequencing for bacterial identification and discovery of novel bacteria in clinical microbiology laboratories. Clinical Microbiology and Infection 14: 908-934.
26. Forsman M, Sandström G, Jaurin B (1990) Identification of Francisella species and discrimination of type A and type B strains of F. tularensis by 16S rRNA analysis. Applied and Environmental Microbiology 56: 949-955.
27. Klijn N, Weerkamp AH, de Vos WM (1991) Identification of mesophilic lactic acid bacteria by using polymerase chain reaction-amplified variable regions of 16S rRNA and specific DNA probes. Applied and Environmental Microbiology 57: 3390-3393.
28. Marsh TL (1999) Terminal restriction fragment length polymorphism (T-RFLP): an emerging method for characterizing diversity among homologous populations of amplification products. Current opinion in microbiology 2: 323-327.
29. Lozupone CA, Stombaugh JI, Gordon JI, Jansson JK, Knight R (2012) Diversity, stability and resilience of the human gut microbiota. Nature 489: 220-230.
30. Shendure J, Ji H (2008) Next-generation DNA sequencing. Nature biotechnology 26: 1135.

31. Song H, Tice JD, Ismagilov RF (2003) A Microfluidic System for Controlling Reaction Networks in Time. Angewandte Chemie International Edition 42: 768-772.
32. Garstecki P, Fuerstman MJ, Stone HA, Whitesides GM (2006) Formation of droplets and bubbles in a microfluidic T-junction—scaling and mechanism of break-up. Lab on a Chip 6: 437-446.
33. Livak-Dahl E, Sinn I, Burns M (2011) Microfluidic chemical analysis systems. Annu Rev Chem Biomol Eng 2: 325-353.
34. Guo MT, Rotem A, Heyman JA, Weitz DA (2012) Droplet microfluidics for high-throughput biological assays. Lab on a Chip 12: 2146-2155.
35. Baret J-C (2012) Surfactants in droplet-based microfluidics. Lab on a Chip 12: 422-433.
36. Teh S-Y, Lin R, Hung L-H, Lee AP (2008) Droplet microfluidics. Lab on a Chip 8: 198-220.
37. Mazutis L, Baret J-C, Griffiths AD (2009) A fast and efficient microfluidic system for highly selective one-to-one droplet fusion. Lab on a Chip 9: 2665-2672.
38. Abate AR, Hung T, Mary P, Agresti JJ, Weitz DA (2010) High-throughput injection with microfluidics using picoinjectors. Proceedings of the National Academy of Sciences.
39. Paik P, Pamula VK, Fair RB (2003) Rapid droplet mixers for digital microfluidic systems. Lab on a Chip 3: 253-259.
40. Brouzes E, Medkova M, Savenelli N, Marran D, Twardowski M, Hutchison JB, et al. (2009) Droplet microfluidic technology for single-cell high-throughput screening. Proceedings of the National Academy of Sciences 106: 14195-14200.
41. Lederberg J (1954) A simple method for isolating individual microbes. Journal of bacteriology 68: 258.
42. Bjork SM, Sjostrom SL, Andersson-Svahn H, Joensson HN (2015) Metabolite profiling of microfluidic cell culture conditions for droplet based screening. Biomicrofluidics 9: 044128.
43. Najah M, Griffiths AD, Ryckelynck M (2012) Teaching single-cell digital analysis using droplet-based microfluidics. ACS Publications.
44. Boedicker JQ, Li L, Kline TR, Ismagilov RF (2008) Detecting bacteria and determining their susceptibility to antibiotics by stochastic confinement in nanoliter droplets using plug-based microfluidics. Lab on a Chip 8: 1265-1272.
45. Churski K, Kaminski TS, Jakiela S, Kamysz W, Baranska-Rybak W, Weibel DB, et al. (2012) Rapid screening of antibiotic toxicity in an automated microdroplet system. Lab on a Chip 12: 1629-1637.
46. Agresti JJ, Antipov E, Abate AR, Ahn K, Rowat AC, Baret JC, et al. (2010) Ultrahigh-throughput screening in drop-based microfluidics for directed evolution. Proc Natl Acad Sci U S A 107: 4004-4009.
47. Kintses B, Hein C, Mohamed MF, Fischlechner M, Courtois F, Lainé C, et al. (2012) Picoliter cell lysate assays in microfluidic droplet compartments for directed enzyme evolution. Chemistry & biology 19: 1001-1009.
48. Grodrian A, Metze J, Henkel T, Martin K, Roth M, Köhler JM (2004) Segmented flow generation by chip reactors for highly parallelized cell cultivation. Biosensors and bioelectronics 19: 1421-1428.

49. Park J, Kerner A, Burns MA, Lin XN (2011) Microdroplet-Enabled Highly Parallel Co-Cultivation of Microbial Communities. PLoS ONE 6: e17019.
50. Weitz M, Mückl A, Kapsner K, Berg R, Meyer A, Simmel FC (2013) Communication and computation by bacteria compartmentalized within microemulsion droplets. Journal of the American Chemical Society 136: 72-75.
51. Ma L, Kim J, Hatzenpichler R, Karymov MA, Hubert N, Hanan IM, et al. (2014) Gene-targeted microfluidic cultivation validated by isolation of a gut bacterium listed in Human Microbiome Project's Most Wanted taxa. Proceedings of the National Academy of Sciences 111: 9768-9773.
52. Choi J-W, Oh KW, Thomas JH, Heineman WR, Halsall HB, Nevin JH, et al. (2002) An integrated microfluidic biochemical detection system for protein analysis with magnetic bead-based sampling capabilities. Lab on a Chip 2: 27-30.
53. Wang C, Oleschuk R, Ouchen F, Li J, Thibault P, Harrison DJ (2000) Integration of immobilized trypsin bead beds for protein digestion within a microfluidic chip incorporating capillary electrophoresis separations and an electrospray mass spectrometry interface. Rapid Communications in Mass Spectrometry 14: 1377-1383.
54. Oku Y, Uesaka Y, Hirayama T, Takeda Y (1988) Development of a Highly Sensitive Bead-ELISA to Detect Bacterial Protein Toxins. Microbiology and Immunology 32: 807-816.
55. Sinn I, Kinnunen P, Albertson T, McNaughton BH, Newton DW, Burns MA, et al. (2011) Asynchronous magnetic bead rotation (AMBR) biosensor in microfluidic droplets for rapid bacterial growth and susceptibility measurements. Lab on a Chip 11: 2604-2611.
56. Ali MF, Kirby R, Goodey AP, Rodriguez MD, Ellington AD, Neikirk DP, et al. (2003) DNA Hybridization and Discrimination of Single-Nucleotide Mismatches Using Chip-Based Microbead Arrays. Analytical Chemistry 75: 4732-4739.
57. Ng JK, Selamat ES, Liu W-T (2008) A spatially addressable bead-based biosensor for simple and rapid DNA detection. Biosensors and Bioelectronics 23: 803-810.
58. Lim CT, Zhang Y (2007) Bead-based microfluidic immunoassays: The next generation. Biosensors and Bioelectronics 22: 1197-1204.
59. Hindson BJ, Ness KD, Masquelier DA, Belgrader P, Heredia NJ, Makarewicz AJ, et al. (2011) High-Throughput Droplet Digital PCR System for Absolute Quantitation of DNA Copy Number. Analytical Chemistry 83: 8604-8610.
60. Pinheiro LB, Coleman VA, Hindson CM, Herrmann J, Hindson BJ, Bhat S, et al. (2012) Evaluation of a Droplet Digital Polymerase Chain Reaction Format for DNA Copy Number Quantification. Analytical Chemistry 84: 1003-1011.
61. Dewan A, Kim J, McLean RH, Vanapalli SA, Karim MN (2012) Growth kinetics of microalgae in microfluidic static droplet arrays. Biotechnology and Bioengineering 109: 2987-2996.
62. Moon H, Cho SK, Garrell RL (2002) Low voltage electrowetting-on-dielectric. Journal of applied physics 92: 4080-4087.
63. Lee J, Moon H, Fowler J, Schoellhammer T, Kim C-J (2002) Electrowetting and electrowetting-on-dielectric for microscale liquid handling. Sensors & Actuators: A Physical 95: 259.

64. Shah GJ, Ohta AT, Chiou EPY, Wu MC, Kim C-JCJ (2009) EWOD-driven droplet microfluidic device integrated with optoelectronic tweezers as an automated platform for cellular isolation and analysis. Lab on a Chip - Miniaturisation for Chemistry and Biology 9: 1732.
65. Cho SK, Zhao Y, Kim CJ (2007) Concentration and binary separation of micro particles for droplet-based digital microfluidics. Lab Chip 7: 490-498.
66. Zhao Y, Chakrabarty K. Synchronization of washing operations with droplet routing for cross-contamination avoidance in digital microfluidic biochips; 2010. ACM. pp. 635-640.
67. Teste B, Ali-Cherif A, Viovy JL, Malaquin L (2013) A low cost and high throughput magnetic bead-based immuno-agglutination assay in confined droplets. Lab Chip 13: 2344-2349.
68. Pan X, Zeng S, Zhang Q, Lin B, Qin J (2011) Sequential microfluidic droplet processing for rapid DNA extraction. Electrophoresis 32: 3399-3405.
69. Brouzes E, Kruse T, Kimmerling R, Strey HH (2015) Rapid and continuous magnetic separation in droplet microfluidic devices. Lab Chip 15: 908-919.
70. Lee H, Xu L, Oh KW (2014) Droplet-based microfluidic washing module for magnetic particle-based assays. Biomicrofluidics 8: 044113.
71. Kim JA, Kim M, Kang SM, Lim KT, Kim TS, Kang JY (2015) Magnetic bead droplet immunoassay of oligomer amyloid beta for the diagnosis of Alzheimer's disease using micro-pillars to enhance the stability of the oil-water interface. Biosens Bioelectron 67: 724-732.
72. Jung JH, Destgeer G, Ha B, Park J, Sung HJ (2016) On-demand droplet splitting using surface acoustic waves. Lab on a Chip 16: 3235-3243.
73. Fornell A, Nilsson J, Jonsson L, Periyannan Rajeswari PK, Joensson HN, Tenje M (2015) Controlled Lateral Positioning of Microparticles Inside Droplets Using Acoustophoresis. Analytical Chemistry 87: 10521-10526.
74. Kurup GK, Basu AS (2012) Field-free particle focusing in microfluidic plugs. Biomicrofluidics 6: 022008.
75. Hein M, Moskopp M, Seemann R (2015) Flow field induced particle accumulation inside droplets in rectangular channels. Lab on a Chip 15: 2879-2886.
76. Brosseau Q, Vrignon J, Baret J-C (2014) Microfluidic Dynamic Interfacial Tensiometry ([small mu]DIT). Soft Matter 10: 3066-3076.
77. Tan Y-C, Cristini V, Lee AP (2006) Monodispersed microfluidic droplet generation by shear focusing microfluidic device. Sensors and Actuators B: Chemical 114: 350-356.
78. Baret JC, Miller OJ, Taly V, Ryckelynck M, El-Harrak A, Frenz L, et al. (2009) Fluorescence-activated droplet sorting (FADS): efficient microfluidic cell sorting based on enzymatic activity. Lab Chip 9: 1850-1858.
79. Cao Z, Chen F, Bao N, He H, Xu P, Jana S, et al. (2013) Droplet sorting based on the number of encapsulated particles using a solenoid valve. Lab on a Chip 13: 171-178.
80. Ahmed R, Jones TB (2006) Dispensing picoliter droplets on substrates using dielectrophoresis. Journal of Electrostatics 64: 543-549.
81. Ahmed R, Jones TB (2007) Optimized liquid DEP droplet dispensing. Journal of Micromechanics and Microengineering 17: 1052-1058.

82. Choi W-K, Lebrasseur E, Al-Haq MI, Tsuchiya H, Torii T, Yamazaki H, et al. (2007) Nano-liter size droplet dispenser using electrostatic manipulation technique. Sensors and Actuators A: Physical 136: 484-490.
83. Garrell AIaRL (2010) Pico-droplet dispensing control in digital microfluidic systems. 49th IEEE Conference on Decision and Control (CDC): pp. 4583-4586.
84. FerraroP, CoppolaS, GrilliS, PaturzoM, VespiniV (2010) Dispensing nano-pico droplets and liquid patterning by pyroelectrodynamic shooting. Nat Nano 5: 429-435.
85. Kuoni A, Boillat M, Derooij N (2003) Two-dimensional parallel dispenser for microarray printing. Journal of the Association for Laboratory Automation 8: 24-28.
86. Mazutis L, Gilbert J, Ung WL, Weitz DA, Griffiths AD, Heyman JA (2013) Single-cell analysis and sorting using droplet-based microfluidics. Nat Protoc 8: 870-891.
87. Sciambi A, Abate AR (2015) Accurate microfluidic sorting of droplets at 30 kHz. Lab Chip 15: 47-51.
88. Brouzes E, Carniol A, Bakowski T, Strey HH (2014) Precise pooling and dispensing of microfluidic droplets towards micro- to macro-world interfacing. RSC Advances 4: 38542-38550.
89. Au SH, Shih SC, Wheeler AR (2011) Integrated microbioreactor for culture and analysis of bacteria, algae and yeast. Biomed Microdevices 13: 41-50.
90. Mazutis L, Araghi AF, Miller OJ, Baret J-C, Frenz L, Janoshazi A, et al. (2009) Droplet-Based Microfluidic Systems for High-Throughput Single DNA Molecule Isothermal Amplification and Analysis. Analytical Chemistry 81: 4813-4821.
91. Edgcomb VP, McDonald JH, Devereux R, Smith DW (1999) Estimation of Bacterial Cell Numbers in Humic Acid-Rich Salt Marsh Sediments with Probes Directed to 16S Ribosomal DNA. Applied and Environmental Microbiology 65: 1516-1523.
92. Blanco L, Bernad A, Lazaro JM, Martin G, Garmendia C, Salas M (1989) Highly efficient DNA synthesis by the phage phi 29 DNA polymerase. Symmetrical mode of DNA replication. J Biol Chem 264: 8935-8940.
93. Zong C, Lu S, Chapman AR, Xie XS (2012) Genome-wide detection of single-nucleotide and copy-number variations of a single human cell. Science 338: 1622-1626.
94. Liang L, Wang CT, Sun X, Liu L, Li M, Witz C, et al. (2013) Identification of chromosomal errors in human preimplantation embryos with oligonucleotide DNA microarray. PLoS One 8: e61838.
95. de Bourcy CFA, De Vlaminck I, Kanbar JN, Wang J, Gawad C, Quake SR (2014) A Quantitative Comparison of Single-Cell Whole Genome Amplification Methods. PLOS ONE 9: e105585.
96. Lizardi PM (2000) Multiple displacement amplification. Google Patents.
97. Paez JG, Lin M, Beroukhim R, Lee JC, Zhao X, Richter DJ, et al. (2004) Genome coverage and sequence fidelity of phi29 polymerase-based multiple strand displacement whole genome amplification. Nucleic Acids Res 32: e71.
98. Dean FB, Hosono S, Fang L, Wu X, Faruqi AF, Bray-Ward P, et al. (2002) Comprehensive human genome amplification using multiple displacement amplification. Proc Natl Acad Sci U S A 99: 5261-5266.

99. Raghunathan A, Ferguson HR, Bornarth CJ, Song W, Driscoll M, Lasken RS (2005) Genomic DNA Amplification from a Single Bacterium. Applied and Environmental Microbiology 71: 3342-3347.
100. Wu L, Liu X, Schadt CW, Zhou J (2006) Microarray-based analysis of subnanogram quantities of microbial community DNAs by using whole-community genome amplification. Appl Environ Microbiol 72: 4931-4941.
101. Yokouchi H, Fukuoka Y, Mukoyama D, Calugay R, Takeyama H, Matsunaga T (2006) Whole-metagenome amplification of a microbial community associated with scleractinian coral by multiple displacement amplification using ϕ29 polymerase. Environmental Microbiology 8: 1155-1163.
102. Rhee M, Light YK, Meagher RJ, Singh AK (2016) Digital Droplet Multiple Displacement Amplification (ddMDA) for Whole Genome Sequencing of Limited DNA Samples. PLoS One 11: e0153699.
103. Yilmaz S, Allgaier M, Hugenholtz P (2010) Multiple displacement amplification compromises quantitative analysis of metagenomes. Nat Methods 7: 943-944.
104. Nishikawa Y, Hosokawa M, Maruyama T, Yamagishi K, Mori T, Takeyama H (2015) Monodisperse Picoliter Droplets for Low-Bias and Contamination-Free Reactions in Single-Cell Whole Genome Amplification. PLoS One 10: e0138733.
105. Sidore AM, Lan F, Lim SW, Abate AR (2016) Enhanced sequencing coverage with digital droplet multiple displacement amplification. Nucleic Acids Res 44: e66.
106. Chang HW, Sung Y, Kim KH, Nam YD, Roh SW, Kim MS, et al. (2008) Development of microbial genome-probing microarrays using digital multiple displacement amplification of uncultivated microbial single cells. Environ Sci Technol 42: 6058-6064.
107. Leung K, Klaus A, Lin BK, Laks E, Biele J, Lai D, et al. (2016) Robust high-performance nanoliter-volume single-cell multiple displacement amplification on planar substrates. Proc Natl Acad Sci U S A 113: 8484-8489.
108. Leung K, Zahn H, Leaver T, Konwar KM, Hanson NW, Page AP, et al. (2012) A programmable droplet-based microfluidic device applied to multiparameter analysis of single microbes and microbial communities. Proc Natl Acad Sci U S A 109: 7665-7670.
109. Koschwanez JH, Carlson RH, Meldrum DR (2009) Thin PDMS Films Using Long Spin Times or Tert-Butyl Alcohol as a Solvent. PLoS ONE 4: e4572.
110. Magoc T, Salzberg SL (2011) FLASH: fast length adjustment of short reads to improve genome assemblies. Bioinformatics 27: 2957-2963.
111. Joshi NA, Fass JN (2011) Sickle: A sliding-window, adaptive, quality-based trimming tool for FastQ files.
112. Langmead B, Salzberg SL (2012) Fast gapped-read alignment with Bowtie 2. Nat Meth 9: 357-359.
113. Li H, Handsaker B, Wysoker A, Fennell T, Ruan J, Homer N, et al. (2009) The Sequence Alignment/Map format and SAMtools. Bioinformatics 25: 2078-2079.
114. R Development Core Team (2010) R: A language and environment for statistical computing. Vienna, Austria: R Foundation for Statistical Computing.
115. Benjamini Y, Speed TP (2012) Summarizing and correcting the GC content bias in high-throughput sequencing. Nucleic Acids Research 40: e72-e72.

116. Dohm JC, Lottaz C, Borodina T, Himmelbauer H (2008) Substantial biases in ultra-short read data sets from high-throughput DNA sequencing. Nucleic Acids Res 36: e105.
117. Cowles CE, Nichols NN, Harwood CS (2000) BenR, a XylS homologue, regulates three different pathways of aromatic acid degradation in Pseudomonas putida. J Bacteriol 182: 6339-6346.
118. Ibekwe AM, Grieve CM (2003) Detection and quantification of Escherichia coli O157:H7 in environmental samples by real-time PCR. J Appl Microbiol 94: 421-431.
119. Shreiner AB, Kao JY, Young VB (2015) The gut microbiome in health and in disease. Current opinion in gastroenterology 31: 69-75.
120. Nelson KE, Weinstock GM, Highlander SK, Worley KC, Creasy HH, Wortman JR, et al. (2010) A catalog of reference genomes from the human microbiome. Science 328: 994-999.
121. Nielsen HB, Almeida M, Juncker AS, Rasmussen S, Li J, Sunagawa S, et al. (2014) Identification and assembly of genomes and genetic elements in complex metagenomic samples without using reference genomes. Nat Biotech 32: 822-828.
122. Qin J, Li R, Raes J, Arumugam M, Burgdorf KS, Manichanh C, et al. (2010) A human gut microbial gene catalogue established by metagenomic sequencing. Nature 464: 59-65.
123. Stewart EJ (2012) Growing Unculturable Bacteria. Journal of Bacteriology 194: 4151-4160.
124. Yu F, Blainey PC, Schulz F, Woyke T, Horowitz MA, Quake SR (2017) Microfluidic-based mini-metagenomics enables discovery of novel microbial lineages from complex environmental samples. bioRxiv.
125. Andrews S FastQC A Quality Control tool for High Throughput Sequence Data.
126. Nurk S, Bankevich A, Antipov D, Gurevich AA, Korobeynikov A, Lapidus A, et al. (2013) Assembling single-cell genomes and mini-metagenomes from chimeric MDA products. J Comput Biol 20: 714-737.
127. Gurevich A, Saveliev V, Vyahhi N, Tesler G (2013) QUAST: quality assessment tool for genome assemblies. Bioinformatics 29: 1072-1075.
128. Camacho C, Coulouris G, Avagyan V, Ma N, Papadopoulos J, Bealer K, et al. (2009) BLAST+: architecture and applications. BMC Bioinformatics 10: 421-421.
129. Kang DD, Froula J, Egan R, Wang Z (2015) MetaBAT, an efficient tool for accurately reconstructing single genomes from complex microbial communities. PeerJ 3: e1165.
130. Eren AM, Esen ÖC, Quince C, Vineis JH, Morrison HG, Sogin ML, et al. (2015) Anvi'o: an advanced analysis and visualization platform for 'omics data. PeerJ 3: e1319.
131. gridengine – Project home[http://gridengine.sunsource.net/%5D.
132. SQLite[http://www.sqlite.org/%5D.
133. Paarmann D, Paczian T, Meyer F: SEED-Viewer – a web user interface for studying genomics datasets. unpublished.

134. Altschul SFl, Madden TL, Schaffer AA, Zhang J, Zhang Z, Miller W, et al. (1997) Gapped BLAST and PSI-BLAST: a new generation of protein database search programs. Nucleic Acids Res 25.
135. Aziz RK, Bartels D, Best AA, DeJongh M, Disz T, Edwards RA, et al. (2008) The RAST Server: Rapid Annotations using Subsystems Technology. BMC Genomics.
136. Cole JR, Chai B, Farris RJ, Wang Q (2007) The ribosomal database project (RDP-II): introducing myRDP space and quality controlled public data. Nucleic Acids Res.
137. DeSantis TZ, Hugenholtz P, Larsen N, Rojas M, Brodie EL, Keller K, et al. (2006) Greengenes, a chimera-checked 16S rRNA gene database and workbench compatible with ARB. Appl Environ Microbiol 72.
138. Dinsdale EA, Edwards RA, Hall D, Angly F, Breitbart M, Brulc JM, et al. (2008) Functional Metagenomic Profiling of Nine Biomes. Nature.
139. Edwards RA, Rodriguez-Brito B, Wegley L, Haynes M, Breitbart M, Peterson DM, et al. (2006) Using pyrosequencing to shed light on deep mine microbial ecology. BMC Genomics 7.
140. Field D, Morrison N, Selengut J, Sterk P (2006) Meeting report: eGenomics: Cataloguing our Complete Genome Collection II. Omics 10.
141. Fierer N, Breitbart M, Nulton J, Salamon P, Lozupone C, Jones R, et al. (2007) Metagenomic and small-subunit rRNA analyses reveal the genetic diversity of bacteria archaea, fungi, and viruses in soil. Appl Environ Microbiol 73.
142. Huse SM, Huber JA, Morrison HG, Sogin ML, Welch DM (2007) Accuracy and quality of massively parallel DNA pyrosequencing. Genome biology 8.
143. Jarvie T (2006). personal communication.
144. Krause L, Diaz NN, Bartels D, Edwards RA, Puhler A, Rohwer F, et al. (2006) Finding novel genes in bacterial communities isolated from the environment. Bioinformatics 22.
145. Leplae R, Hebrant A, Wodak SJ, Toussaint A (2004) ACLAME: a CLAssification of Mobile genetic Elements. Nucleic Acids Res.
146. Liang F, Holt I, Pertea G, Karamycheva S, Salzberg SL, Quackenbush J (2000) An optimized protocol for analysis of EST sequences. Nucleic Acids Res 28.
147. Margulies M, Egholm M, Altman WE, Attiya S, Bader JS, Bemben LA, et al. (2005) Genome sequencing in microfabricated high-density picolitre reactors. Nature 437.
148. McHardy AC, Martin HG, Tsirigos A, Hugenholtz P, Rigoutsos I (2007) Accurate phylogenetic classification of variable-length DNA fragments. Nature methods 4.
149. McNeil LK, Reich C, Aziz RK, Bartels D, Cohoon M, Disz T, et al. (2007) The National Microbial Pathogen Database Resource (NMPDR): a genomics platform based on subsystem annotation. Nucleic Acids Res.
150. Meyer F, Overbeek R, Rodriquez A (2008). FIGfams – Yet another protein family collection.
151. Meyer F, Paarmann D, D'Souza M, Olson R, Glass E, Kubal M, et al. (2008) The metagenomics RAST server – a public resource for the automatic phylogenetic and functional analysis of metagenomes. BMC Bioinformatics 9: 386.

152. Mou XSS, Edwards RA, Hodson RE, Moran MA (2008) Generalist Species Dominate Bacterial Carbon Processing in the Coastal Ocean. Nature.
153. Overbeek R, Begley T, Butler RM, Choudhuri JV, Diaz N, Chuang H-Y, et al. (2005) The Subsystems Approach to Genome Annotation and its Use in the Project to Annotate 1000 Genomes. Nucleic Acids Res.
154. Rodriguez-Brito B, Rohwer F, Edwards RA (2006) An application of statistics to comparative metagenomics. BMC bioinformatics [electronic resource] 7.
155. Rohwer F (2007). personal communication.
156. Tringe SG, von Mering C, Kobayashi A, Salamov AA, Chen K, Chang HW, et al. (2005) Comparative metagenomics of microbial communities. Science 308.
157. Tyson GW, Chapman J, Hugenholtz P, Allen EE, Ram RJ, Richardson PM, et al. (2004) Community structure and metabolism through reconstruction of microbial genomes from the environment. Nature 428.
158. Venter JC, Remington K, Heidelberg JF, Halpern AL, Rusch D, Eisen JA, et al. (2004) Environmental genome shotgun sequencing of the Sargasso Sea. Science 304.
159. Wegley L, Edwards R, Rodriguez-Brito B, Liu H, Rohwer F (2007) Metagenomic analysis of the microbial community associated with the coral Porites astreoides. Environmental microbiology 9.
160. Wuyts J, Peer YVande, Winkelmans T, De Wachter R (2002) The European database on small subunit ribosomal RNA. Nucleic Acids Res 30.
161. Goodman AL, Kallstrom G, Faith JJ, Reyes A, Moore A, Dantas G, et al. (2011) Extensive personal human gut microbiota culture collections characterized and manipulated in gnotobiotic mice. Proceedings of the National Academy of Sciences 108: 6252-6257.
162. Nayfach S, Pollard KS (2015) Average genome size estimation improves comparative metagenomics and sheds light on the functional ecology of the human microbiome. Genome Biology 16: 51.
163. Ekblom R, Wolf JBW (2014) A field guide to whole-genome sequencing, assembly and annotation. Evolutionary Applications 7: 1026-1042.
164. Vollmers J, Wiegand S, Kaster A-K (2017) Comparing and Evaluating Metagenome Assembly Tools from a Microbiologist's Perspective - Not Only Size Matters! PLOS ONE 12: e0169662.
165. Sakamoto M, Benno Y (2006) Reclassification of Bacteroides distasonis, Bacteroides goldsteinii and Bacteroides merdae as Parabacteroides distasonis gen. nov., comb. nov., Parabacteroides goldsteinii comb. nov. and Parabacteroides merdae comb. nov. Int J Syst Evol Microbiol 56: 1599-1605.
166. Comstock LE (2009) Importance of Glycans to the Host-Bacteroides Mutualism in the Mammalian Intestine. Cell Host & Microbe 5: 522-526.
167. Fierer N, Schimel JP, Holden PA (2003) Variations in microbial community composition through two soil depth profiles. Soil Biology and Biochemistry 35: 167-176.
168. Waldrop M, Balser T, Firestone M (2000) Linking microbial community composition to function in a tropical soil. Soil Biology and Biochemistry 32: 1837-1846.

169. Handelsman J, Rondon MR, Brady SF, Clardy J, Goodman RM (1998) Molecular biological access to the chemistry of unknown soil microbes: a new frontier for natural products. Chemistry & biology 5: R245-R249.
170. Cydzik-Kwiatkowska A, Zielińska M (2016) Bacterial communities in full-scale wastewater treatment systems. World Journal of Microbiology and Biotechnology 32: 66.
171. Daims H, Nielsen JL, Nielsen PH, Schleifer K-H, Wagner M (2001) In Situ Characterization ofNitrospira-Like Nitrite-Oxidizing Bacteria Active in Wastewater Treatment Plants. Applied and environmental microbiology 67: 5273-5284.
172. Rinehart KL (2000) Antitumor compounds from tunicates. Medicinal research reviews 20: 1-27.
173. Rinehart KL, Holt TG, Fregeau NL, Stroh JG, Keifer PA, Sun F, et al. (1990) Ecteinascidins 729, 743, 745, 759A, 759B, and 770: potent antitumor agents from the Caribbean tunicate Ecteinascidia turbinata. The Journal of Organic Chemistry 55: 4512-4515.
174. Fayette J, Coquard IR, Alberti L, Ranchere D, Boyle H, Blay JY (2005) ET-743: a novel agent with activity in soft tissue sarcomas. Oncologist 10: 827-832.
175. Moss C, Green DH, P□rez B, Velasco A, Henr□quez R, McKenzie JD (2003) Intracellular bacteria associated with the ascidian Ecteinascidia turbinata : phylogenetic and in situ hybridisation analysis. Marine Biology 143: 99-110.
176. Moss C, Green DH, Pérez B, Velasco A, Henríquez R, McKenzie JD (2003) Intracellular bacteria associated with the ascidian Ecteinascidia turbinata: phylogenetic and in situ hybridisation analysis. Marine Biology 143: 99-110.
177. Cockrell DC, Beare PA, Fischer ER, Howe D, Heinzen RA (2008) A Method for Purifying Obligate Intracellular Coxiella burnetii that Employs Digitonin Lysis of Host Cells. Journal of microbiological methods 72: 321-325.
178. Honarmand H (2012) Q Fever: An Old but Still a Poorly Understood Disease. Interdisciplinary Perspectives on Infectious Diseases 2012: 8.
179. Simon RD (1974) The use of an ultrasonic bath to disrupt cells suspended in volumes of less than 100 µliters. Analytical Biochemistry 60: 51-58.
180. Jury MR (2011) Long-Term Variability and Trends in the Caribbean Sea. International Journal of Oceanography 2011: 9.